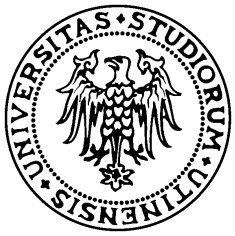

UNIVERSITY OF UDINE

DEPARTMENT OF EXPERIMENTAL CLINICAL MEDICINE

PHD COURSE IN BIOMEDICAL SCIENCES AND BIOTECHNOLOGY

XXVI CYCLE

Differential responses by aortic valve interstitial cells using *in vitro* models mimicking metastatic and dystrophic calcification: critical role of inorganic phosphate and additional effects of other pro-calcific agents including LDLs

PhD Student:
Alberto Della Mora

Supervisor:
Professor Maurizio Marchini

ACADEMIC YEAR 2013/2014

Alle persone importanti della mia vita

Abstract

Calcific aortic valve stenosis (CAVS) is the most severe valvulopathy affecting western world population. In the present thesis, *in vitro* models stimulating metastatic or dystrophic calcification in cultured bovine aortic valve interstitial cells (AVICs) were studied. Multivaried stimulations of primary cultures of AVICs were performed using inorganic phosphate (Pi) at critical concentrations, bacterial endotoxin lipopolysaccharide (LPS), and conditioned medium (CM) from cultures of allogeneic LPS-stimulated macrophages. Spectrophotometric estimations revealed calcification primarily to depend on elevated Pi levels (≥ 2.0 mM), which were comparable with the most elevated normophosphatemic levels and hyperphosphatemic ones. Pi-dependent effects resulted to be enhanced by adding LPS and CM together but not alone. Ultrastructurally, the calcific process consisted in a distinct AVIC degeneration as found for actual CAVS, in which the crucial event was a progressive plasmamembrane and organelle membrane colliquation that culminated in the generation of an acid-phospholipid-rich material outlining dying cells and their remnants and acting as major hydroxyapatite (HA) nucleator. AVIC remnants included rounded paracrystalline calcospherulae mirroring those described for CAVS. Consistently, Raman micro-spectroscopy applied to calcifying cultured AVICs revealed peripheral localization of HA and acidic phospholipids. Formation of calcific nodules also in the presence of apoptosis inhibitors and negative immunoreactivity to cleaved caspase 3 and annexin V led to exclude apoptosis to occur for calcifying AVICs. Conversely, surviving AVICs were found to undergo initial autophagocytosis, as revealed by immunopositivity to marker MAP1-LC3A, and subsequent derangement as revealed by ultrastructural detection of unusual hypertrophy of endoplasmic reticulum correlating with incubation time course and Pi concentration. In CAVS-affected valves atherosclerosis-like features were detected, with (i) Raman analysis showing colocalization between HA, phospholipids, cholesterol and carotenoids, and (ii) parallel electron microscopy revealing the presence of typical intra- and extracellular cholesterol crystals. Thus, the effects exerted by native low density lipoproteins in both native (nLDL) and aggregated (agLDL) form were explored on cultured AVICs using thin layer chromatography (TLC), spectrophotometry, histochemistry and electron microscopy. The chromatographically detected amounts of internalized esterified cholesterol differently correlated with the spectrophotometrically calcium estimations. Concerning pro-calcific effects, nLDLs and agLDLs alone induced mild calcification, whereas their combination with pro-calcific Pi+LPS+CM mixture unexpectedly provoked negligible calcification for nLDLs but prominent calcification for agLDLs. In conclusion, LDLs are further potential candidates for conditioning AVIC-dependent calcification in addition to Pi and other pro-calcific factors.

TABLE OF CONTENTS

LIST OF ABBREVIATIONS

agLDL	aggregated LDL
ALP	Alkaline Phosphatase
ATP	Adenosine Triphosphate
AVIC	Aortic Valve Interstitial Cell
bCM	bovine Conditioned Medium
BMP	Bone Morphogenic Protein
Ca	Calcium
CAII	Carbonic Anhydrase II
Ca-PL-PO_3	Calcium-Phospholipid-Phosphate
CAVS	Calcific Aortic Valve Stenosis
CCP	Calciprotein Particles
CDP	Cell-Derived Products
CRD	Chronic Renal Disease
CUA	Calcific Uremic Arteriolopathy
CuB	Cuprolinic Blue
CVC	Calcific Vascular Cell
DMEM	Dulbecco's Modified Eagle's Medium
EC	Esterified Cholesterol
ECM	Extracellular Matrix
ER	Endoplasmic Reticulum
ESRD	End-Stage Renal Disease
FBS	Foetal Bovine Serum
FC	Free Cholesterol
FGF	Fibroblast Growth Factor
GAG	Glycosoaminoglycan
Gla	γ-carboxyglutamic acid
HA	Hydroxyapatite
HDL	High Density Lipoprotein
ICAM	Intercellular Adhesion Molecule

IL	Interleukin
LC3	Light Chain 3
LDL	Low Density Lipoprotein
LDLr	LDL receptor
LPS	Lipopolysaccharide
Lrp	Lipoprotein receptor-like protein
LRP	LDL-Related Protein
MAP	Microtubule-Associated Protein
mCM	murine Conditioned Medium
MGP	Matrix Gla Protein
MMP	Matrix Metalloproteinase
MV	Matrix Vesicle
NFκB	Nuclear Factor κ B
nLDL	native LDL
NPP	Nucleotide Pyrophosphatase/Phosphodiesterase
OCN	Osteocalcin
OPG	Osteoprotegerin
OPN	Osteopontin
oxLDL	Oxidized LDL
P	Phosphorus
PA	Phosphatidic Acid
PC	Phosphatidylcholine
PI	Phosphatidylinositol
Pi	inorganic Phospahate
PiT	Phosphate Transporter
PPi	inorganic Pyrophosphate
PPL	Phthalocyanin Positive Layer
PPM	Phthalocyanin Positive Material
PS	Phosphatidylserine
RANK	Receptor Activator of Nuclear Factor kB
RANKL	RANK Ligand
RER	Rough ER
RGD	Arginine-Glycine-Aspartate

ROS	Reactive Oxygen Species
SM	Sphingomyelin
SMC	Smooth Muscle Cell
T2DM	Type 2 Diabetes Mellitus
TG	Triglycerides
TGF-β	Transforming Growth Factor-beta
TLC	Thin Layer Chromatography
TLR	Toll-like Receptor
TNF-α	Tumor Necrosis Factor-alpha
UPR	Unfolded Protein Response
VCAM	Vascular Cell Adhesion Molecule
VIC	Valve Interstitial Cell
VSMC	Vascular Smooth Muscle Cell

1. INTRODUCTION

Calcification is a process that takes place physiologically, in so-called hard tissues, or pathologically, in so-called soft tissues. Namely, physiological (orthopic) calcification includes endochondral and intramembranous ossification of bones as well as the biomineralization of dentin and enamel in the teeth. By contrast, extraskeletal mineralization occurs ectopically on respect orthopic one, i.e. various parenchymatous organs, cardiovascular structures or tumoral masses. Indeed there are a number of clinical conditions, including aging, cancer, diabetes, autoimmune diseases, and other disorders closely correlate with calcific processes.

These pathologies tissue can be related to histogenetic factors or to degenerative conditions. In both cases the inherent alterations seems to depend on multifactorial phenomena, even occurring according to distinctive condition-dependent and/or tissue-related patterns (Anderson H.C., 1983; Bonucci E., 1984; Boskey A.L. *et al.*, 1988).

This pathological mineralization was reported to consist in an aberrant deposition of calcium phosphate salts, including hydroxyapatite (HA), but also calcium oxalates and octacalcium phosphate, with detrimental effects (Kim K.M. 1995; Giachelli C.M., 1999).

In serum and extracellular fluids calcium (Ca) and inorganic phosphate (Pi) exist in metastable equilibrium that is, their levels are too low for spontaneous precipitation but sufficient to cause HA formation once crystal nucleation has started (Whyte M.P., 2006). Thus, the fundamental step in the process leading to ectopic calcification is the formation of HA crystals, which were demonstrated also to bind proteins, lipids, and other biomolecules, causing loss of soft tissue flexibility and pliability, encrusting organs and vessels so leading to painful outcomes and even lethal ones for patients.

Ectopic calcification in soft tissues was largely supposed to be a passive, degenerative process elicited by the presence of dead and dying cells. During the last decade a great number of studies showed that soft tissue calcification is a complex and highly regulated phenomenon, with some researchers hypothesizing it even associates with bone-like neo-formation. In healthy patients, extra-skeletal biomineralization is prevented by a variety of inhibitors of mineralization such as inorganic pyrophosphate (PPi), which was reported to be a major regulator of vascular calcification during human development (Anderson H.C., 1983;

Rutsch F. *et al.*, 2001; Johnson K. *et al.*, 2003). Giachelli and coworkers hypothesized that ectopic mineralization results from an imbalance between pro-calcific and anti-calcific regulatory molecules (Giachelli C.M., 2005).

Ectopic calcification can be associated with either abnormal serum levels of calcium and/or phosphate or normal ones being called metastatic calcification and dystrophic respectively.

The correlations of metastatic or dystrophic calcification with etiologically associated diseases are reported in Table 1.

TABLE 1: DISORDERS ASSOCIATED WITH ECTOPIC CALCIFICATION

- A. Metastatic calcification
  - I. Hypercalcemia
    - a. Milk-alkali syndrome
    - b. Sarcoidosis
    - c. Hyperparathyroidism
    - d. Renal failure
  - II. Hyperphosphatemia
    - a. Tumoral calcinosis
    - b. Hypoparathyroidism
    - c. Pseudohypoparathyroidism
    - d. Cell lysis after chemotherapy for leukemia
    - e. Renal failure
- B. Dystrophic calcification
  - I. Calcinosis (universalis or circumscripta)
    - a. Childhood dermatomyositis
    - b. Scleroderma
    - c. Systemic lupus erythematosus
  - II. Post-traumatic event

adapted from Whyte M.P. (2006)

When calcium-phosphorus solubility product (Ca x P) in extracellular fluid surpasses the critical value of 60 mg^2/dl^2 (Vattikuti R. and Towler D.A., 2004), mineral precipitation occurs in vital tissues. Initially, metastatic calcification consists in a precipitation of amorphous material, whereas crystalline HA is deposited later.

Hypercalcemia is usually associated with mineral deposits in kidney, lung, and stomach. In addition, tunica media of large arteries, endocardial elastic tissue, conjunctiva, and periarticular soft tissues are often affected (Whyte M.P., 2006). Other causes leading to hypercalcemia are augmented secretion of parathyroid hormone, i.e. hyperparathyroidism (Marcocci C. and Cetani F., 2011), malignancies (Lumachi F. *et al.*, 2009) and milk-alkali

syndrome, due to massive ingestion of calcium and absorbable basic salts (Abreo K. *et al.*, 1993). Finally, it was assumed to depend on elevated levels of vitamin D3, as in sarcoidosis (Baughman R.P. *et al.*, 2013).

Conversely a condition of hyperphosphatemia, with elevated serum levels of phosphorus occurs in idiopathic hypoparathyroidism or pseudohypoparathyroidism (Maeda S.S. *et al.*, 2006). It can be also associated with tumoral calcinosis because of releasing of intracellularcellular phosphate from cells lysed by chemotherapeutic drugs (Farrow E.G. *et al.*, 2011; Slavin R.E. *et al.*, 2012). Moreover, abnormal mineral imbalance associated with hyperphosphatemia, is commonly observed in glomerulosclerosis resulting from diabetes, as well as in severe chronic renal disease (CRD), an advanced renal failure, commonly called end-stage renal disease (ESRD), that requires dialysis or kidney transplantation. As a consequence of CRD, secondary hyperparathyroidism implies an increase of parathyroid hormone levels, with resulting changes in plasma vitamin D3, calcium, phosphorus, and an increase of their Ca x P product (Liebermann M. *et al.*, 2013). Patients with CRD are often subjected to advanced atherosclerosis and a high cardiovascular mortality rate. CRD severity and complexity causes a prominent metabolic dysfunction, leading to accelerated, extensive calcification in intimal and medial layers of arterial walls.

An example of a calcifying disorder in hyperphosphatemic conditions is metastatic calcinosis occurring in the skin and implying the formation of nodular deposits of calcium and phosphate, overall in periarticular sites. Hyperphosphatemia can be also associated with vascular calcification, as in vascular calciphylaxis.

In absence of a systemic mineral imbalance, dystrophic calcification occurs in soft tissues as a result of injury, aging, disease (Giachelli C.M., 1999) or metabolic alterations, such as hypercholesterolemia or hyperglycemia, which causes osmotic and oxidative stresses (Vattikuti R. and Towler D.A., 2004).

Of the soft tissues that potentially undergo ectopic calcification, blood vessels, heart valves, and the kidney, are the most susceptible to develop this pathology (Anderson H.C. and Morris D.C., 1993).

1.1 VASCULAR CALCIFICATION

Growing evidence exists that vascular calcification is on the verge of an epidemic disease concerning the westernized societies (Towler D.A., 2008), being shared risk factors aging, renal failure, and type II diabetes mellitus (T2DM) and shared hypertriglyceridemia, increased serum low density lipoproteins (LDL), decreased serum high-density lipoproteins

(HDL), obesity, and hypertension (O'Brien K.D. *et al.*, 1996; Olsson M. *et al.*, 1999; Pohle K. *et al.*, 2001).

In dystrophic calcification, vascular mineral deposition was described to occur according to three histoanatomic variants consisting in cardiac valve calcification (tricuspid valves, mitral valves, pulmonary valves and aortic valves), calcification of arterial tunica intima (intimal calcification) or calcification of arterial tunica media (medial calcification) (Vattikuti R. and Towler D.A., 2004; Lau W.L. and Ix J.H., 2013). In all these three cases the mineralization process shared different but overlapping mechanisms. Intimal calcification affects atherosclerotic plaques in the context of the disease called "atherosclerosis", whereas medial calcification is also called "arteriosclerosis" (Table 2).

TABLE 2: MACROVASCULAR CALCIFICATION: A HISTOANATOMIC VIEW

Cardiac valve calcification	Interstitial cell activation/inflammation	Senile calcific aortic sclerosis
	Dystrophic calcium deposition	Bicuspid aortic valve calcification
	T cells, macrophages, interstitial adipocytes, and myofibroblasts	Bioprosthetic valve calcification
	Osteogenesis, intramembranous bone formation	
	Rare cartilage metaplasia/calcified cartilage, infrequent endochondral bone formation	
	Marrow formation with hematopoiesis visualized in advanced disease	
Atherosclerotic calcification	Cellular necrosis and debris	Atherosclerosis
	Evolution of fibro-fatty plaque	Hypercholesterolemia
	Calcium deposition with lipoproteins, cellular lipid debris	Similar histology in calcifying fibrotic myocardial infarct
	Macrophages, T cells, endothelial dysfunction, platelet and myofibroblast activation	
	Cartilage metaplasia/calcified cartilage, endochondral bone formation	
	Marrow formation with hematopoiesis visualized in advanced disease	
Medial artery calcification	Adventitial activation/inflammation	Type 2, type 1 diabetes
	Macrophages, T cells, myofibroblasts, adipocytes,medial VSMCs and CVCs	End-stage renal disease
	Matrix vesicles, with osteogenesis resembling intramembranous bone formation	
	No cartilage formation	

adapted from Vattikuti R. and Towler D.A. (2004)

The present thesis primarily focuses on ectopic mineralization and underlying mechanisms at level of aortic valve leaflets affected by calcific aortic valve stenosis (CAVS).

1.1.1 AORTIC VALVE CALCIFICATION

CAVS affects 2.8% of adults over 75 years old is by at different extents (Nkomo V.T. *et al.*, 2006), being the second most common indication for cardiac surgery (Roberts W.C. and Ko J.M., 2005), which is associated with an 80% risk of progression to heart failure, valve replacement or death within five years (Otto C.M. *et al.*, 1997). In addition, surgical cusp replacement is still the sole therapeutic approach to the most severe form of CAVS, to date.

Even more worrying, the incidence and prevalence of valve disease is increasing worldwide due to the world population increasing age. Yacoub M.H. and Takkenberg J.J.M. (2005) reported that in the next forty years, the world population will increase as well as the proportion of over 60 aged people. Thus, the annual number of patients requiring heart valve replacement is estimated to triple from approximately 290,000 in 2003, to over 850,000 by 2050. Notably, the largest increase in the world population will be seen in third-world countries, in which not all patients will have access to this treatment. Strategies to address this global problem could have an important impact.

The risk factors shared by CAVS and atherosclerosis, hypertension, older age, male gender, smoking, hypercholesterolemia and diabetes have been reported (Stewart B.F. *et al.*, 1997; Pohle K. *et al.*, 2001; Peltier M. *et al.*, 2003; Freeman R.V. and Otto C.M., 2005; Messika-Zeitoun D. *et al.*, 2007). All Likely, these factors increase the incidence of aortic stenosis contributing to leaflet damage including endothelial defects and dysfunction (Mohler E.R. 3rd, 2004).

However, although risk factors and downstream mediators appear similar for these diseases, about 50% of patients with valve calcification are exempt from clinically significant atherosclerosis (Mazzone A. *et al.*, 2007; Qian J. *et al.*, 2010).

The semilunar aortic valve is a pentalayered anatomical entity that opens and closes almost 100,000 times a day permitting unidirectional forward blood flow maintaining sufficient strength and durability to tolerate repetitive mechanical stress over a lifetime.

Valve pliability and elasticity are guaranteed by the distinct texture of the constitutive extracellular matrix (ECM). A monolayer of endothelial cells envelopes the aortic and ventricular surfaces of the valve leaflet, forming two of its five layers together with a weak subendothelial, intimal-like sheet, whereas the inner valve interstitial cells (VICs) are represented by a mixed population of fibroblasts, myofibroblasts and smooth muscle cells

(SMCs) (Della Rocca F. *et al.*, 2000). VICs populate the ECM, which is composed by three highly organized sheets, named (i) *tunica fibrosa,* at the aortic side, (ii) *tunica spongiosa*, intermediate, and (iii) *tunica ventricularis*, at the ventricular side. A strictly controlled balance between synthesis and degradation of ECM components is controlled by VICs, which mediate constant repair and remodelling. Of the major components, collagen fibers are more abundant in the *fibrosa*, glycosoaminoglycans (GAGs) in the *spongiosa*, and elastin fibers in the *ventricularis*.

The early morphological stage of aortic valve disease is named aortic valve sclerosis, consisting in a mild valve thickening without obstruction of blood flow. Aortic sclerosis is present in almost 25% of adults 65 years of age, being associated with a 50% increase risk of cardiovascular events (Otto C.M. *et al.*, 1999).

Otherwise the later pathological stage, known as aortic valve stenosis, is a degenerative condition in which a massive calcification of the leaflets (Fig. 1.1) impairs theirs motion and can lead to obstruction of the blood outflow, with subsequent left ventricular hypertrophy, heart failure, and sudden death.

Macroscopically, sclerosis is characterized by an increased leaflet thickness and stiffening, whereas stenosis implies additional leaflet commissural fusion and subsequent calcification (Stewart B.F. *et al.*, 1997). Progression of aortic valve disease is showed in Figure 1.1. The calcific process begins at level of the *fibrosa*, along the leaflet adherent margin. With a slowly gradual progression, the calcific nodules spread toward the *fibrosa* invading the entire cusp.

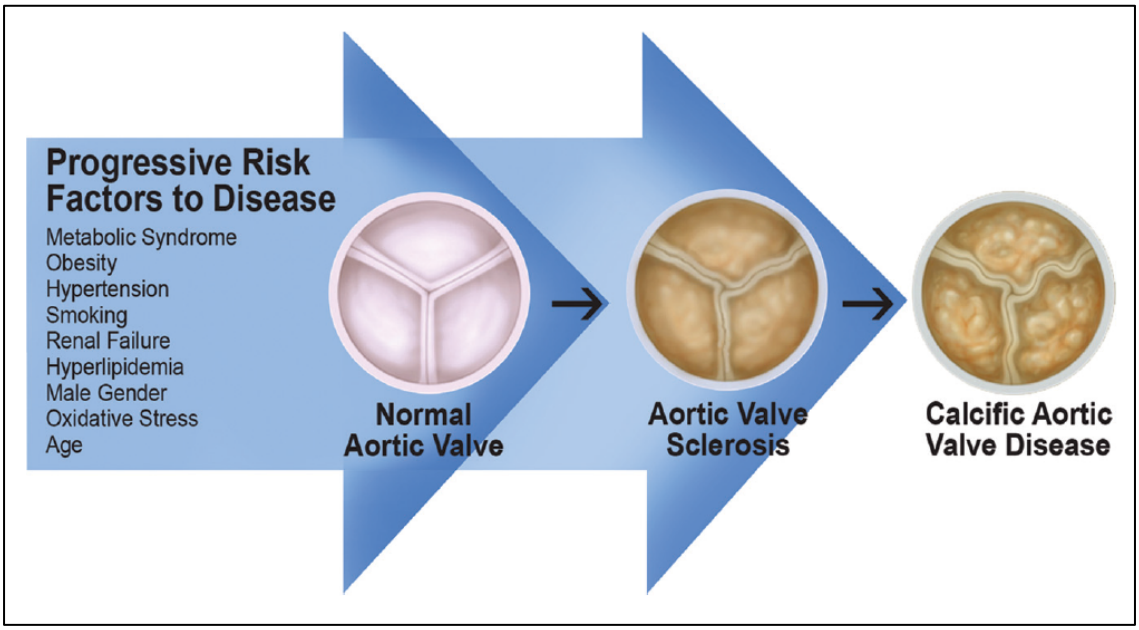

Figure 1.1. The identified cardiovascular risk factors involved in the development of aortic valve disease from sclerosis to CAVS (Rajamannan N.M. *et al.*, 2011).

In the past, calcification process was thought to be unmodifiable, because the gradual wear and tear of the leaflets with passive calcium deposition (Mönckeberg J.C., 1904). Now, histopathologic and clinical data suggest that CAVS is an active pathobiological process of valve modification similar to atherosclerosis because of lipoprotein deposition (O'Brien K.D. *et al.*, 1996; Olsson M. *et al.*, 1999), chronic inflammation, and calcium deposition as HA (Otto C.M. *et al.*, 1994; Rajamannan N.M. *et al.*, 2003).

1.1.2 ATHEROSCLEROTIC (INTIMAL) CALCIFICATION

Atherosclerosis occurs in aorta and in large elastic arteries and consists in intimal lipid deposits forming plaques of variable size that lead to eccentric lumen obliteration.

The atherosclerotic plaque stability depends on the formation of a thick fibrous cap, which envelops a small lipid core (Doherty T.M. and Detrano R.C., 1994). 5 to 10μm long, needle-shaped HA mineral crystals appear in early lesions in the third decade of life. It was previously believed that calcification occurs only in the most advanced, end-stage plaque in the elderly. Calcifications near the luminal surface may be subjected to erosion. However, Lin and colleagues found that calcification does not seem to increase plaque vulnerability when testing *in vitro* the mechanical response of a calcified plaque model to fluid stress (Lin T.C. *et al.*, 2006).

As mentioned above, risk factors of atherosclerosis are hypercholesterolemia, increased low-density lipoprotein cholesterol, increased lipoproteins, increased triglycerides, decreased high-density lipoprotein cholesterol, male gender, cigarette smoking, hypertension and diabetes.

Atherosclerotic calcification is initially characterized by cellular necrosis, inflammation, and lipoprotein and phospholipid complexes (Demer L.L., 2002). Calcium deposition occurs at level of lipoproteins as well as lipid complexes, derived from cellular membranes, located within the atherosclerotic plaques. Oxidized lipid products provide several signals that recruit and activate macrophages and T cells. Whether atherosclerotic calcification is cause or consequence of cardiovascular disease is still controversial.

Atherosclerotic calcium deposits could stiffen the aorta and affect plaque stability (Sage A.P. *et al.*, 2010) as well as atherosclerosis could induce cellular osteogenic differentiation in vascular smooth muscle cells (VSMCs) implying calcification of neoformed bone matrix (Böstrom K. *et al.*, 1993).

Indeed, calcium deposits cause compliance mismatch at the interface of the rigid mineral with the more distensible artery wall tissue. Under mechanical stress, this interface has a

greater risk for mechanical failure, resulting in a break of the fibrous cap (Richardson P.D. *et al.*, 1989; Farb A. *et al.*, 1996). Plaque rupture, or ulceration, is believed to cause most myocardial infarction and stroke as well as thrombotic phenomena. Calcium deposits dramatically redistribute stress in plaque, reducing it in some regions and increasing it in others (Hoshino T. *et al.*, 2009) with the exposition to rupture risk depending on the anatomic orientation of the calcium deposits on respect to the plaque and associated necrotic core.

In arterial walls, calcification positively correlates with atherosclerotic plaque burden (Beadenkopf W.G. *et al.*, 1964) and increasing in risk of (i) myocardial infarction, (ii) ischemic episodes in peripheral vascular system, and (iii) rupure after angioplasty.

1.1.3 ARTERIOSCLEROTIC (MEDIAL) CALCIFICATION

Medial artery calcification, also known as Mönckeberg's sclerosis, is the circumferential, contiguous, and confluent calcification afflicting the muscular medial layer of arterial walls, occurring independently from atherosclerosis. This type of calcification is common in elderly patients and linearly afflicts increasing aged population (Reid J.D and Andersen M.E., 1993; Elliott R.J. and McGrath L.T., 1994; Tohno Y. *et al.*, 1996), but also normal young patients with no overt metabolic disease (Mori H. *et al.*, 1992; Top C. *et al.*, 2002).

Medial calcification has been linked to disorders characterized by generalized metabolic alterations, as well as derangements concerning electrolytes or pH. Correlations are reported with hypervitaminosis D (Mallick N.P. and Berlyne G.M., 1968), hyperphosphatemia, as in ESRD (Foley R.N. *et al.*, 1998), and overall diabetes mellitus (Everhart J.E. *et al.*, 1988; Lehto S. *et al.*, 1996; Chantelau E. *et al.*, 1997; Edmonds M.E., 2000) and its complications such as autonomic neuropathy (Edmonds M.E. *et al.*, 1992; Gentile S. *et al.*, 1990).

Furthermore, the medial artery calcification is an emerging important predictor of (i) diabetes severity and duration, (ii) lower extremity amputation, and (iii) cardiovascular mortality risk (Lehto S. *et al.*, 1996).

Medial calcification can occur frequently in aorta wall, but it is typically encountered in arteries having low propensity to develop atherosclerosis, such as abdominal visceral arteries, arteries of thyroid and breast, and arteries supplying the extremities (reviewed by Doherty T.M. *et al.*, 2004).

Medial calcification has been reported rarely to occur in coronary arteries, whose calcification is associated with atherosclerotic plaque (Nakamura S. *et al.*, 2009).

In small- and medium-sized vessels, medial calcification is known as calcific uremic arteriolopathy (CUA), or calciphylaxis, and occurs when the physiological calcium phosphate

solubility threshold is elevated (Qunibi W.Y. *et al.*, 2002). CUA causes ischemic and ulcerating tissue necrosis of dermis, subcutaneous tissue, muscles, and internal organs (visceral calciphylaxis) (reviewed by Ng A.T. and Peng D.H., 2011).

Aortic stiffness is an important consequence of medial calcification, and calcification has the greatest effect on aortic rigidity (Demer L.L., 1991) resulting in hypertension, left ventricular hypertrophy, ischemia, heart failure, lower limb amputation, and death (Shao J.S. *et al.*, 2010).

A comparison between intimal and medial calcification is showed in Figure 1.2.

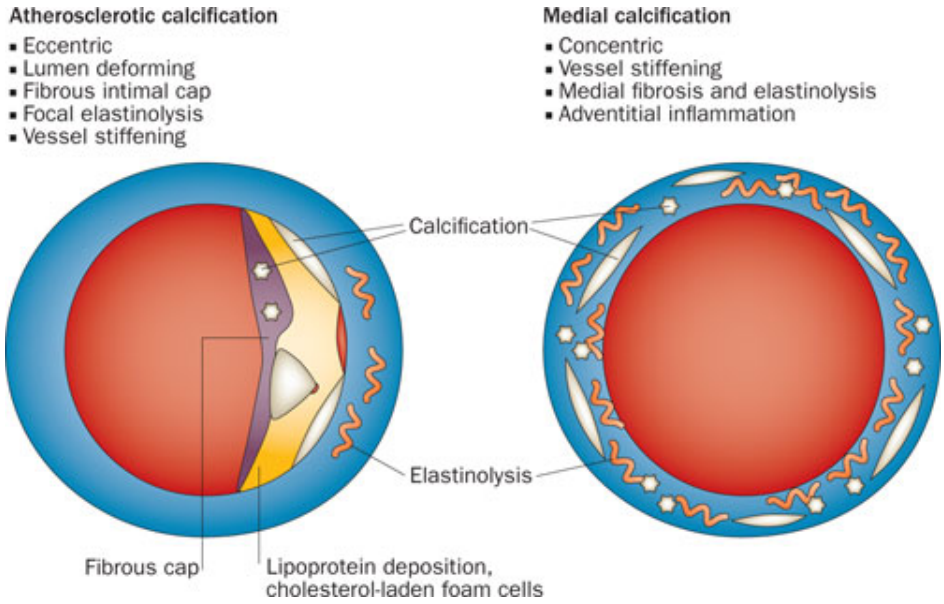

Figure 1.2. Atherosclerotic *vs* medial arterial calcification. Both types stiffen arterial conduit vessels. The eccentric remodeling of atherosclerotic calcification also reduces lumen diameter, and predisposes to acute thrombosis. (Thompson B. and Towler D.A. 2012).

1.2 CALCIFICATION MECHANISMS IN CARDIOVASCULAR SYSTEM

An unsolved problem concerning the calcific processes is the identification of the starting point of HA nucleation. Mineralization results from physicochemical and biochemical processes eliciting HA crystal deposition in topic areas in the ECM.

In ectopic calcification a primary role was ascribed to the cells, similarly to physiological mineralization occurring in bone and pre-calcific cartilage, in which an involvement exists of matrix vesicles (MVs) resulting from budding of 50-to-200 nm sized cytoplasmic bodies by osteoblasts and hypertrophic chondrocytes, respectively (Bonucci E., 1967; Anderson H.C., 1967; Bonucci E., 1971; Wuthier R.E., 1982).

Polarized release of MVs was reported to occur at level of (i) chondrocyte edges during biomineralization in growth plate cartilage (Anderson H.C., 1969; Cecil R.N.A. and Anderson H.C. 1978), (ii) osteoid-facing surfaces of osteoblasts in newly formed bone (Anderson H.C. *et al.*, 1973; Palumbo C., 1986), and (iii) apical surfaces of odontoblasts in the tooth pre-dentine (Bernard G.W., 1972; Eisenmann D.R. and Glick P.L., 1972). Usually, increasing electron density of MVs, because of amorphous $CaPO_4$ mineral pre-deposition, precedes HA crystal formation.

The polarized vesiculation from these types of cells, as well as the specific molecule composition of MVs versus the mother cell, denotes a highly organized process involving a great number of molecules. For example, in the membranes of MVs lipid bilayer is unusually enriched by acidic phospholipids (Wuthier R.E., 1976). In addition, their outer surfaces show prominent concentration of alkaline phosphatase (ALP), which promotes calcification by reducing pyrophosphate (PPi) levels (Rachow J.W. and Ryan L.M., 1988; Hessle L. *et al.*, 2002), and annexins, in particular, annexin II, V and VI. Annexins are Ca^{2+} and phospholipid binding integral proteins, which can form calcium channels through MV membranes, stimulating calcium uptake (Wuthier R.E. *et al.*, 1992; Kirsh T. and Wuthier R.E., 1994; Kirsh T. *et al.*, 1997). Otherwise, the Pi enters via a type III Na^{+}-dependent phosphate transporter (PiT), to form apatite within MVs (Li X. and Giachelli C.M., 2004). Additionally, Pi is delivered by ALP, that degrades PPi and adenosine triphosphate (ATP), commonly known as mineralization inhibitors (Anderson H.C. *et al.*, 2004).

Anderson and Sajdera reported that the initial calcification occurs at level of the inner membrane of the vesicle wall, being the early crystals of HA detected in that location (Anderson H.C. and Sajdera S.W., 1976; Anderson H.C., 1980).

Essentially, physiological mineralization is a biphasic phenomenon (Anderson H.C., 1995). During the first phase, intravesicular calcium concentration increases due to its affinity for acidic phospholipids and Ca-binding proteins of the vesicle membrane interior. Phosphatases, for example ALP, act on ester phosphate of matrix vesicle fluid producing a local increase in PO_4 in the vicinity of vesicle membrane. The intravesicular ionic product Ca x P is raised, resulting in initial deposition of calcium-phosphate at membrane inner side. When sufficient Ca^{2+} and $PO4^{3-}$ have accumulated within the MVs, $CaPO_4$ mineral begins to precipitate in non-crystalline form. Amorphous $CaPO_4$ is converted to octacalcium phosphate, whose crystals are then transformed into the highly insoluble HA (Anderson H.C., 1969; Wu L.N. *et al.*, 1993). Accumulation and growth of intravesicular crystals leads to their penetration of the MV membrane and the subsequent exposition to the extravesicular

environment. In addition, hydrolytic action of phospholipases (Wuthier R.E. *et al.*, 1978) and proteases of MVs (Dean D.D. *et al.*, 1992) result in MV breakdown.

The second phase consists in epitaxial mineral propagation, because the extravesicular fluid is supersaturated of calcium, enabling further crystal nucleation to take place (Anderson H.C. *et al.*, 2004).

Then new self-nucleated crystals of HA accumulate forming spherical clusters at MV surfaces.

Cells and cell-derived products (CDP) as well as matrix vesicles-like structures, were considered initiators of calcific process of both native and bioprosthetic valves, whereas collagen is considered to play a secondary role, linked to the subsequent propagation of calcific phenomena in the ECM (Kim K.M. and Huang S., 1971; Kim K.M., 1976; Schoen F.J. *et al.*, 1985; Valente M. *et al.*, 1985; Schoen F.J. *et al.*, 1986; Schoen F.J. and Levy R.J., 1992; Girardot M.N. *et al.*, 1995; Ortolani F. *et al.*, 2002a; Ortolani F. *et al.*, 2002b). These final pro-calcific products, called *calcospherulae* or spherulites, appear as target-like bodies being often coated by needle-like apatite crystals oriented perpendicularly to their membrane (Fig. Valente). These cell-derived pseudocrystalline structures were found not only in native valves (Kim K.M., 1976) but also in bioprosthetic valves (Valente M. *et al.*, 1985) and in *in vitro* calcifying aortic VICs (Bonetti A. *et al.*, 2012).

Alternatively, the initial phase of intracellular calcification was also assumed to occur at nuclear envelope and/or mitochondria of dead or dying cells, with initial HA accumulation (Schoen F.J. *et al.*, 1985; Girardot M.N. *et al.*, 1995).

Ortolani and colleagues shed light on the events underlying valve mineralization modifying classical pre-embedding histochemical reactions for electron microscopy (i) phthalocyanin cuprolinic blue (CuB) or (ii) diaminotriphenyilmethane dye malachite green combined with (iii) post-embedding silver salt staining. Thus, parallel preservation and visualization of acidic mixtures of phospholipid-containing proteo-lipidic material and HA removal with unmasking of calcific sites were achieved (Ortolani F. *et al.*, 2002a; Ortolani F. *et al.*, 2002b; Ortolani F. *et al.*, 2003; Ortolani F. *et al.*, 2007).

Namely, in *in vivo* subdermal model of valve calcification, cell involvement was found to occur throughout the release of lipids by degenerating organules and their release into cytoplasm as phthalocyanin positive material (PPM) and its subsequent peculiar outcropping at cell edges as phthalocyanin positive layers (PPLs) lining cells and cell-derived matrix-vesicle-like bodies. In addition, PPLs were found to represent the major HA crystal nucleators Moreover, PPL-like material was observed to spread outside mineralized cells enveloping

collagen fibrils and elastin fibres so also triggering ECM calcification.

Additional precipitation of HA crystals was reported to occur at level of the gap zones of collagen fibrils as later extra-vesicular event (Arsenault, A. L. *et al.*, 1991) as well as early MV-independent calcific process (Glimcher M.J., 1981).

The increase of acidic phospholipids in the membranes of pro-calcific MVs led to the hypothesis of direct involvement of phosphatidylserine (PS), phosphatidylinositol (PI) and phosphatidic acid (PA) (Wuthier R.E., 1973; Vogel J.J. and Boyan-Salyers B.D., 1976; Wuthier R.E., 1976). Such an involvement was also assessed by Odutuga and colleagues, in the same years (Odutuga A.A *et al.*, 1975). They demonstrated that these phospholipids extracted from both hard and soft tissues are able to precipitate HA from calcium-phosphate metastable solutions in *in vitro* conditions.

Since 1970s, a considerable insight was the discovery of specific complexes isolated from mineralized or mineralizing tissues (Boskey A.L. and Posner A.S., 1976; Boskey A.L. *et al.*, 1977; Wuthier R.E. and Gore S.T., 1977) each formed by calcium, acidic phospholipids and phosphate (Ca-PL-PO_3).

These complexes were not believed to be composed by apatite crystals adsorbed on the surface of phospholipids, but a distinct material (an intermediate), which could lead initial nucleation, and growth of apatite crystals by orientating suitably the bound calcium and phosphate ions.

In detail, the enzymatic deletion of serine or inositol suggests that calcium bind to both the phosphate and carboxyl groups for PS and phosphate and hydroxyl groups for PI.

Thus Ca-PL-PO_3 complexes were assumed to act as calcification nucleator by promoting HA formation. Moreover, an influence on calcification by magnesium, HCO_3, citrate, enzymes, proteins, proteoglycans and other factors was found.

The high content of acidic phospholipids in MV membrane not only allow them to bind Ca^{2+}, but also facilitate binding with calcium-dependent annexins (Wuthier R.E. *et al.*, 1992; Kirsh T. *et al.*, 1997).

As above mentioned, the role of acidic phospholipids was ultrastructurally confirmed by Ortolani and colleagues in subdermally implanted porcine aortic valve leaflets (Ortolani F. *et al.*, 2003).

Thus the Ca-PL-PO_3 complexes could interact with a lot of different molecules, such as ALP, proteolipids, cholesterol, etc. suggesting the existence of more composite nucleators (named “nucleational core complex”), as biochemically shown in hypertrophic cartilage (Boyan B.D. and Boskey A.L., 1984; Wu L.N. *et al.*, 1991; Wu L.N. *et al.*, 1993; Kirsch T. *et*

al., 1994; Wu L.N. *et al.*, 1996). The involvement of a great number of these molecules was also assessed in aortic valves and bioprosthetic ones, supporting the idea that different types of mineralization could share common mechanisms of action (Kim K.M. and Huang S., 1971; Kim K.M., 1976; Levy R.J. *et al.*, 1980; Levy R.J. *et al.*, 1983b; Maranto A.R. and Schoen F.J., 1988; Levy R.J *et al.*, 1991; Jorge-Herrero E. *et al.*, 1991; Jorge-Herrero E. *et al.*, 1994).

Furthermore, acidic membrane phospholipids are present at greater extents in necrotic areas, being associated with CDPs and *calcospherulae*, thereby eliciting calcification of necrotic tissues. In particular, these structures are abundant in aortic atherosclerotic lesions (Kim K.M., 1976; Tanimura A. *et al.*, 1983). Ca-PL-PO_3 complexes were identified in human atheroslerotic aortas, suggesting that calcification mechanism may occur in a series of surgical specimens affected by pathological calcification besides in bone and calcifying cartilage (Dmitrovsky E. & Boskey A.L., 1985; Boskey A.L. *et al.*, 1988). These findings suggested a possible correlation between these cell debris and MVs acting in physiologically calcifying tissues.

The two structures are not identical, but it is likely that both guarantee a favorable environment for mineralization. Interestingly, these pro-calcific bodies could represent a link between physiological and dystrophic calcification (Anderson H.C., 1983).

1.3 MOLECULAR DETERMINANTS

The etiopathogenesis of cardiovascular tissue is the result of active processes such as lipid accumulation and/or alteration, inflammatory responses, loss of inhibition cell osteogenetic differentiation and cell death. It is still debated which factors represent the major triggers of the calcific process. Besides, mineralization seems to depend by the balanced action of promoters and inhibitors.

1.3.1 INORGANIC PHOSPHATE

Growing evidence indicates that Pi is an important driver of vascular calcification affecting VSMCs and VICs.

Pi is fundamental in most cellular processes, including energy metabolism, signal transduction, storage and translation of genetic information and maintenance of lipid membrane structure. The majority of phosphate in humans (85%) is located in bone, in which it is complexed with calcium under form of HA. Normal phosphate serum levels are conventionally comprised within a range between a minimum of 0.8 to 1.45 mM (Tonelli M. *et al.*, 2005; Osuka S. and Razzaque M.S, 2012) up to a maximum of 2.0 to 2.1 mM (Jono S.

et al., 2000; Rodriguez-Benot A. *et al.*, 2005). Disturbances outside this range, resulting in hypo- and hyperphosphatemia, are known to be clinically relevant. Several observational studies showed a link between cardiovascular morbidity and mortality and higher serum phosphate levels (Tonelli M. *et al.*, 2005; Dhingra R., *et al.*, 2007; Foley R.N. *et al.*, 2009; Larsson T.E. *et al.*, 2010). Furthermore, even relatively small elevations of Pi in the high normophosphatemic range have been correlated with increased risk of cardiovascular diseases, including ectopic calcification (Tonelli M. *et al.*, 2005; Ellam T.J. and Chico T.J., 2012; Osuka S. and Razzaque M.S., 2012).

Phosphate levels are predominantly maintained by fibroblast growth factor (FGF)-23, which is secreted by osteocytes and reduces calcitriol levels (Fukumoto S., 2005). Additionally, FGF-23 acts on kidneys causing phosphaturia, and therefore reduces serum phosphate levels (Nabeshima Y., 2008).

Another active component of calcification is the functional sodium-dependent phosphate transport system, including phosphate transporter PiT1 (Jono S. *et al.*, 2000; Li X. *et al.*, 2006; Villa-Bellosta R. *et al.*, 2007). Moreover, Giachelli and colleagues demonstrated that Pi induces VSMCs calcification *in vitro* by a direct mechanism involving Pit-1 (Jono S. *et al.*, 2000).

Another enzyme implied in phosphate axis is a metalloenzyme known as phosphate-monoester phosphohydrolase, commonly named alkaline phosphatase, which was demonstrated to have two roles in promoting mineralization. First, it supplies substrate for HA mineral deposition inducing Pi releasing from organic phosphate conjugates. The second role involves the hydrolysis of PPi (Lomashvili K.A. *et al.*, 2008) thereby increasing Pi concentration and in parallel decreasing its anti-calcific role.

Additionally, calcium uptake was found inversely to correlate with ALP activity (Genge B.R. *et al.*, 1988), the decline of which was found to depend on loss of metal ions Zn^{2+} and Mg^{2+} rather than the action of a specific protease.

Wuthier and colleagues hypothesized an additional role of ALP, which might facilitate the attachment of MV to collagen fibrils, inducing the formation of nucleation complexes (Wu L.N. *et al.*, 1996).

Being ALP an enzyme working in bone tissue, a great number of researchers correlated an increase of ALP activity with the priming of osteogenetic differentiation by vascular cells in the context of various models of vascular tissue calcification (Chen N.X. *et al.*, 2002; Giachelli C.M. *et al.*, 2005; Mathieu P. *et al.*, 2005; Osman L. *et al.*, 2007).

1.3.2 INFLAMMATORY MEDIATORS

Inflammation is a prominent feature in aortic valve calcification, being present in both early and advanced aortic valvular lesions (Olsson M. *et al.*, 1994; Otto C.M. *et al.*, 1994).

Cellular inflammatory infiltrates are not common in normal aortic valves. In fact, T-lymphocytes were absent and only rare macrophages were found to be scattered within the *interstitium* of normal valve leaflets, whereas inflammatory infiltrate composed of macrophages and T cells characterized early valvular lesions (Otto C.M. *et al.*, 1994). These activated inflammatory cells lying in the subendothelium and in the *fibrosa* are reported to induce a chronic inflammation with release of cytokines and enzymes such as interleukins IL-2 (Olsson M. *et al.*, 1994) and IL-1β (Kaden J.J. *et al.*, 2003), transforming growth factor beta 1 (TGF-β1) (Jian B. *et al.*, 2003), tumor necrosis factor alpha (TNF-α) (Kaden J.J. *et al.*, 2005b), and matrix metalloproteinases (MMPs) (Edep M.E. *et al.*, 2000), which contribute to ECM remodeling, inflammatory activation of myofibroblasts which, in turn, seem to develop an osteoblast-like phenotype, with subsequent calcification.

Interestingly, Toll-like receptors (TLR) and the complement system seem to be also involved in the pathogenesis of CAVS (Helske S. *et al.*, 2008; Meng X. *et al.*, 2008), as well as *in-vitro* stimulation of TLR can promote an osteogenic transdifferentiation by VICs.

Epidemiologic data indicated that bacterial endocarditis leads to calcification in aortic valves (Otto C.M. *et al.*, 1999). Babu and colleagues postulated that osteoblastic phenotype acquirement by VICs take place in response to circulating bacterial products, thereby contributing to the pathogenesis of CAVS (Babu A.N. *et al.*, 2008).

1.3.2.1 TRANSFORMING GROWTH FACTOR-BETA (TGF-β)

The TGF-β proteins superfamily comprises cytokines and peptide growth factors that regulate biological functions in many systems including cardiovascular one. TGF-β1 is present in human calcific aortic stenotic cusps. Interestingly, in sheep aortic VIC cultures TGF-β1 was found to promote calcification through mechanisms involving apoptosis (Jian B. *et al.*, 2003).

Otherwise, TGF-β blocking antibody prevented nodule formation. Consistently, increased expression of TGF-β in the ECM correlated with increased ALP activity in both *in vitro* and *ex vivo* conditions (Clark-Greuel J.N. *et al.*, 2007).

In addition, TGF-β treatments were reported to induce tissue remodelling during calcification of human aortic valves by increasing the active form of MMP-2 and MMP-9 pro-enzyme, in *in-vitro* experiments, as well as the expression of MMP-9 and tissue inhibitor of

MMPs (TIMPs) in *ex vivo* specimens (Clark-Greuel J.N. *et al.*, 2007). In VSMC cultures rich in phosphate, neutralization of TGF-β does not inhibit calcification, indicating that this cytokine is not directly involved in calcium deposition (Wang N. *et al.*, 2010).

Interestingly, exogenous addition of TGF-β to the wound was found to modulate VIC response to injury by increasing VIC activation and proliferation, wound closure rate, and stress fibers expression (Liu A.C. and Gotlieb A.I., 2008).

1.3.2.2 TUMOR NECROSIS FACTOR-ALPHA (TNF-α)

Tumor necrosis factor-α (TNF-α) is a pleiotropic cytokine secreted by several types of cells, including activated macrophages, T lymphocytes, SMCs, and fibroblasts. It is involved in acute and/or chronic inflammation as a response to many factors such as oxidized LDLs (Jovinge S. *et al.*, 1996), damaged ECM (Alexandraki K. *et al.*, 2006) and bacterial infection (Guzik T.J. *et al.*, 2006).

TNF-α involvement in vascular calcification was firstly reported by Tintut and colleagues who treated bovine aortic SMCs with TNF-α also demonstrating this cytokine to elicit downstream upregulation of ALP (Tintut Y. *et al.*, 2000). Further studies identified TNF-α in both human and mouse atherosclerotic lesions and calcified aortic valves (Frostergård J. *et al.*, 1999; Boesten L.S. et al., 2005; Yu Z. *et al.*, 2011).

Concerning aortic valve calcification, TNF-α was found to act as an inducer of ECM remodelling (Kaden J.J. *et al.*, 2005a), cell proliferation and differentiation (Kaden J.J. *et al.*, 2005b), and calcification (Yu Z. *et al.*, 2011).

1.3.2.3 RANK/OPG/RANKL SYSTEM

The transmembrane protein receptor activator of nuclear factor κB (RANK), its ligand (RANKL), and its decoy receptor osteoprotegerin (OPG) constitute a cytokine system of the TNF superfamily, which is involved in the regulation of bone resorption and vascular calcification (Bucay N. *et al.*, 1998; Kiechl S. *et al.*, 2006; Panizo S. *et al.*, 2009).

OPG is a soluble receptor that binds to RANKL, thereby inhibiting the interaction of RANKL and RANK, once expressed by a variety of tissues and cell types including SMCs and endothelial cells, whereas RANKL and RANK are not expressed in vascular tissue under physiologic conditions (Simonet W.S. *et al.*, 1997). Deletion of the OPG gene leads to severe calcification of aorta and renal arteries, associated with the expression of RANKL and RANK in the calcified areas, suggesting RANKL to promote vascular calcification, with OPG playing a protective role (Min H. *et al.*, 2000). Consistently, OPG-null mice resulted to

develop arterial calcification. An involvement of OPG in mineralization was also demonstrated in VSMC calcification, where it seems to exert inhibitory effects on calcification (Bucay N. *et al.*, 1998). Otherwise RANKL has reported to promote extracellular mineralization in VSMC cultures via a BMP4-dependent mechanism (Panizo S. *et al.*, 2009).

Mouse studies have shown that the RANKL-RANK pathway is the gatekeeper of osteoclast differentiation and activation (Nakagawa N. *et al.*, 1998).

Kaden and colleagues firstly demonstrated the role of RANKL/OPG pathway in aortic valve myofibroblasts, showing that RANKL promotes matrix calcification in *in vitro* mineralizing conditions. In addition, increasing in ALP activity and synthesis of osteocalcin was found; hence this system was hypothesized to induce an osteogenetic phenotype in the cultured cells (Kaden J.J. *et al.*, 2003).

1.3.3 CALCIFIC INHIBITORS

A lot of findings have showed that most tissues, including heart valves and blood vessels, normally express inhibitors of mineralization. The lack of these molecules, named "loss of inhibition", indicate that calcium phosphate deposition starts when pro-calcifying conditions overwhelm the anticalcifying capacity of tissues, leading to calcification.

1.3.3.1 PYROPHOSPHATE

In humans, a pathologic example of the importance of calcifying inhibitor mechanism is heritable deficiency of the small molecule PPi, which leads to idiopathic infantile arterial calcification (Rutsch F. *et al.*, 2001).

PPi is the anionic form of pyrophosphoric acid and resulted to be regulated by the opposite activity of two enzymes. Of these, ectonucleotide pyrophosphatase/phosphodiesterase 1 (NPP1) catalyses its synthesis hydrolysing ATP, whereas ALP catalyses its hydrolysis (Rachow J.W. and Ryan L.M., 1988; Hessle L. *et al.*, 2002; Harmey D. *et al.*, 2004). Additionally, PPi is released with the involvement of ANK, a protein that shuttles intracellular PPi to the extracellular milieu (Harmey D. *et al.*, 2004).

PPi is present in almost all ECMs, and several studies have shown that PPi is a potent inhibitor of medial vascular calcification *in vitro* conditions (Lomashvili K.A. *et al.*, 2004; Villa-Bellosta R. *et al.*, 2011) and *in vivo* (Schibler D. *et al.*, 1968). It performs the inhibitory activity by binding nascent HA crystals and preventing further incorporation of Pi ions into these crystals (Hessle L. *et al.*, 2002; Harmey D. *et al.*, 2004). Additionally, it acts as inhibitor of calcific phenotype acquirement by VSMCs (Johnson K. *et al.*, 2005) occurring in

normopyrophosphatemic conditions (Fleisch H. *et al.*, 1966).

In animal models, vascular calcification was induced via lowering of PPi levels, as it occurs in mice carrying the ANK mutation or in NPP1-null mice, there latter exhibiting cartilage-specific gene expression changes in their SMCs (Johnson K. *et al*., 2005).

Villa-Bellosta and Sorribas highlighted that PPi is able to completely inhibit all HA deposition under physiological conditions, but it can inhibit only one third of calcium deposition during hyperphosphatemia (Villa-Bellosta R. and Sorribas V. 2011).

1.3.3.2 OSTEOPONTIN

Osteopontin (OPN) is an acidic, multifunctional protein with a primary structure including several structural domains such as an arginine-glycine-aspartate (RGD) adhesive domain and a calcium-binding domain, which is rich in aspartic acid. In addition, OPN can be highly phosphorylated on serine and threonine residues, a structural feature which is required for mineral inhibitory effects (Jono S. *et al.*, 2000).

The combination of electronegative-glutamic and aspartic acid residues, putative specific calcium-binding motifs and sites acting as substrate for serine/threonine kinases endows OPN with ability to bind prominent Ca^{2+}amounts (50 moles of calcium per 1 mole of OPN) (Chen Y. *et al.*, 1992). OPN was discovered in mineralized tissues such as bones and teeth, but has a wide tissue distribution and was also identified in calcified vascular lesions (Giachelli C.M. *et al.*, 1993). Although OPN is not present in normal arteries, Fitzpatrick and colleagues as well as Giachelli and co-workers reported OPN to be abundant at calcification sites of human atherosclerotic plaques and in calcific aortic valves (Fitzpatrick L.A. *et al.*, 1994; O'Brien K.D. *et al.*, 1995).

The role of OPN in vascular calcification has been investigated using both *in vitro* and *in vivo* approaches (Steitz S.A. *et al*., 2002). In first case, OPN was demonstrated to inhibit the calcification of SMC, cultured with elevated phosphate with a dose-dependent fashion. OPN was intimately associated with growing apatite crystals, suggesting physical inhibition of the crystal growth to represent one of the mechanisms for inhibition (Jono S. *et al.*, 2000).

In *in vivo* experiments using OPN double null mice showed earlier and more severe mineralization of vessels was found in comparison with matrix Gla protein deficient mice (Speer M.Y. *et al.*, 2002). Another *in vivo* approach was applied by Steitz and co-workers, consisting in implantation of glutaraldehyde-fixed porcine aortic valves into OPN null mice. They showed a very greater degree of calcification compared with valves implanted into wild type mice (Steitz S.A. *et al.*, 2002). Furthermore, OPN not only inhibited HA deposition but

also caused its regression. Such a regression correlated with the carbonic anhydrase II (CAII) expression in the macrophages surrounding the implants and led to acidification of the implants.

Steitz and colleagues proposed that OPN secreted by stromal or inflammatory cells at sites of ectopic mineralization binds bioapatite so representing a recognition site or providing a concentration gradient for macrophage and giant cells leading to their topical accumulation with parallel up-regulation of CAII via cell surface OPN receptors. This leads to increased proton efflux, acidification of the local microenvironment, and dissolution of the bioapatite (Steitz S.A. *et al.* 2002). Thus, OPN may function not only as a physical inhibitor of apatite crystal growth, but also may promote mineral regressive mechanisms by controlling the cellular gene expression patterns that favour mineral resorption.

In immunohistochemical study on calcium-binding proteins in failed bioprosthetic porcine valves retrieved from humans, OPN was found to be associated with the calcifications areas exclusively, whereas bone markers such as osteocalcin, bone sialoprotein and osteonectin were unreactive (Shen M. *et al.*, 1997).

In failed bioprosthetic porcine valves retrieved from humans, OPN was immunohistochemically detected with the calcifications areas exclusively, whereas no immunohistochemical positivity resulted for other bone proteins such as osteocalcin, bone sialoprotein and osteonectin (Shen M. *et al.*, 1997).

1.3.3.3 FETUIN-A

Fetuin-A, a hepatocyte derived serum glycoprotein, is the most abundant non-collagenic protein in bone tissue (Termine J.D. *et al.*, 1981). Clinically, low serum levels of fetuin-A affect patients with moderate to severe chronic kidney disease, especially dialysis patients.

This cysteine protease inhibitor belongs to the cystatin superfamily of calcium binding proteins being characterized by a cystatin-like domain containing a lot of acidic aspartic and glutamic acid side chains and acts sequestrating calcium phosphates (Heiss A. *et al.*, 2003).

Fetuin-A binds calcium phosphate and calcium carbonate, but not calcium alone, with high affinity (Schinke T. *et al.*, 1996) and plays the additional role of binding directly to transforming growth factor beta (TGF-β1, TGF-β2) and bone morphogenic protein (BMP2, BMP4, BMP6) and also inactivating them (Binkert C. et al, 1999).

In contrast with OPN, fetuin-A only inhibits *de novo* formation of calcium phosphate rather than to dissolve preformed mineral, thus preventing the growth and aggregation of

calcific nuclei as well as subsequent formation of larger entities and ultimately mineral precipitation (Rochette C.N. 2009).

Fetuin-A is considered an opsonizing serum protein because of its capability of shielding spontaneously formed small mineral complexes of calcium-phosphate, making colloidal, nanoscopic particles which should be otherwise insoluble. Jahnen-Dechent and colleagues named these fetuin-calcium-phosphate complex as "calciprotein particles" (CCPs) and hypothesized that fetuin mediates their cellular uptake and clearing by phagocytosis (Jahnen-Dechent W. *et al.*, 2008; Jahnen-Dechent W. *et al.*, 2011).

Fetuin-A was shown to inhibit VSMC calcification experimentally induced by elevated concentrations of extracellular mineral ions (Reynolds J.L. *et al.*, 2004; Reynolds J.L. *et al.*, 2005). Fetuin-A enhanced uptake by phagocytosis with vesicular recycling of fetuin-mineral complexes reducing both apoptosis and calcification. In addition, subsequent fetuin-A release from apoptotic and viable VSMCs abrogated extracellular calcium phosphate precipitation.

Fetuin-A was thought to be a mineral chaperone mediating the uptake of mineral from the extracellular space and general circulation, thereby contributing in prevention from of ectopic calcification at level of plasma and tissue fluids (Westenfeld R. *et al.*, 2009).

In addition to its anti-calcific properties effects, fetuin-A has found to play a role in diabetes, via inhibition of insulin receptor autophosphorylation and tyrosine kinase activity in *in vitro* and *in vivo* conditions, with the involvement of the acidic amino acids clustered within the cystatin-like domain 1 (briefly reviewed by Burke A.P. *et al.*, 2007; Mathews S.T. *et al.*, 2006).

1.3.3.4 MATRIX GLA PROTEIN

Matrix γ-carboxyglutamic acid (Gla) protein (MGP) is considered an inhibitor of cardiovascular calcification and its function depends on vitamin K-dependent γ-carboxylation of glutamate residues, a process inhibited by warfarin.

MGP is thought to be a potent regulator of calcium deposition *via* (i) direct binding calcium ions and nascent crystals, (ii) inhibition of bone morphogenetic proteins, and (iii) regulation of apoptosis (Proudfoot D. and Shanahan C.M., 2006). MGPs reported to be also associated to both physiological (Hauschka P.V. *et al.*, 1975) and pathological calcification (Lian J.B. *et al.*, 1976; Levy R.J. *et al.*, 1979), including human aortic valves (Levy R.J. *et al.*, 1980).

Their involvement in calcification was also found for porcine aortic valves implanted in rat

subcutis (Fishbein M.C. *et al.*, 1982) as well as their inhibitory role in both arterial calcification in MGP null mice (Luo G. *et al.*, 1997; Murshed, M. *et al.*, 2004) and arterial and valvular calcification after warfarin intake (Price P.A. *et al.*, 1998; Schurgers L.J. *et al.*, 2004).

Osteocalcin (OCN) is the major Gla-containing bone protein, which was found to be involved in the regulation of bone mineralization. OCN is not normally expressed in vascular cells, but its expression by human SMCs is induced in calcific arterial walls and in *in vitro* pro-calcific environment (Jono S. *et al.*, 2000). It has been also found in explanted human calcified cardiac valves (Levy *et al.*, 1983a) and in porcine glutaraldehyde-preserved bioprostheses after implantation in bovine aortic roots (Levy *et al.*, 1983b) or in rat *subcutis* (Levy *et al.*, 1983c). Although the existing correlation between this vitamin-K-dependent protein amount and tissue calcium levels, lacking of calcification after vitamin K-antagonist therapy suggested no significant OCN involvement in this pathogenesis, so being regarded as an useful monitoring factor of calcification (Levy R.J. *et al.*, 1983c). By contrast, no positivity to OCN was revealed by immonostaining with polyclonal antibodies against calcium-binding proteins, in failed bioprosthetic porcine valves retrieved from humans (Shen M. *et al.*, 1997). *In vitro* studies (Boskey A.L. *et al.*, 1985) OCN was found to inhibit the growth of seeded HA, whereas it had some effects on the initial crystallization of HA in the presence of Ca-PL-PO_3 complexes, albeit without direct interactions. In addition, OCN resulted to differ from the other Gla-containing proteins, because of its high affinity for both HA crystals and acidic phospholipids.

1.3.4 LIPID FACTORS

Aortic valve degeneration mechanism is similar to that underlying atherosclerosis, with lipids playing a fundamental role in calcific process induction. In fact, epidemiologic data indicated a link between dyslipidaemia (high levels of LDLs, triglycerides, and low levels of high-density lipoproteins) and development of CAVS, as in metabolic syndrome (Briand M. *et al*., 2006; Goldbarg S.H. *et al*., 2007; Rabuş M.B. *et al*., 2009).

Histological and immunohistochemical studies showed that early valvular lesions are characterized by a subendothelial thickening of the leaflet *tunica fibrosa* with presence of intra- and extracellular lipids and microscopical calcification (Otto C.M. *et al.*, 1994). One of the main causes of these injuries is the damage of the endothelial layer overlying the valve due to elevated shear stress, with its increased permeability and initial infiltration and accumulation of circulating lipids. Subsequent endothelium destruction elicits an increasing

influx of atherogenic LDLs, followed by invasion into the valve of inflammatory cells, such as monocytes and T-lymphocytes. LDLs accumulate in valvular interstitial tissue with inflammatory consequences that could drive to calcification (O'Brien K.D. *et al.*, 1996).

Peculiar LDL structure allows nonpolar lipids to be transported by blood stream as soluble molecules. LDL particles are formed by a hydrophobic core containing esterified cholesterol and triglycerides and shielded by a phospholipid monolayer including unesterified cholesterol, and apolipoprotein apoB-100 (Fig. 1.3).

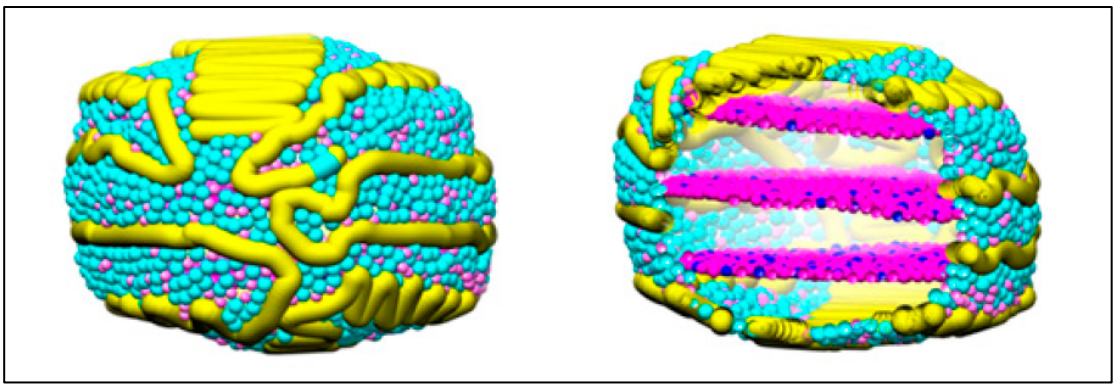

Figure 1.3. Three-dimensional reconstruction of LDL particle using electron cryomicroscopy. Image left shows an outside view of LDL and the disposition of apo B-100 (yellow cable) on external shield. The cut-away view of the particle (right) shows the internal organization of cholesteryl ester moieties. Phospholipid head groups, cholesteryl ester and triglycerides are displayed as cyan, magenta, and blue balls respectively (adapted from Ren G. *et al*., 2009).

Overall, LDL particles contain about 1,600 esterified cholesterol molecules, 700 phospholipid molecules, 600 unesterified cholesterol molecules, and 170 triglyceride molecules (Esterbauer H. *et al.*, 1992; Oörni K. *et al*., 2000). Phosphatidylcholine (PC) and sphingomyelin (SM), represent about 70% (500 molecules) and 30% (200 molecules) of LDL phospholipids. The peripheral molecules specifically interact to each other forming distinct domains on the LDL surface: there is evidence that apoB-100 is irreversibly associated with the PC molecules, whereas cholesterol interacts preferentially with SM (Sommer A. *et al.*, 1992; Mattjus P. and Slotte J.P., 1996; Murphy H.C. *et al.*, 1997).

At least in part, lipoprotein deposition within the *subintima* is mediated by accumulated ECM proteoglycans, including biglycans and decorins, with apolipoprotein positively charged amino acids binding negatively charged glycosaminoglycan side chains of proteoglycans (O'Brien K.D. *et al.*, 1995; Olsson U. *et al.*, 1997).

LDLs trapped in the subendothelial spaces undergo modifications such as oxidation, aggregation and fusion (Olsson M. *et al.*, 1999). Oxidized lipoproteins (oxLDL) were firstly detected in human and rabbit atherosclerotic lesions (Ylä-Herttuala S. *et al.*, 1989). These modified lipoproteins are highly cytotoxic and capable to promote inflammatory responses

and subsequent mineralization (Demer L.L., 2002). In an *in vitro* study, a role of oxLDL in stimulation of osteoblastic differentiation of vascular fibroblasts was suggested (Parhami F. *et al.*, 1997). In an *in vivo* study, a single injection of human LDL resulted in their accumulation within rat arterial walls, with oxidative modification within six hours (Calara F. *et al.*, 1998). The presence of oxidized LDL was associated with activation of transcription factor nuclear factor κ B (NFκB) in the endothelium, as well as with endothelial expression of intercellular adhesion molecule-1 (ICAM-1). Even mild oxidative modification alters LDL particle structure making them capable to aggregate (Hoff H.F. and O'Neil J., 1991).

oxLDLs are present in stenotic valves (Olsson M. *et al.*, 1999), with high content correlating with severe sclerosis, greater leukocyte infiltration, and expression of inflammatory cytokines, such as TNF-α (Mohty D. *et al.*, 2008). Moreover, *in vitro* studies showed oxidized cholesterol to stimulate calcified nodule formation by valve fibroblasts (Mohler E.R. 3rd, *et al.*, 1999)

High contents of valve oxLDL seem to correlate with high serum levels of so called "small dense LDL", which represents a subclass of LDL with distinct atherogenic properties (Packard C. *et al*., 2000; Rizzo M. and Berneis K., 2006), due to their characteristics, such as (i) small size, that permits to easily penetrate into the arterial wall, (ii) high affinity for proteoglycans of the arterial wall which results in a prolonged residence time in the subendothelial space (Anber V. *et al*., 1996), and (iii) lacking in vitamin E making them highly susceptible to oxidization (Goulinet S. and Chapman M.J., 1997; Tribble D.L. *et al*., 2001).

Valvular endothelial dysfunction or injury also leads to increased expression of adhesion molecules VCAM-1, ICAM-1, and E-selectin with associated recruitment of inflammatory cells (Müller A.M. *et al.*, 2000).

In vivo studies on hypercholesterolemic rabbits (Rajamannan N.M. *et al.*, 2002; Zeng Z. *et al.*, 2007) as well as *in vitro* studies on myofibroblasts (Rajamannan N.M. *et al.*, 2002) showed extracellular aggregated and fused lipid particles to accumulate in the stenotic aortic valves and revealed aortic valve calcification to be mediated in part by the lipoprotein receptor-like protein 5 (Lrp5)/β-catenin pathway.

Modifications of the surface structure of LDL particles can result in loss of their stability leading to LDL aggregation and subsequent fusion. Aggregation of LDL implies their surfaces to touch each other without particle merging as well as size changing. More extensive particle modifications lead to energetic stabilization resulting in their fusion (Pentikäinen M.O. *et al.*, 1996).

Aggregated LDL (agLDL) isolated from atherosclerotic lesions were demonstrated to be 10- to 50-fold enriched in ceramide, which is the lipolytic product of sphingomyelinase resulted from the hydrolysis of SM (Schissel S.L. *et al.*, 1996). Furthermore, secretory sphingomyelinase and secretory phospholipase A_2 were found to play roles in the modification of LDL during arterial intima atherogenesis. Indeed, sphingomyelinase induced both aggregation and fusion, whereas only LDL aggregation was caused by phospholipase A_2 (Öörni K. *et al.*, 1998; Schissel S.L. *et al.*, 1998).

Aggregation of normal LDLs by vortexing was found to convert them into a form that was readily uptaken by mouse peritoneal macrophages through a LDL-receptor-dependent mechanism (Khoo J.C. *et al.*, 1988).

In *in vivo* and *in vitro* experiments, macrophages were shown to internalize variously modified LDLs including agLDLs, becoming foam cells, whereas lipid accumulation into VSMCs was restricted to agLDLs and according **to** a peculiar pattern of internalization (Llorente-Cortés V. *et al.*, 1998).

Compared with native LDL (nLDL), which are taken up through endocytic LDL receptor (LDLr), agLDL are taken up with different pathway, involving LDL-related protein 1 (LRP1) (Llorente-Cortés V. *et al.*, 2000; Llorente-Cortés V. *et al.*, 2002a; Llorente-Cortés V. *et al.*, 2002b). LRP1-mediated selective uptake of agLDL induced high intracellular cholesteryl ester accumulation in lipid droplets surrounded by lipid-binding protein adipophilin contributing to the transformation of human VSMCs into foam cells (Llorente-Cortés V. *et al.*, 2006).

1.4 CALCIFICATION AND CELL DEATH

Ectopic calcification is associated with cell death. In particular, apoptosis-derived or autophagocytosis-derived bodies are reported as HA-nucleating structures, so playing the same pro-calcific role of matrix vesicles in mineralizing cartilage and bone (Kim K.M., 1995; Lee Y.S. and Chou Y.Y., 1998; Proudfoot D. *et al.*, 2000; Jian B. *et al.*, 2003; Somers P. *et al.*, 2006; Clarke M.C.H *et al.*, 2008).

Apoptotic processes were detected to occur around calcific loci interspersed throughout (i) the *media* of arteries affected by Mönckeberg's sclerosis, (ii) neointimal atherosclerotic plaques, and (iii) the *fibrosa* of aortic valves affected by calcific stenosis (Lee Y.S. and Chou Y.Y., 1998; Schoppet M. *et al.*, 2004). Pro-apoptotic protein containing MV-like remnants were found in advanced carotid atherosclerotic plaques (Kockx M.M., *et al.*, 1998). Moreover, a role of apoptosis was suggested in *in vitro* calcification because of the

identification of apoptotic markers in mineralized nodules of calcified VSMCs (Proudfoot D. *et al.*, 2000).

Sheep AVIC cultures stimulated with TGFβ-1 developed calcified, ALP-enriched nodules also containing apoptotic cells (Jian B. *et al.*, 2003). However, although apoptosis has been implicated in the formation of calcified cell nodules *in vitro* (Proudfoot D. *et al.*, 2000), administration of an apoptosis inhibitor to cultured cells did not affect the formation of calcific nodules (Jian B. *et al.*, 2003).

Macroautophagocytosis (here referred as autophagy) was reported to be involved in degenerative aortic valve disease (Somers P. *et al.*, 2006). Autophagy is described as surviving process for recycling cellular components such as long-lived proteins and damaged organelles by sequestering them within double-membrane vesicles called autophagosomes, which fuse with primary lysosomes with subsequent degradation.

It can be stimulated by stress, such as starvation, hormones and by cellular damage. If cell damage is irreversible, too cell components are enzymatically digested, resulting in cell death without release of toxic substances so avoiding inflammation in the surrounding tissue. Thus, autophagy can be also referred as a primarily caspase-independent cell death mechanism executed by lysosomal enzymes triggered when caspase-dependent routes fails as a response to cytotoxic agents such as oxLDL (Olsson M. *et al*., 1999).

After treatment with oxysterol, in cultured human VSMCs myelin figure formation was observed as well as processing of microtubule-associated protein (MAP) 1A/1B-light chain 3 (LC3) (Martinet W. *et al*., 2004). This is a ubiquitous soluble protein, which represents an important autophagic marker. In fact, during autophagy, cytosolic form of LC3 (LC3-I) is conjugated to phosphatidylethanolamine to form LC3-phosphatidylethanolamine conjugate (LC3-II), which is recruited to autophagosomal membranes (Klionsky D.J. *et al*., 2012). Since in the same study great amounts of ubiquitinated cells were detected in calcified aortic valves, compared to apoptotic cells, it was suggested that autophagic cell death rather than apoptosis might play a role in the release of matrix vesicles in degenerative aortic valves.

In contrast, shared degeneration steps other than those characterizing both apoptosis and autophagy were found to affect calcifying AVICs in three conditions: (i) actual valvular stenosis (Ortolani F. *et al.*, 2010; unpublished results), (ii) *in vivo* experimental calcification in xenogenically implanted aortic valve leaflets (Ortolani F. *et al.*, 2002a; Ortolani F. *et al.*, 2002b; Ortolani F. *et al.*, 2003; Ortolani F. *et al.*, 2007), and (iii) *in vitro* calcification in AVIC cultures after addition of different pro-calcific agents (Ortolani F. *et al.*, 2010; Bonetti A. *et al.*, 2012).

Such a degenerative steps consisted in (i) initial formation of cytoplasmic vacuolization, lysosome-like dense bodies, cytoplasmic protrusions and general increase of membrane components; (ii) overall dissolution of plasmalemmas, nuclear envelopes and organule membranes; (iii) increasing cytoplasm electrondensity due to the accumulation of dark amorphous PPM because of its positivity to histochemical reaction with the phthalocyanin CuB; (iv) centrifugal exudation of this material, giving rise to the formation of the marginal PPL; (v) PPL budding and pinching off generating thick walled CDPs and CDP-derived paracrystalline by-products named *calcospherulae.* The final cell derived particles were someway identifiable as MV-like bodies due to their size and shared capacity to nucleate HA crystals.

1.5 *IN VIVO* PRO-CALCIFIC MODELS

Animal model are useful systems in elucidating the complex molecular and cellular mechanisms underlying cardiovascular pathologies including CAVS in the native hemodynamic and biochemical environment. Besides understanding pathophysiologic factors and disease natural progression, the reliable tests of the effects exerted by various therapeutic agents are provided.

Some species such as swine can develop spontaneous vascular and valvular atherosclerotic lesions (Skold B.H. and Getty R., 1961) in contrast with others, such as rabbits and mice. In vivo studies of CAVS focused on animals, in which the pathologic process is elcited or accelerated by (i) exposure to known risk factors such as high-cholesterol, high-fat, or high-carbohydrate diets (Nievelstein-Post P. *et al.*, 1994; Rajamannan N.M. *et al.*, 2002; Drolet M.C. *et al.*, 2003; Cimini M. *et al.*, 2005; Zeng Z. *et al.*, 2007), (ii) knockout crucial genes such as apolipoprotein E, LDL receptor, or MGP (Luo G. *et al.*, 1997; Tanaka K. *et al.*, 2005; Weiss R.M. *et al.*, 2006; Aikawa E. *et al.*, 2007), (iii) or combination of both injuries (Drolet M.C. *et al.*, 2006).

Several studies concerning calcification of implanted bioprosthetic valves were developed. Circulatory *in vivo* models are most predictive of the success of a new valve designs or anti-calcification studies, however they are expensive and rate of calcification is slow.

Alternatively, an interesting approach was a model consisting in xenogenic implantations of porcine aortic valve into rat subdermal tissue. With this economical model, calcification occurs rapidly exhibiting histologic and chemical features that resemble those in failed clinical specimens (Levy R.J. *et al.*, 1983c; Schoen F.J. *et al.*, 1985).

1.6 *IN VITRO* PRO-CALCIFIC MODELS

In the attempt to clarify the mechanisms underlying cardiovascular tissue mineralization, in the last decade several *in vitro* models have been developed simulating metastatic calcification by using elevated levels (>2.0 mM) of either organic phosphate (Mathieu P. *et al.*, 2005) or Pi (Jono S. *et al.*, 2000; Steitz S.A. *et al.*, 2001; Giachelli C.M. *et al.*, 2005). In addition, attention was focused on inflammation involvement by treating cells with either bacterial endotoxin lipopolysaccharide (LPS) (Babu A.N. *et al.*, 2008) or inflammatory cytokines, such as TGF-β (Watson K.E. *et al.*, 1994; Jian B. *et al.*, 2003; Clark-Greuel J.N. *et al.*, 2007), TNF-α (Tintut Y. *et al.*, 2000), or IL-1β (Kaden J.J. *et al.*, 2003). Moreover, an intriguing approach that mimics *in vivo* conditions was the treatment of so called calcifying VSMC subset with conditioned medium from cultures of heterogenic macrophages stimulated with LPS (Tintut Y. *et al.*, 2002), likely containing pro-inflammatory cytokines, as confirmed by subsequent studies (Xu *et al.*, 2007; Wu L.N. *et al.*, 2009). Pro-calcific effects on cultured AVICs were also achieved by co-stimulations with high Pi concentrations plus inflammatory stimuli, such as TNF-α (Kaden J.J. *et al.*, 2005b) or LPS (Rattazzi M. *et al.*, 2008).

Finally, *in vitro* models were developed simulating either severe dystrophic calcification (Ortolani F. *et al.*, 2010) or metastatic one (Bonetti A. *et al.*, 2012), using elevated Pi alone and/or combined with LPS and pro-inflammatory mediators derived from allogenic cultures of LPS-stimulated macrophages.

2. AIMS OF THE THESIS

Calcific aortic valve stenosis (CAVS) takes place in the great field of ectopic soft tissue calcification representing the third cause of cardiovascular disease in the western world population. Although CAVS has been largely investigated in the last decades, the causes and mechanisms are still not clear. It is still debated whether the calcific processes start at the intracellular level or matrix level. Semilunar aortic valves are particularly prone to mineralization with surgical valve transplantation still representing the sole therapeutic approach to this pathology, to date. In the present work, CAVS was studied applying different experimental techniques on cultured aortic valve interstitial cells (AVICs).

In order to study the calcific process, the present thesis has been designed as follows:

1) elucidation of the specific role played by pro-calcific agents alone, or combined as revealed by histochemical, ultrastructural and spectrophotometrical investigations on cultured calcific AVICs using *in vitro* models mimicking both metastatic and dystrophic calcification. Results concerning metastatic calcification have been published (Bonetti A. *et al*., 2012) (Appendix);
2) identification of cell responses to pro-calcific and pro-inflammatory agents correlating with a distinct pro-calcific cell death;
3) ultrastructural characterization of actual CAVS on calcified aortic valves explanted from patients;
4) identification and localization of distinct chemical components characterizing CAVS-affected human aortic valves and cultured AVICs, using Raman microspectroscopic analysis;
5) study of the effects exerted by native- and aggregated low density lipoproteins (LDLs) on AVICs, using an in *in vitro* model mimicking pro-atherosclerotic environment, combined or not with pro-calcific one.

3. MATERIALS AND METHODS

3.1 ISOLATION AND CULTURE OF AVICs

Primary cultures of AVICs were obtained by enzymatic digestion of aortic valve leaflets isolated from hearts of slaughtered healthy bovines (age 1⁄4 15 months), as previously described by Rattazzi and colleagues (Rattazzi M. et al., 2008). Namely, excised aortic roots were placed in Dulbecco's Modified Eagle's Medium (DMEM, Sigma) plus 1% penicillin/streptomycin and 1 mg/ml amphotericin B kept cool in ice. Then, aortic valve leaflets were isolated, depleted of endothelial cells by gentle surface scraping, and minced into 2-3 mm^3 pieces, which were digested with type-I collagenase (125 U/ml; Sigma), elastase (8 U/ml; Sigma), and soybean trypsin inhibitor (0.375 mg/ml; Sigma) for 30 min at +37°C. After digestion, the pieces were transferred into tissue culture Petri dishes (Greiner) and cultured in DMEM plus 20% Foetal Bovine Serum (FBS; Gibco), 1% L-glutamine, and 1% penicillin/streptomycin for 7-10 days. Once drawn from the digested pieces, AVICs were cultured in complete DMEM as above until pre-confluent state and expanded up to 10 folds. Cells from passages 4 to 6 were used. Light microscopy monitoring was made using an Olympus IX70 inverted microscope.

3.2 SAMPLING OF HUMAN AORTIC VALVES

Native, tricuspid aortic valves were surgically explanted from patients (n = 4; mean age = 78.3 years) subjected to cardiac valve replacement at the Cardiothoracic Surgery Unit of the University-Hospital Enterprise of Udine. All aortic valves were affected by severe, non-rheumatic stenosis as diagnosed by the evaluation of pre-operative clinical and echocardiographic parameters (valve area < 1cm2; middle transvalvular gradient > 65mmHg). After explantation, aortic valves were transiently maintained in sterile physiological solution to allow (i) macroscopic examination, which revealed the presence of large calcific nodules protruding at cusp aortic surface, and (ii) excision of cusps, each of which was then subdivided into two emicusps such that one was destined to cooling and the other to electron microscopy processing. Emi-cusps were cooled by dipping into 2-methylbutane liquid kept cool in liquid nitrogen.

3.3 CONDITIONED MEDIUM FROM RAW264.7 MACROPHAGES

Murine RAW264.7 macrophages were plated on tissue culture flasks (Falcon) and cultured in DMEM supplemented with 10% FBS, 1% L-glutamine, and 1% penicillin/ streptomycin. At pre-confluence, RAW cells (passage 4) were stimulated with LPS (100 ng/ml; Sigma) for 1 h at +37°C, rinsed twice with DMEM plus 10% FBS, and additionally cultured in complete DMEM for 12 hs achieving macrophage degranulation. After culture medium collection and centrifugation, supernatant was 0.22-µm-filtered, added with 1% polymyxin B (BioChemika) to neutralize residual LPS, and stored at -20°C until use.

3.4 CONDITIONED MEDIUM FROM BOVINE FRESH MACROPHAGES

Fresh lympho/monocytes were collected by Ficoll® (1:2; GE Healthcare) density gradient centrifugation of peripheral blood from healthy bovines and then plated on tissue culture flasks and maintained in complete DMEM, supplemented with 10% FBS, 1% L-glutamine, and 1% penicillin/ streptomycin, overnight. After lymphocyte removing by rinsing with DMEM plus 10% FBS, monocytes were cultured in complete DMEM for 3 days to promote cell differentiation. These monocytes/macrophages were stimulated with LPS (100 ng/ml) for 1 h at +37°C, rinsed twice with DMEM plus 10% FBS, and additionally cultured in complete DMEM for 12 hs achieving macrophage degranulation. After medium collection and centrifugation, supernatant was 0.22-µm-filtered, added with 1% polymyxin B, and stored at -20°C until use.

3.5 LDL ISOLATION AND AGGREGATION

Human LDLs (1.019 to 1.063 g/mL) were obtained from pooled sera of normocholesterolemic volunteers and isolated by sequential ultracentrifugation. LDLs were dialyzed three times against 200 volumes of 150 mmol/L NaCl, 1 mmol/L EDTA, and 20 mmol/L Tris-HCl, pH 7.4, overnight and once against 150 mmol/L NaCl. LDL protein concentration was determined by the bicinchoninic acid (BCA) method and cholesterol concentration by a commercial kit (Pierce).

Aggregated LDLs (agLDLs) were prepared by vortexing in PBS at room temperature. agLDLs (precipitable fraction) were separated from the non-aggregated LDLs (non-precipitable fraction) and their percentage was calculated by measuring the fraction of protein recovered in the pellet obtained after centrifugation at 10 000 g for 10 minutes.

3.6 AVIC TREATMENTS

At pre-confluence, AVICs seeded on 35 mm culture plates (Greiner) were cultured in DMEM plus 10% FBS, 1% L-glutamine, and 1% penicillin/streptomycin (i) alone (control-cultures) or supplemented with: (ii) 20% (v/v) murine RAW264.7 macrophage conditioned medium (mCM-cultures); (iii) 20% (v/v) bovine macrophage conditioned medium (bCM-cultures); (iv) 100 ng/ml LPS (LPS-cultures); (v) 3.0 mM Pi (Pi-cultures); (vi) 3.0 mM Pi and 100 ng/ml LPS (Pi-LPS-cultures); (vii) 3.0 mM Pi plus 20% (v/v) bovine macrophage conditioned medium (Pi-bCM-cultures); (viii) 3.0 mM Pi, plus 100 ng/ml LPS, plus 20% (v/v) murine RAW264.7 macrophage conditioned medium (Pi-LPS-mCM-cultures); (ix) 3.0 mM Pi, plus 100 ng/ml LPS, (Pi-LPS-bCM-cultures). In each cell culture supplemented with 3.0 mM Pi, the final concentration of Pi was 3 mM. The treatments were performed for 3, 6, and 9 days, renewing the culture medium every 3 days.

Concerning dystrophic-like conditions, pre-confluent AVICs were cultured using 4 sets of culture media each consisting in (i) DMEM plus 10% FBS, plus 1% L-glutamine, plus 1% penicillin/streptomycin (control cultures) or added with different volumes of 0.5 M sodium dihydrogen phosphate solution, thereby obtaining final Pi concentrations of (ii) 0.8 mM Pi (0.8-Pi-cultures), (iii) 1.3 mM Pi (1.3-Pi-cultures), and (iv) 2.0 mM Pi (2.0-Pi-cultures). Moreover, 4 sets were prepared of 0.8-, 1.3-, and 2.0-Pi-cultures with further addition of 100 ng/mL LPS and 20% (v/v) bovine macrophage conditioned medium (0.8-Pi-LPS-CM-cultures, 1.3-Pi-LPS-CM-cultures, and 2.0-Pi-LPS-CM-cultures, respectively). The treatments were performed for 3, 9, 15, 21, 25, and 28 days, renewing the culture medium every three days.

To ascertain whether apoptosis is involved in AVIC pro-calcific degenerative processes, a parallel set of 2.0-Pi-LPS-CM-cultures was treated with a pre-validated concentration of 20 μM pancaspase inhibitor Boc-D-FMK (Sigma-Aldrich) for 28 days renewing culture medium every three days.

In order to assess the effects of low density lipoproteins (LDLs) in pro-calcific degenerative process, AVICs were cultured with 50 μM of native LDLs (nLDL-clutures) or aggregated LDLs (agLDL-cultures) alone or combined with pro-inflammatory stimuli Pi (2.0 or 3.0), LPS and bCM (2.0-Pi-LPS-bCM-nLDL-, 2.0-Pi-LPS-bCM-agLDL-, 3.0-Pi-LPS-bCM-nLDL- and 3.0-Pi-LPS-bCM-nLDL-cultures, respectively). The treatments were performed for 3, 6, and 9 days in metastatic-like conditions, and for 3, 9, 15, and 21 days in dystrophic-like conditions culture medium was renewed every three days.

3.7 LIGHT MICROSCOPY

3.7.1 ALIZARIN RED S CALCIUM STAINING

After culture medium removal, AVIC monolayers were rinsed with phosphate buffer and fixed with neutral-buffered 5% formalin for 10 min. After further rinsing, cultured cells were treated with an aqueous solution of 2% alizarin red S (Carlo Erba Reagents), pH 4.2, for 5 min, rinsed again to remove exceeding staining solution, and covered with distilled water. As negative control, parallel AVIC monolayers were treated with a decalcifying solution containing 0.05 M sodium acetate buffer and 0.05 M magnesium chloride, pH 4.8, for 1 h at room temperature prior to alizarin red staining. Observations and photographic records were made using an Olympus IX70 inverted microscope.

3.7.2 VON KOSSA SILVER STAINING

8-μm-thick cryosections were serially cut and mounted on poly-L-lysine pre-coated glass slides, air-dried, fixed with phosphate-buffered 5% formaldehyde, and subjected to von Kossa silver reaction for the evidentiation of calcium binding sites. Namely, the cryosections were treated with 1% silver nitrate aqueous solution, with exposure to direct sunlight, for 15 min, rinsed with distilled water, dipped into a 5% sodium thiosulfate reducing solution for 5 min, and rinsed again. von-Kossa-reacted cryosections were weakly counterstained with hematoxylin and eosin, dehydrated in graded ethanols, cleared with xylene, and mounted with Eukitt® mounting medium. Observations and photographic recording were made using Zeiss AxioImager and Leica DM 2500 photomicroscopes, the latter being a part of an InVia Raman microscope (Renishaw).

3.8 TRANSMISSION ELECTRON MICROSCOPY

3.8.1 PRE-EMBEDDING CUPROLINIC BLUE REACTION

After culture medium removal, AVIC monolayers were washed twice with 0.1 M phosphate buffer and subjected to pre-embedding reaction with 0.05% phthalocyanin Cuprolinic Blue (CuB; Electron Microscopy Sciences) dissolved in 25 mM sodium acetate buffer, containing 0.05 M magnesium chloride and 2.5% glutaraldehyde, pH 4.8, overnight, at room temperature. After further washing, AVICs were post-fixed with phosphate-buffered 2% osmium tetraoxide (OsO_4) (Agar Scientific) for 1 h at +4°C, washed again, dehydrated in graded ethanols, and embedded in Epon 812 resin.

Similarly, samples obtained from explanted human valve leaflets were minced into 1-2

mm^3 pieces and subjected to pre-embedding CuB reaction for polyanion evidentiation. Namely, samples were treated with 0.05% CuB dissolved in acid (pH 4.8) 25 mM sodium acetate buffer, added with 0.05 M magnesium chloride and 2.5% glutaraldehyde, for 3 days at room temperature under continuous agitation using an Agar rotator. After washing with acid buffer as above, samples were post-fixed with phosphate-buffered 2% OsO_4, dehydrated in graded ethanols, and embedded in Epon/Araldite.

Ultrathin sections were collected on formvar-coated 2x1-mm-slot copper grids and contrasted with uranyl acetate and lead citrate. Ultrastructural examination and photographic recordings were made using a Philips CM12 STEM transmission electron microscope.

3.8.2 POST-EMBEDDING VON KOSSA SILVER REACTION

Semithin sections of CuB-reacted AVIC monolayers were mounted on glass slides, covered with a drop of 1% silver nitrate aqueous solution, and placed on an +80°C warm plate for 15 min under direct sunlight. After washing with distilled water and drying, semithin sections were covered with a drop of 5% sodium thiosulfate reducing solution and warmed at 80°C for 5 min. After further washing and drying, reacted semithin sections were re-embedded by gluing onto the slides top-less conic Beem capsules (Agar Scientific), so encircling each semithin section, which were filled with Epon-Araldite fluid. After resin polymerization, re-embedded sections were detached from slides and subjected to standard electron microscopy processing.

3.8.3 ULTRASTRUCTURAL LOCALIZATION OF ACID PHOSPHATASE ACTIVITY

Acid phosphatase activity was revealed according to Gomori's method. Briefly, AVIC monolayers were fixed with 3% paraformaldehyde for 30 min, washed with sodium acetate buffer, pH 5.0, and incubated with 0.05 M sodium acetate buffer, containing 0.01 M beta-glycerophosphate and 0.004 M lead nitrate, pH 5.0, for 45 min at 37°C. As negative control, incubating solutions lacking in beta-glycerophosphate were used. After washing with cooled sodium acetate buffer to block enzymatic activity, AVIC monolayers were (i) fixed with 2% glutaraldehyde for 15 min, (ii) post-fixed with 2% osmium tetraoxide for 1 h at 4°C, (iii) dehydrated in graded ethanols, and (iv) embedded in Epon 812 resin. Thin sections were collected, contrasted, observed, and recorded as above.

3.9 RAMAN MICROSPECTROSCOPY

Concerning AVIC cultures, cells were seeded on CaF_2 slides and treated with DMEM plus 10% FBS, 1% L-glutamine, and 1% penicillin/streptomycin (i) alone (control cultures) or (ii) combined with 3.0 mM Pi, LPS, and bCM (Pi-LPS-bCM-cultures). The treatments were performed for 9 days, renewing the culture medium every three days. At day 9, slides were dried and stored at room temperature until microspectroscopic examination.

Concerning histological samples, longitudinal, 15-μm-thick cryosections were mounted on CaF_2 slides, air-dried, and stored at -20°C until microspectroscopic examination.

Raman maps were collected in back scattering geometry, with the above InVia Raman microscope (Renishaw) equipped with a 785 nm diode laser (Renishaw) delivering 90 mW of laser power at the sample. The CaF_2 slide supporting the tissue samples was mounted on a ProScan II motorized stage under the microscope. A Leica 50× microscope objective (N.A. 0.85) focused the laser on the sample. A 1200 l/mm grating yielded a spectral resolution of 4 cm^{-1}. A thermoelectrically cooled charge coupled device (CCD) camera was used for detection. The spectrograph was calibrated using the lines of a Ne lamp. Mapping was achieved collecting spectra with steps of 12 μm, with 10 s exposure time for each spectrum, for a total of 5708 spectra, each consisting of 1203 data points. Spectra were obtained in the 600-1800 cm^{-1} region using the synchro mode of the instrument software WiRETM 3.2 (Renishaw), in which the grating is continuously moved to obtain Raman spectra of extended spectral regions. Data preprocessing (i.e. baseline subtraction, vector normalization) and analysis were made using the hyperSpec package (Beleites C. and Sergo V., 2013) for R (R Core Team, 2013).

3.10 CALCIUM QUANTIFICATION

After culture medium recovering, cells were scraped from each culture plate, centrifuged, and treated with an aqueous lysis buffer containing 50 mM TRIS-HCl, 150 mM NaCl, 5 mM EDTA, and 1% Triton X-100, pH 7.4, for 1 h at +4°C. After centrifugation at 2000 g for 5 min, part of supernatant (500 ml) was recovered for ALP activity/protein assay and remaining lysed samples were rejoined to their original culture media and transferred into distinct Teflon vessels. Samples were added with 1 ml of 65% supra-pure grade nitric acid (Merck) and 500 ml of 30% supra-pure hydrogen peroxide (Merck), irradiated using the High Performance Microwave Digestion Unit mls 1200 mega (Milestone; 2 min at 250 W, 2 min at 0 W, 5 min at 300 W, 5 min at 450 W, and 6 min at 650 W), and diluted with ultra-pure water until

obtaining 100 ml of total solution. Calcium quantification was assessed using the O-cresolphtalein complexone method (Chema Diagnostica) and absorbance was read at 575 nm with a Cary 50 Bio spectrophotometer (Varian). Each estimation came from 10 readings of five distinct experiments.

3.11 ALKALINE PHOSPHATASE ACTIVITY ASSAY

Supernatants (500 μL) obtained from micro-centrifugation of lysed samples were used to determine ALP activity and protein content. ALP activity was assessed using a kinetic method based on measurement of 4-nitrophenol production (Chema Diagnostica) reading the absorbance at 405 nm at +37°C within 5 min of enzymatic activity using the Cary 50 Bio spectrophotometer. Values corresponding to the trend line gradients coming from reading of five distinct experiments were normalized on the basis of protein content spectrophotometrically estimated by Bradford method using a commercial kit (Pierce).

3.12 IMMUNOCYTOCHEMISTRY

Control-cultures, 1.3-Pi-LPS-CM-cultures, and 2.0-Pi-LPS-CM-cultures were obtained by seeding AVICs on 24x24 mm cover slips placed at the bottom of 35 mm culture plates and culturing them for 3, 9, 15, and 21 days. After culture medium removal, AVIC monolayers were incubated with (i) 0.1% Triton X-100 solution for 10 min, (ii) 3% hydrogen peroxide solution for 5 min, (iii) 3% normal serum solution for 30 min, (iv) 1:600 anti-MAP1LC3-A polyclonal antibody (Merck Millipore) or 1:25 anti-annexin-V polyclonal antibody (Santa Cruz Biotechno-logy) for 2 hs at room temperature in a humidified chamber. Primary antibodies were replaced by normal serum, as negative control. After washing, AVIC monolayers were incubated with peroxidase-conjugated secondary antibodies (Jackson ImmunoResearch) for 30 min at room temperature. Peroxidase activity was revealed by incubation with diaminobenzidine tetrahydrochloride (DAB) and hydrogen peroxide (Vector Laboratories) for 3-6 min. After rinsing with distilled water to block enzymatic activity, AVIC monolayers were weakly counterstained with hematoxylin. Cover slips were then mounted on glass slides using an aqueous mounting medium, observed, and recorded using a Zeiss AxioImager photomicroscope. Percentages of immunopositive cells were estimated using the ImageJ software.

3.13 POLYACRYLAMIDE GEL ELECTROPHORESIS

Sodium dodecyl sulphate polyacrylamide gel electrophoresis (SDS-PAGE) (Laemmli U.K., 1970) was performed using 10x10x0,1 cm gels. The acrylamide concentration in the separating gel was chosen according to the molecular size of the proteins to be separated, varying from 8 to 13% acrylamide and maintaining a acrylamide: N,N'-methylenebisacrylamide ratio of 37.5:1 (w/w), which were solubilized in 0.25

M glycine, 0.025 M Tris/HCl, pH 8.8 and 0.1% (w/v) SDS. The stacking gel was prepared using 4% (v/v) acrylamide in stacking buffer (0.125 M Tris/HCl, pH 6.8, 0.1% (w/v) SDS). 0.1% ammonium persulfate and 0.0015% (v/v) TEMED were added to start gel polymerization.

Electrophoresis was performed with a limiting voltage of 250 V and a current of 15 mA until the dye front reached at the bottom of the gel. The electrophoresis system was cooled using an internal fan to circulate water. Protein molecular weights were estimated by running standard proteins of known molecular weight in separated lanes (Bio-Rad).

ACRYLAMIDE 17% RUNNING BUFFER (one gel)	
40%Acrylamide/bis-Acrylamide solution (Sigma)	2,55 ml
dH_2O	3,45 ml
10% SDS	60 µl
10% Ammonium persulfate	60 µl
Temed (N,N,N',N'–Tetramethylethylenediamine)	9 µl

ACRYLAMIDE 4% STACKING BUFFER (one gel)	
40%Acrylamide/bis-Acrylamide solution (Sigma)	0,2 ml
dH_2O	1,8 ml
10% SDS	20 µl
10% Ammonium persulfate	20 µl
Temed (N,N,N',N'–Tetramethylethylenediamine)	5 µl

ELECTROPHORESIS BUFFER	
Glycine	250 mM
Tris/HCl pH 8.8	25 mM
SDS	0.1% p/v

3.14 WESTERN BLOT ANALYSIS

After cell lysis and protein quantification, supernatants from 3-, 9-, 15-, and 21-day-long control-cultures, 1.3-Pi-LPS-CM-cultures, and 2.0-Pi-LPS-CM-cultures were separated by SDS-PAGE and transferred to 0.2 μm pore size nitrocellulose membranes (Schleicher & Schuell, Bio Science) using a semi-dry blotting apparatus (TE 22 transfer unit from Amersham Biosciences). The transfer was performed at 2.5 mA/cm^2 for 1 h in the transfer buffer. After staining with Ponceau S solution (ATX Ponceau S red staining solution Fluka), to verify transfer efficiency, the nitrocellulose sheets were saturated with 3% (w/v) non-fat dry milk in PBS buffer plus 0.1% Tween 20 for 1 h at room temperature and then incubated with 1:500 anti-caspase-3 (cleaved form) polyclonal antibody (Cell Signaling Technology) overnight at 4°C.

Blots were then rinsed three times with PBS buffer plus 0.1% Tween 20 and incubated for 1 h 30' with peroxidase-conjugated anti-rabbit-IgG (1:15,000) secondary antibody (Sigma-Aldrich) at room temperature. The membranes were washed again three times in PBS buffer plus 0.1% Tween 20 and developed with chemiluminescence assay SuperSignal® West Dura (Thermo Scientific) with maximum exposure time of 4 hs. For accurate estimation of protein molecular weight, Precision Plus Protein Standard (Bio-Rad) was used. AVICs treated with apoptosis inducer etoposide (50 μM) for 18 hs were used as positive control.

High-resolution images of the films were acquired using the scanner SF Launcher and processed using the program ImageQuant TL.

TRANSFER BLOT BUFFER (pH 8.1 - 8.3)	
Tris/HCl	25 mM
Glycin	192 mM
Methanol	20% v/v

3.15 THIN LAYER CHROMATOGRAPHY

Lipid extraction was done according to the method of Bligh and Dyer with less modifications (Bligh E.G. and Dyer W.J., 1959).

According to estimated protein concentration, one aliquot of the cell suspension was extracted with methanol/dichloromethane (2:1 v/v). After solvent removal under an N_2 stream, the lipid extract was re-dissolved in dichloromethane. Samples were partitioned by thin layer chromatography (TLC), which was performed on silica G-24 plates. Three different concentrations of standards (a mixture of cholesterol, triglycerides, and cholesterol palmitate) were applied to each plate. The chromatographic developing solution was heptane/diethyl ether/acetic acid (74:21:4 v/v/v). The plate was completely dried and spots were stained with ethanol solution of phosphomolybdic acid (5% p/v) and sulphuric acid (5% v/v). The spots corresponding to free cholesterol (FC), triglycerides (TG), and cholesteryl esters (CE) were quantified by densitometry ImageQuant TL (BioRad) against the standard curve of cholesterol, triglycerides, and cholesterol palmitate, respectively, by using a computing densitometer (Spectra MAX 250, Molecular Devices).

3.16 STATISTICAL ANALYSIS

Concerning spectrophotometrical evaluations of calcium levels and ALP activity in metastatic-like conditions, statistical differences among control and the different AVIC treatments were assessed using the ANOVA test, with Bonferroni correction for multiple comparisons. Values with $p < 0.0001$ were considered to be statistically significant. Values were reported as mean ± standard deviation.

Concerning other experiments, after using the Levene's test for analysis of variances, statistical significance was assessed using either the Student’s t-test for data showing homogeneity of variances or the Mann-Whitney test for data showing no homogeneity of variances. For both tests, values with $p < 0.017$ were considered to be statistically significant. Values were reported as mean ± standard deviation.

4. RESULTS

4.1 METASTATIC CALCIFICATION

The effects of pro-calcific agents in promoting cell-dependent mineralization were evaluated chemically and morphologically.

The primary cultures of bovine aortic valve interstitial cells (AVICs) (Fig. 4.1) were stimulated with elevated (2.6 mM) inorganic phosphate (Pi-cultures) alone or combined with the pro-inflammatory stimuli represented by lipopolysaccharide (LPS-cultures) and conditioned media from cultures of either xeno- or allogeneic macrophages stimulated with LPS (mCM-cultures and bCM-cultures, respectively).

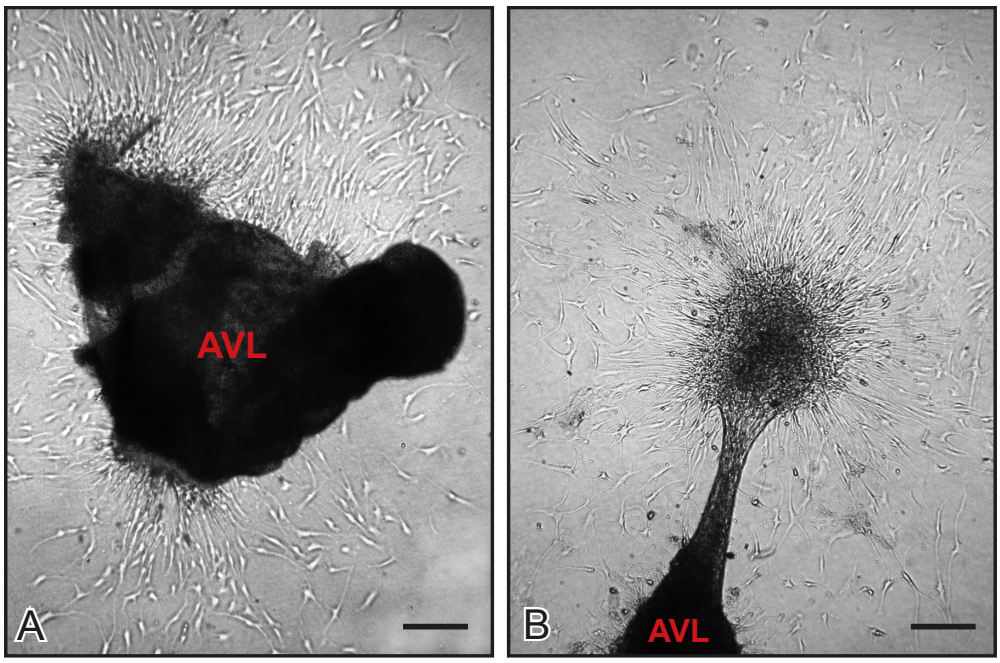

Figure 4.1. Bovine aortic valve interstitial cells (AVICs) spreading out from an aortic-valve-leaflet-derived sample (AVL) on culture Petri dish. Tissues were treated with a cocktail of enzymes in order to digest collagen and elastin, so allowing spontaneous migration of AVICs from the valve *interstitium* and their adhesion to a Petri dish bottom. Scale bar: 50 µm.

Morphologically, the mineralization rates induced by the applied treatments were readily recognizable under the inverted microscope on the basis of size and number of formed calcific nodules. The presence of calcific nodules was apparent only in Pi-cultures as well as the most marked calcification occurring in Pi-LPS-bCM-cultures (Fig. 4.2).

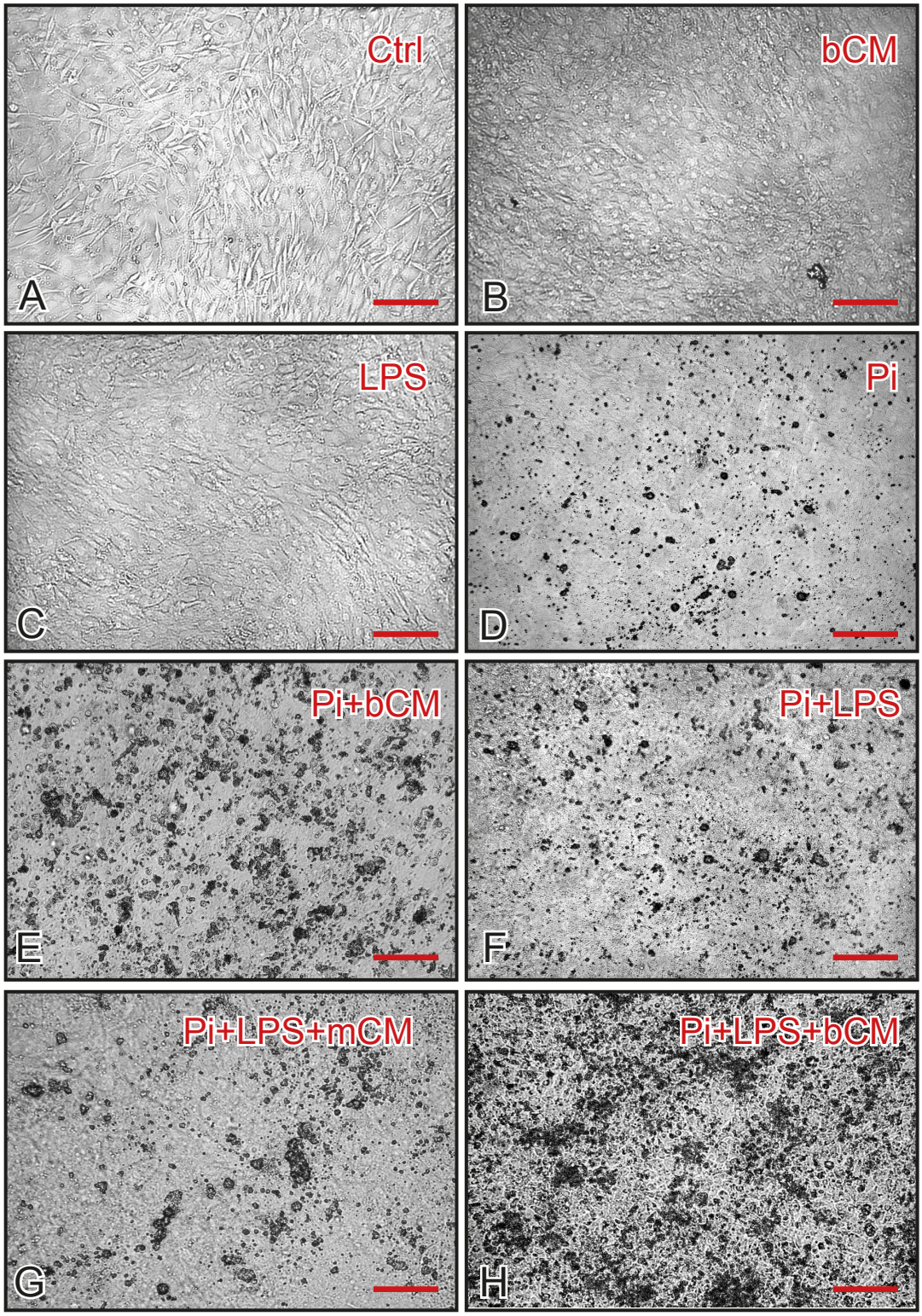

Figure 4.2. Inverted microscope micrographs of unstained AVIC monolayers. A-C: Absence of calcium precipitation in control cultures (A) and cultures treated with bCM alone (B) and LPS alone (C). D-H: Presence of calcium precipitation in monolayer cultures treated with elevated Pi alone (D), or combined with bCM (E), LPS (F), LPS and mCM (G), LPS and bCM (H). Scale bar: 50 µm.

Spectrophotometric estimations of calcium amounts contained in digested samples from AVIC cultures after 9-day-long treatments are reported in Figure 4.3. Consistently with

morphological data, the mean values resulted for samples from control cultures, LPS-cultures, mCM-cultures, and bCM-cultures were similar to each other and were collectively lower than those in samples from the cultures supplemented with elevated Pi. Also, these higher values were similar to each other, except for the Pi-LPS-bCM-cultures, which contained even more mineral.

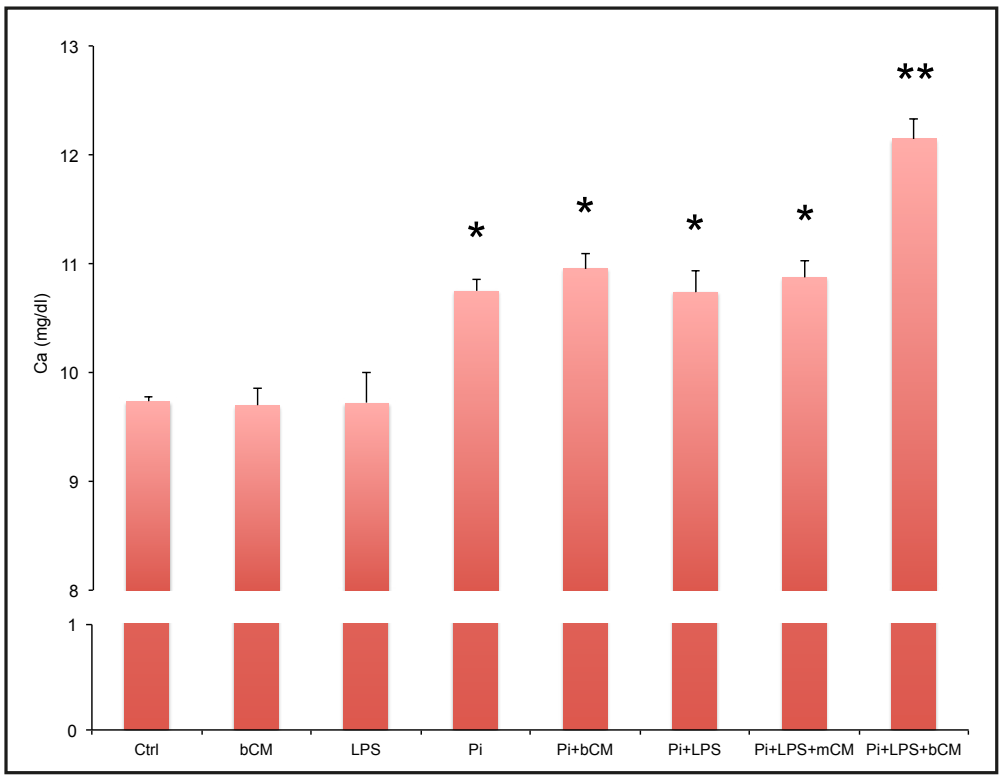

Figure 4.3. Spectrophotometric estimation of calcium amounts for 9-day-long-cultured bovine AVICs with no treatment (Ctrl) or after different stimuli alone or combined, that is, lipopolysaccharide (LPS), murine conditioned medium (mCM), bovine conditioned medium (bCM), and elevated inorganic phosphate (Pi). The values are reported as mean + SD. The values concerning the treated cultures are significantly different (*) from those of control cultures, and those concerning Pi-LPS-bCM-cultures are significantly different (**) from all others; $p < 0.0001$.

Since alkaline phosphatase (ALP) is considered to play a key role in calcification, its enzymatic activity was investigated spectrophotometrically.

The values of ALP activity in the 9-day-long AVIC cultures are reported in Figure 4.4. Compared to control-cultures, no change resulted for bCM-cultures, a weak increase for LPS-cultures, and further weak increase for Pi-cultures. Marked increases resulted for the remaining cultures, being the highest values measured for Pi-LPS-cultures and linearly lower those for Pi-LPS-mCM-cultures and Pi-LPS-bCM-cultures, respectively.

Comparing changes in calcium amounts with those in ALP activity, the values of calcium content were markedly increased for all five cultures containing elevated Pi, whereas higher ALP activity only resulted for the three cultures containing Pi and LPS.

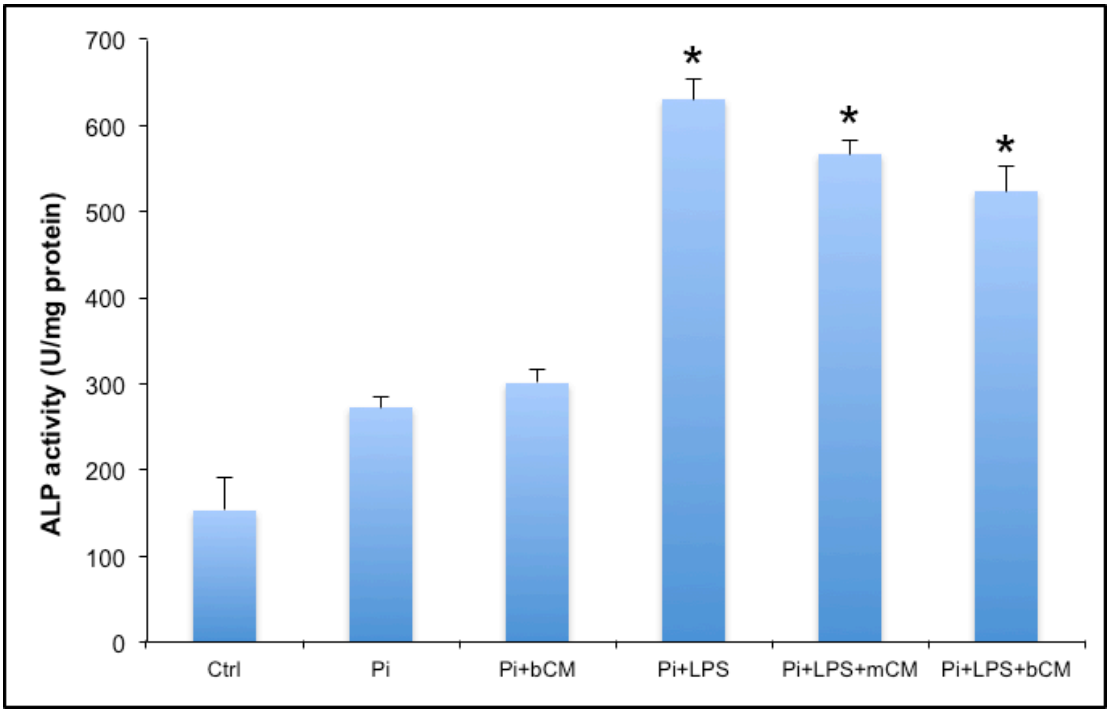

Figure 4.4. Spectrophotometric estimation of ALP activity for 9-day-long-cultured bovine AVICs with no treatment or after the different stimulations as in Fig. 4.2. The values are reported as mean + SD. The values concerning the treated cultures are significantly different (*) from those of control cultures.

Supplementary estimations of this parameter were supplied for all these cultures verifying the time course spanning 3-9 days (Fig. 4.5). In detail, enzymatic activity reached a maximum at 6-day-long incubation for Pi- and Pi-bCM-cultures compared with control-cultures, with a subsequent drop at 9 days. Conversely, enzymatic activity underwent a roughly linear increase up to day 9 for Pi-LPS-cultures, Pi-LPS-mCM-cultures, and Pi-LPS-bCM-cultures.

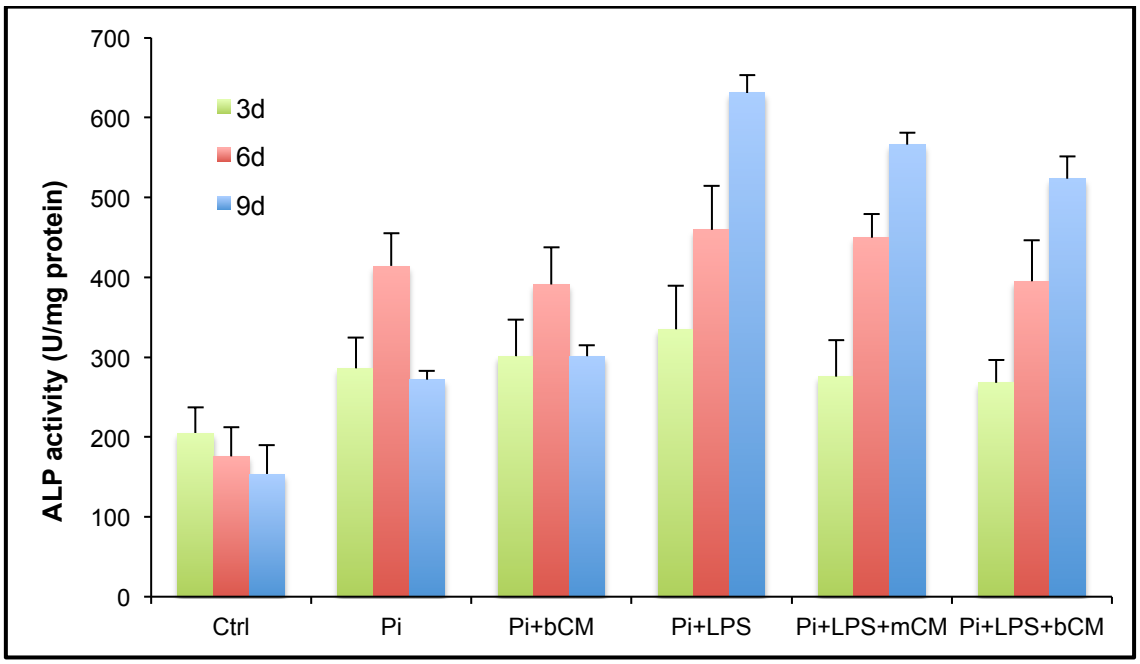

Figure 4.5. Spectrophotometric estimation of ALP activity time course spanning 3-9 days for bovine AVIC cultures after all treatments involving the presence of elevated Pi. The values are reported as mean + SD.

Severity of cell alterations was assessed at the ultrastructural level on samples subjected to pre-embedding histochemical reactions with acidic mixtures of glutaraldehyde and copper phthalocyanin Cuprolinic Blue (CuB). Since this mixture allows sample decalcification with simultaneous retention of acidic-lipid-containing material resulting from the degradation of cytoplasmic organules and membranes, this method permits to detect features not recognizable by using standard technique and previously showed AVICs to undergo a peculiar degeneration for *in vivo* experimental models of accelerated calcification (Ortolani F. *et al.*, 2002a; Ortolani F. *et al.*, 2002b; Ortolani F. *et al.*, 2003; Ortolani F. *et al.*, 2007) as well as *in vitro* models simulating dystrophic calcification (Ortolani F. *et al.*, 2010). In addition, semithin sections of CuB-reacted samples were subjected to post-embedding von Kossa silver reactions based on metallic silver precipitation, widely used on histological sections to detect calcific sites.

On thin sections, control AVICs showed well-preserved intracytoplasmic organules and *lamellipodia* with associated anchoring stress fibres (Fig. 4.6 A, B) and occasional autophagic vacuoles.

As in controls, no apparent damage was appreciable for AVICs from bCM-cultures, and LPS-cultures (not shown). In all cultures containing elevated Pi, a distinct cell degenerative process was observed which included (i) degeneration of cytoplasmic organelles, (ii) release of CuB-reactive material, and (iii) margination of this material and its outward budding. In more detail, initial AVIC alteration consisted in the abnormal dilation of rough endoplasmic reticulum, swelling of mitochondria with progressive dissolution of their cristae, cytoplasm vesiculation, mounting loss of all membrane-bound organules and nuclear envelope, with the appearance of a lot of phthalocyanin-reactive lipid droplets, autophagocytic vacuoles/ lysosomes, and myelin figures (Figs. 4.6 D, G, H and 4.7 A, C, D).

Cytoplasm vacuolization also depended on depletion of swollen mitochondria and was complicated by their joining/fusion into greater vacuoles. During these processes, previously accumulated lipid-like amorphous material seemed to be poured into the major vacuoles, transforming them into lipid inclusions subsequent to fragmentation and dissolution of lining membranes (Figs. 4.6 H and 4.7 C).

The resulting lipid inclusions underwent a progressive increase in reactivity to pre-embedding reaction with CuB (Figs. 4.6 G and 4.7 A) and were selective sites for metallic silver particle deposition, after additional post-embedding von Kossa silver staining (Fig. 4.7 B). An incipient increase in cytoplasm electrondensity seemed to result from the melting of these reactive lipid droplets with associated overgrowing deposition of amorphous

phthalocyanin-positive material (PPM), which entrapped organule-derived remnants and clusters of degrading ribosomes (Figs. 4.6 H and 4.7 D).

More advanced degenerative features were (i) shortening/disappearance of lamellipodia, with cells acquiring smoothed profiles and irregularly roundish shapes, (ii) complete colliquation of organelles, and (iii) their replacement by increasing PPM. Centrifugal PPM spreading in waves followed, resulting in the appearance of multilaminated, CuB-reactive PPLs outlining the body of cell remnants and being 100-200 nm thick (Figs. 4.6 E and 4.7 E). Initial pseudo-orthogonal precipitation of needle-like HA crystals appeared mostly to occur at level of PPLs, revealing their marked involvement as HA nucleators (Fig. 4.7 F). The same role was exhibited by initial PPL- derived bodies, detaching from cell surface and, to a lesser extent, intracellular transitional forms of PPM into PPLs. Co-localization between HA crystal nucleation and metallic silver precipitation was also evident after von Kossa reactions (Fig. 4.7 G).

These degenerative steps appeared to end with the dead PPL-lined cells undergoing fragmentation into heterogeneously sized bubbling bodies (Fig. 4.8 A, B), with overlapping sporulation-like PPL budding and pinching off. The resulting rounded concentrically laminated *calcospherulae* were mostly characterized by a punctate dense core and diameters ranging between 130 nm and 1 μm (Fig. 4.8 A-E). Also these PPL-derivatives were strongly reactive to silver von Kossa reactions (Fig. 4.8 F).

It is worth noting that stimulation with elevated Pi alone was sufficient to give rise to all degenerative patterns including the genesis of *calcospherulae* (Fig. 4.6 D). Of interest, *calcospherulae* phagocytated by still viable AVICs were encountered (Fig. 4.6 C).

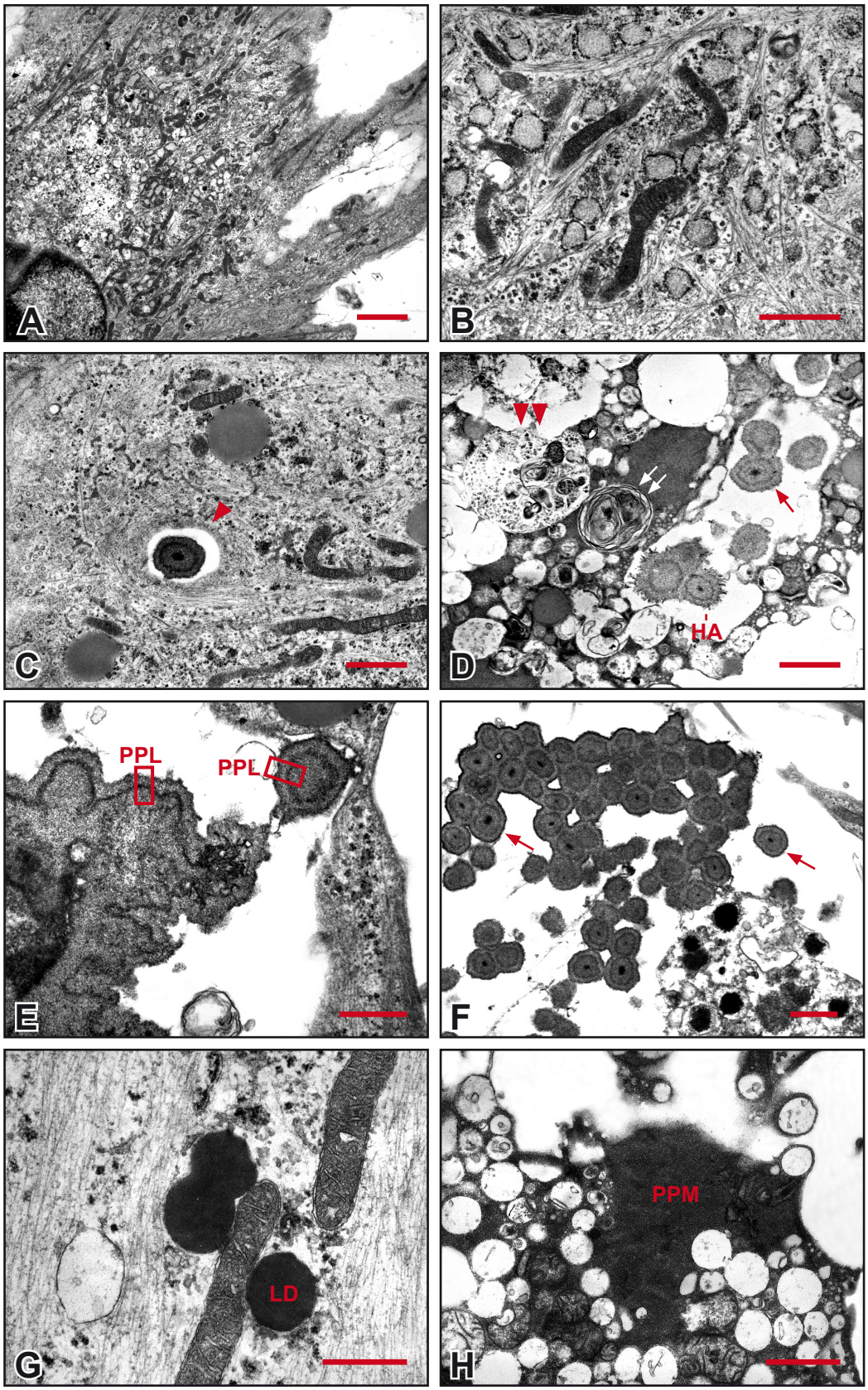

Figure 4.6. A and B: Thin sections showing normal features in AVICs from control-cultures. C-F: Altered features in AVICs from cultures added with 2.6 mM Pi: autophagocytic vacuole (double arrowhead in D); myelin figure (double white arrow in D); CuB-reactive layers (frame-PPL in E); *calcospherulae* (black arrows in D and F); phagocyted *calcospherula* (arrowhead in C); hydroxyapatite crystals (HA in D). G: CuB-reactive lipid droplets (LD) in an AVIC cultured with PiþLPS. H: Vesiculation and CuB-reactive material (PPM) in an AVIC cultured with Pi+LPS+mCM. Scale bars: 2,5 µm (A); 1 µm (B-D); 0.5 µm (E); 1 µm (F); 0.5 µm (G); 1 µm (H).

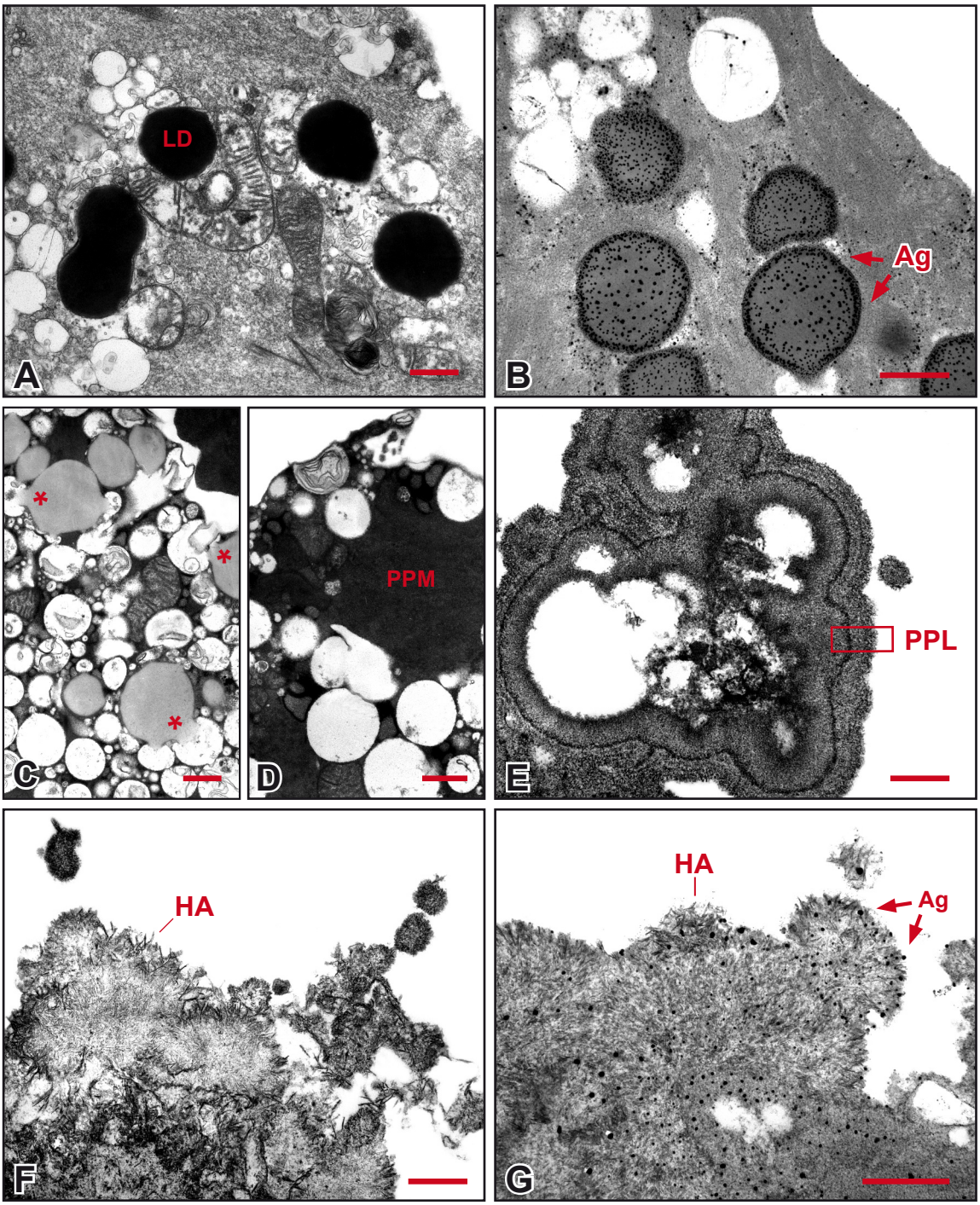

Figure 4.6. A-G: Thin sections showing altered features in AVICs from cultures added with 2.6 mM-Pi+LPS+bCM: CuB-reactive lipid droplets (LD in A); selective precipitation of metallic silver (Ag with arrows in B and G); vesiculation (in C and D) with inter-vesicle lipid material pouring (asterisks in C); CuB-reactive material (PPM in D); CuB-reactive multi-laminated layer (frame-PPL in E); hydroxyapatite crystals (HA in F and G). Scale bars: 0,5 µm.

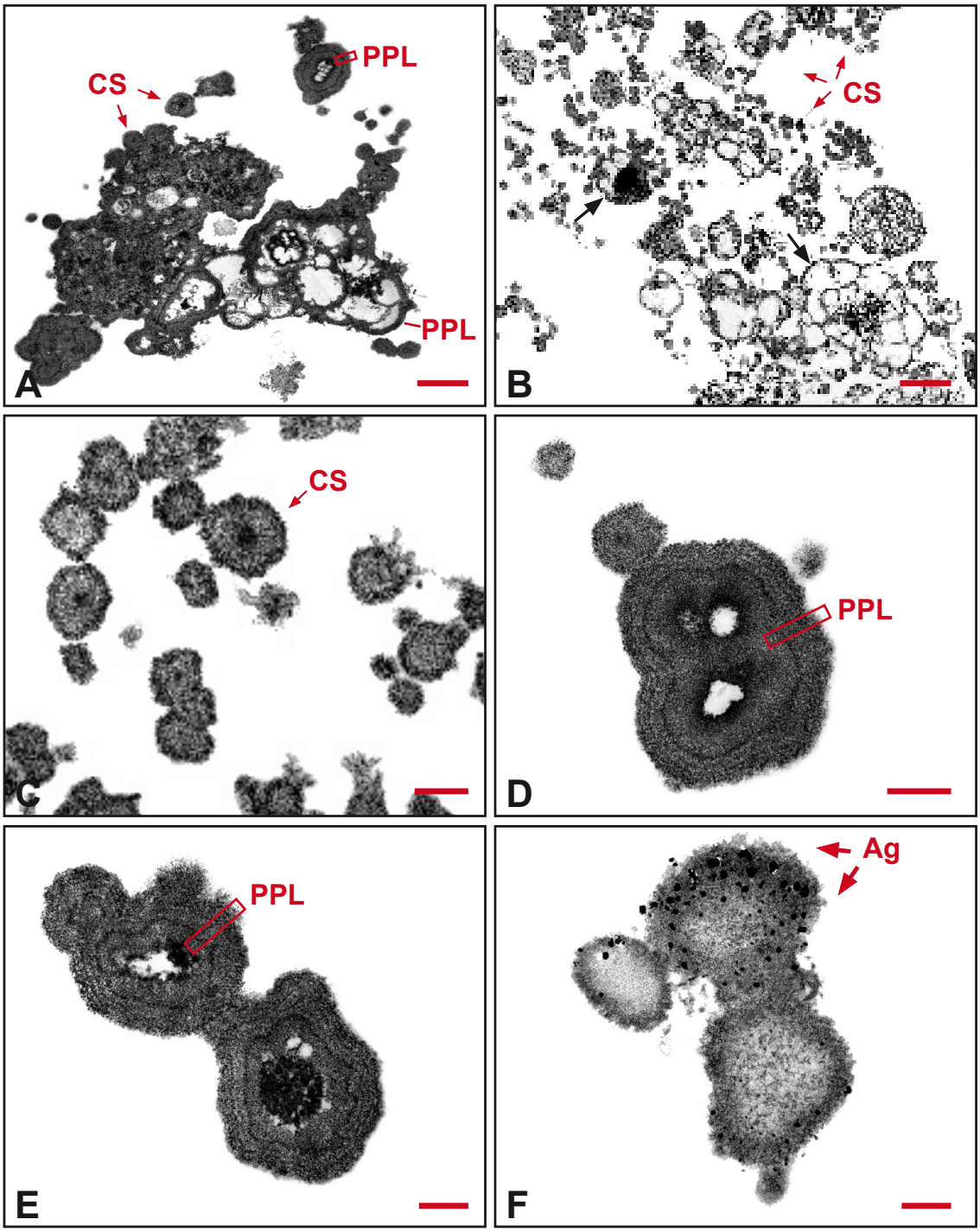

Fig. 4.8. A-F: Thin sections showing cell-derived products subsequent to fragmentation of AVICs from cultures added with 2.6 mM Pi+LPS+bCM: concentrically laminated *calcospherulae* (CS with arrows in A-C); bubbling bodies (single arrows in B); and minor fragments showing CuB-reactive layers (frame-PPL in A, D, and E); selective precipitation of metallic silver (Ag with arrows in F). Scale bars: 2,5 µm (A, B); 0,5 µm (C-F).

Raman microspectroscopy was used to provide further chemical informations about pro-calcific degeneration of cultured AVICs after stimulations with the most effective mineralizing stumulation (Pi-LPS-bCM-cultures). Cultured AVICs were seeded on fluorite glasses because this material expresses a single Raman vibrational band not interferring with the signal generated by the sample.

Raman imaging showed HA to be mainly distributed at cell edges, with additional localization in the cytoplasm under form of HA foci (Fig. 4.9 A). HA major distribution was consistent with that of needle-shaped apatite crystals along AVIC surfaces displayed by electron microscopy (Fig. 4.6 F, G), as well as peripheral PPL location (4.9 B).

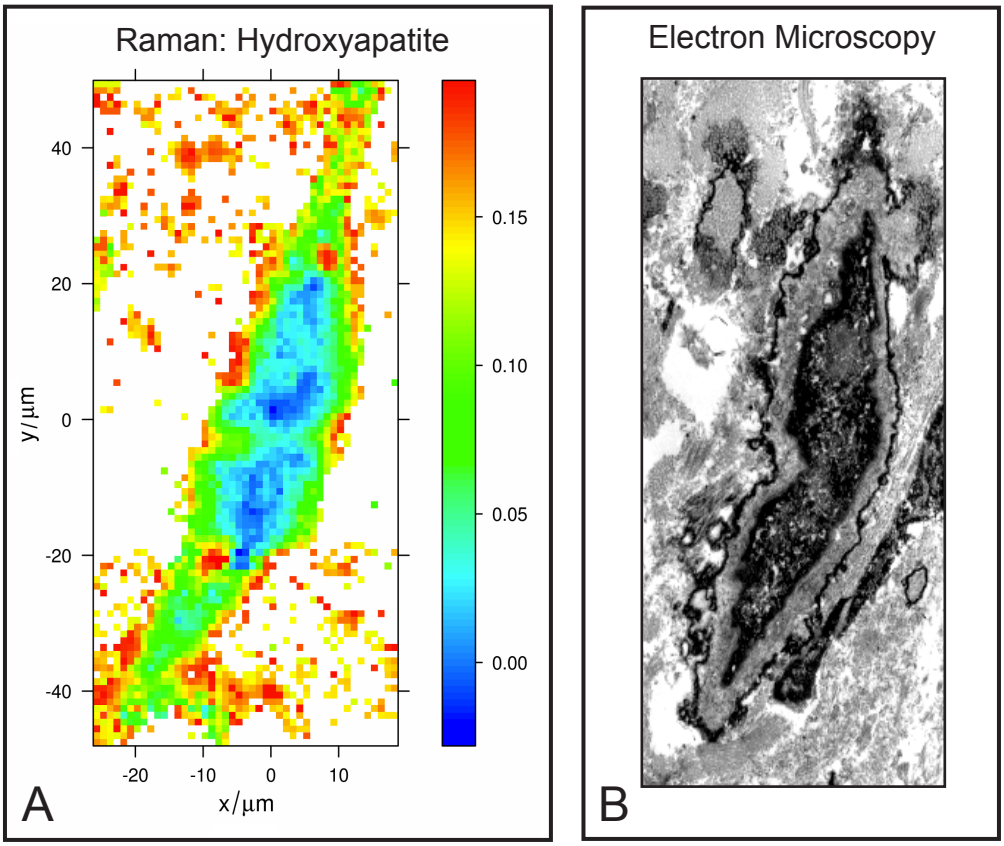

Figure 4.9. **A**: Raman pattern of hydroxyapatite (HA) distribution in the AVIC as in 4.9 B. **B**: Ultrastructural picture showing PPL-lined degenerating AVIC from xenogenic subcutis implant (from human stenotic valve) after pre-embedding Cuprolinic blue reaction. Magnification: 5,000 x.

On the basis of this topographical similarity, the same AVIC shown in Figure 4.9 A was analysed to achieve chemical detection of organic components (Fig. 4.10 B) and compared with control (Fig. 4.10 A). In detail, the Raman spectrum showed the characteristic peaks for HA at 959 cm^{-1} and for nucleic acids at 1570 cm^{-1}. The presence of proteins was inferred by both the phenylalanine peak at 1060 cm^{-1}, and the amide-I protein peak at 1500-1700 cm^{-1}. The peak at 1128 cm^{-1} indicated the presence of saturated fatty acid chains, whereas the peak at 1650 superimposed to that of amide I, revealed the presence of unsaturated lipids. Finally, the deformation peak of acetylic and methylenic groups at almost 1450 cm^{-1} indicated the presence of both types of lipids.

Maxima of HA distribution were displayed by cell-derived extracellular particles. Additionally, clusters of HA, lipids and proteins were detected at peripheral cell cytoplasm

(Fig. 4.10 B). Most HA appeared to be arranged under form of a stratified outer cluster (green coloured pixels) and an adjacent inner cluster (light blue coloured pixels), in which lipids were present too. Characteristically, the multiple stratified cluster pattern depicted the cells as target-like structures, with a core cluster corresponding to nuclear proteins and nucleic acids, and a series of outer clusters corresponding in the order to cytoplasm organules and layers containing various quantities of HA, lipids and proteins. On examining relative peaks on Raman spectra, it is noteworthy that the amount of proteins decreases gradually, moving toward AVIC periphery, with parallel increasing of HA amounts. Concerning lipid components, peak analysis revealed a very weak lowering of lipids within the more and more external layers, indicating a persistent presence of lipids together with HA.

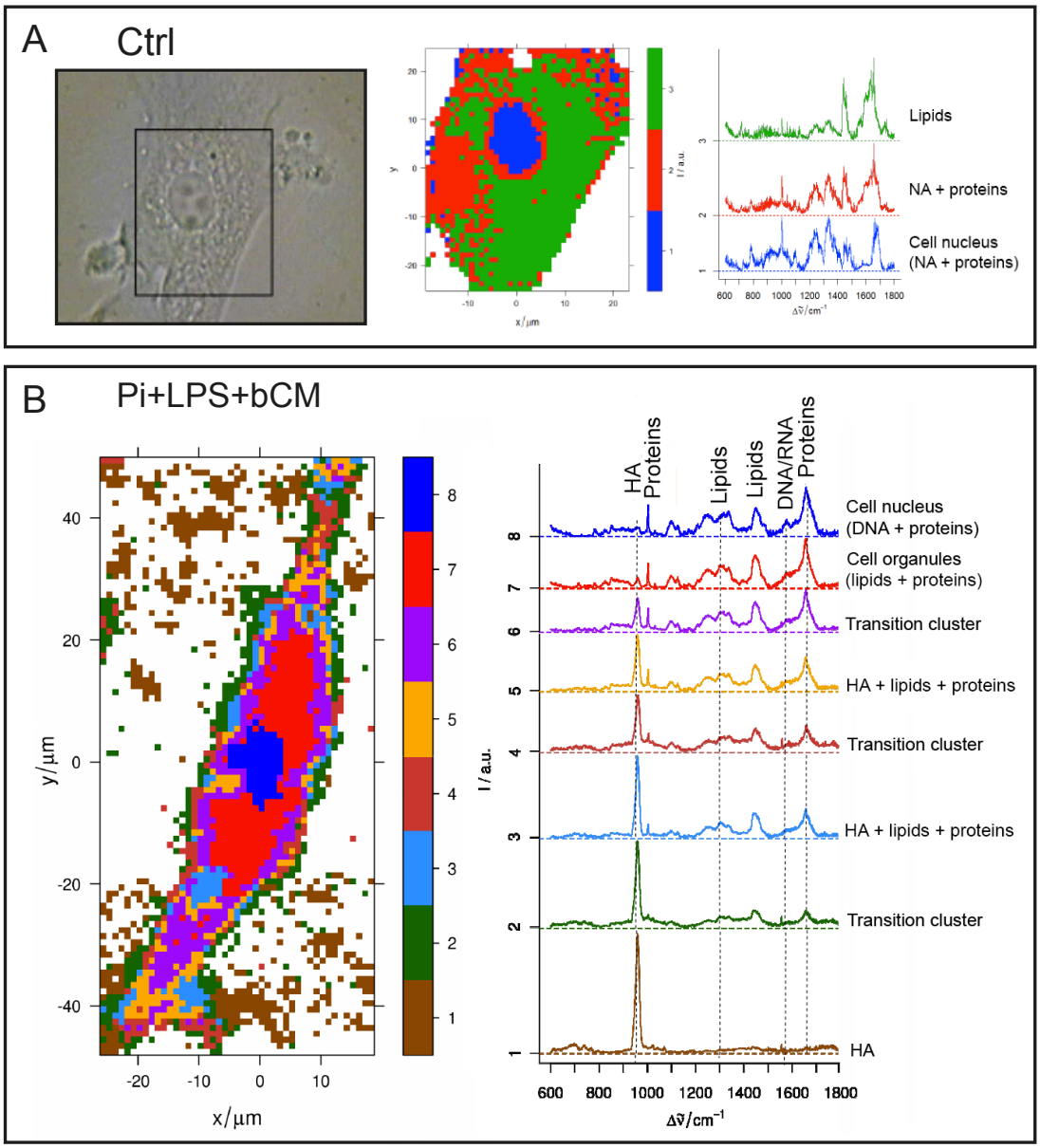

Figure 4.10. A: Map of Raman spectra (centre) corresponding to multivariate hard clustering analysis on an area (square) of a cultured not treated AVIC (left) and relative spectra (right). B: Cluster map (left) and relative spectra (right) as in A on a cultured AVIC after 9-day-stimulation with Pi + LPS + bCM.

4.2 DYSTROPHIC CALCIFICATION

Once characterized the mineralizing process regarding metastatic calcification, the investigation was extended to *in vitro* models simulating dystrophic calcification.

Since Pi was previously found to represent a critical pro-calcific agent, AVICs derived from bovine valve leaflets were stimulated with different concentrations of Pi spanning the entire normophosphatemic range (0.8 mM, 1.3 mM and 2.0 mM) alone or combined with LPS and bCM.

Presence of calcific nodules was histochemically assessed using alizarin red (Fig. 4.11).

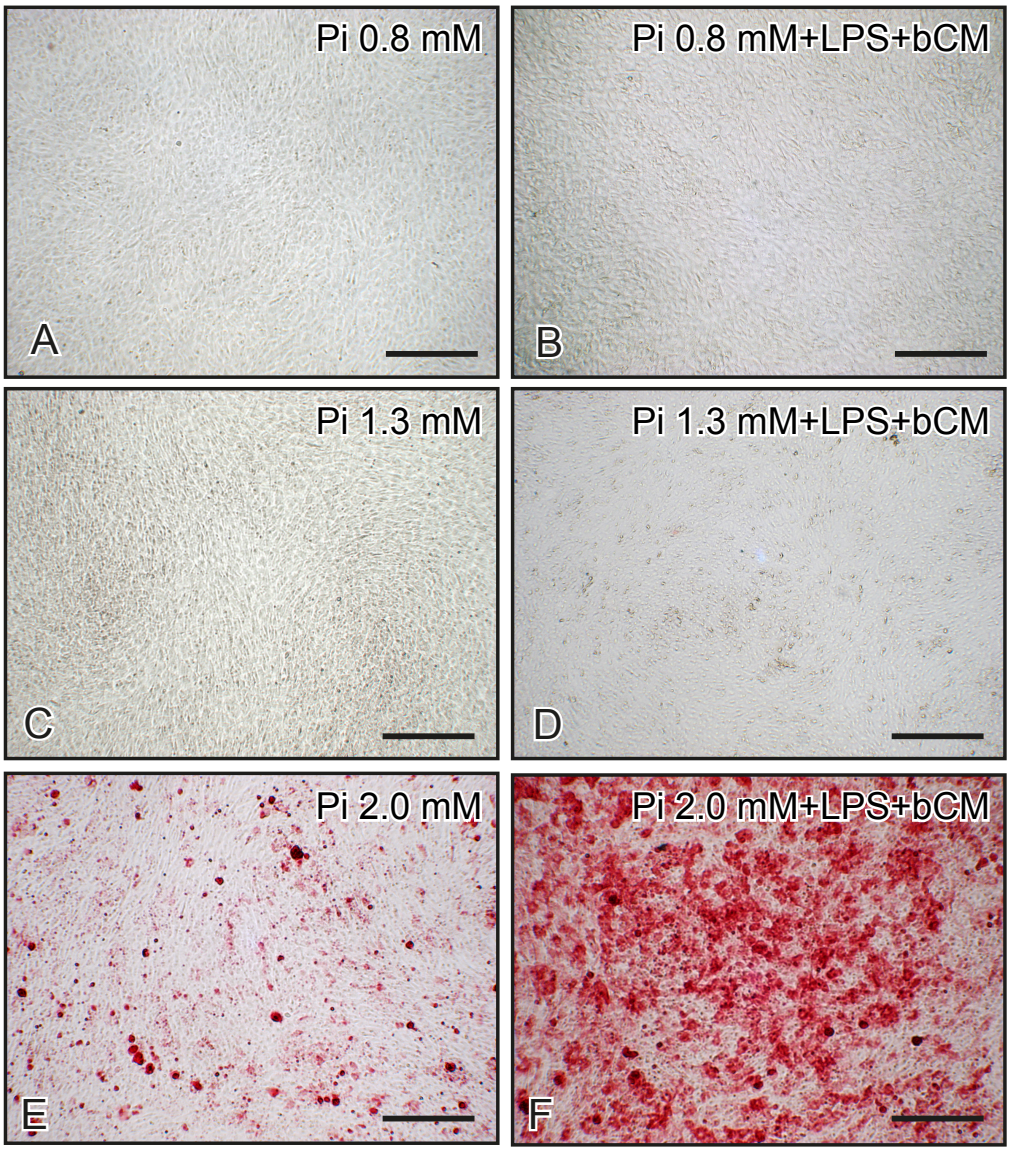

Figure 4.11. Inverted microscope micrographs of alizarin red stained AVIC monolayers at 21 days of stimulation. A-D: Absence of calcium precipitation in 0.8-Pi-cultures (A), 0.8-Pi-LPS-bCM-cultures (B), 1.3-Pi-cultures (C), and 1.3-Pi-LPS-bCM-cultures (D). E and F: Presence of calcium precipitation in 2.0-Pi-cultures (E), and 2.0-Pi-LPS-bCM-cultures (F). Scale bars: 250 μm.

Under inverted microscope, no alizarin red stained calcific nodules appeared for controls, 0.8- Pi-cultures, and 1.3-Pi-cultures as well as 0.8-Pi-LPS-bCM-cultures and 1.3-Pi-LPS-bCM-cultures, whereas nodule formation and increase occurred for 2.0-Pi-cultures, being the calcific process exacerbated for 2.0-Pi-LPS-bCM-cultures.

As for metastatic calcification, spectrophotometrical analyses were performed to gain a quantitative evaluation of calcium amounts and ALP activity in the different AVIC cultures (Fig. 4.12). Both parameters resulted to be correlated with Pi concentrations and incubation times, being mineralization enhanced by the additional stimuli used.

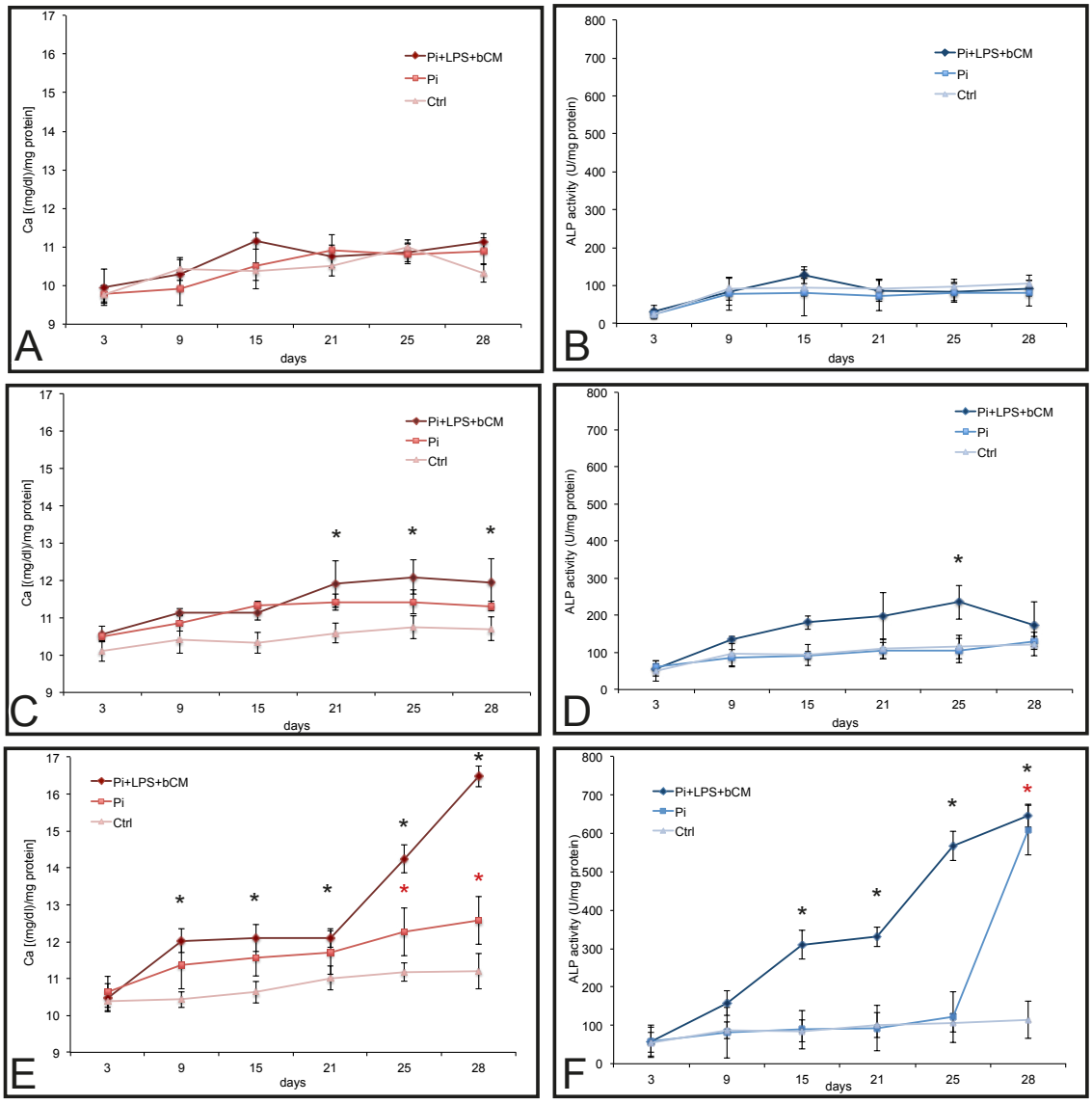

Figure 4.12. Spectrophotometrical estimations of calcium amounts (left column) and ALP activity (right column) for AVICs cultured with Pi at 0.8 mM (A, B), 1,3 mM (C, D) and 2.0 mM (E, F), alone or combined with pro-inflammatory stimuli (LPS+bCM). The values are reported as mean + SD. The values concerning the Pi-LPS-bCM-cultures significantly different from those of control cultures are indicated with black asterisk; the values concerning the Pi-cultures significantly different from those of control cultures are indicated with red asterisk; $p < 0.01$.

As in control cultures (Pi = 0.7mM), in 0.8-Pi-cultures and 0.8-Pi-LPS-bCM-cultures there was neither significant time-dependent changes nor stimulation-dependent ones (Fig. 4.12 A, B).

Compared to control, 1.3-Pi-cultures and 1.3-Pi-LPS-bCM-cultures showed significantly higher Ca^{2+} amounts, which also moderately increased in the time course for 1.3-Pi-LPS-bCM-cultures (Fig. 4.12 C). ALP activity resulted to be higher for only 1.3-Pi-LPS-bCM-cultures whereas 1.3-Pi-cultures did not differed from control ones (Fig. 4.12 D). In addition, this increase in enzymatic activity stopped at 25 day with subsequent decrease as previously assessed for metastatic calcification.

Compared to control, 2.0-Pi-cultures and 2.0-Pi-LPS-bCM-cultures showed similar trends as those for 1.3-Pi-cultures and 1.3-Pi-LPS-bCM-cultures until day 21, although exhibiting higher values (Fig. 4.12 E, F). Namely, at longer incubation times distinct exceptions consisted in (i) drastic increasing in both Ca^{2+} and ALP activity for 2.0-Pi-LPS-bCM-cultures, and (ii) striking increasing in ALP activity for 2.0-Pi-cultures starting from day 25.

Ultrastructurally, in 2.0-Pi-cultures and, at greater extent, 2.0-Pi-LPS-bCM-cultures, severity of cell alterations was found to increase with a time-dependent pattern, according to a lipid-release-associated cell degenerative process which was superimposable to that previously described for cultured AVICs (Ortolani F. *et al.*, 2010). Briefly, initial AVIC degenerative features consisted in (i) a widespread swelling of mitochondria and other organelles and parallel dissolution of their membranes with appearance of lipid droplets undergoing progressive acidification, so acquiring reactivity for the pre-embedding CuB reaction (Fig. 4.13 A), as well as calcium binding capacity, as revealed by post-embedding von Kossa silver staining (Fig. 4.13 B), and (ii) progressive disappearance of these droplets and organelles concurrently with progressive intracytoplasmic release and accumulation of amorphous lipid material showing analogous positivity for this phthalocyanin (PPM) and silver. More advanced degenerative features consisted in centrifugal PPM spreading and segregating at cell surface in form of phthalocyanin positive layers (PPLs) (Fig. 4.13 C), maintaining strong positivity for metallic silver precipitation (Fig. 4.13 D) as well as marked capacity of nucleating HA crystals, being directly exposed to the extracellular Pi-enriched milieu (Fig. 4.13 E). Further feature shared with metastatic calcification was the appearance of final degeneration products consisting in a population of variously sized PPL-lined irregular particles and pinching off of roundish PPL-lined *calcospherulae*, with superimposed affinity to metallic silver deposition, and associated HA nucleation (Fig. 4.13 F-H).

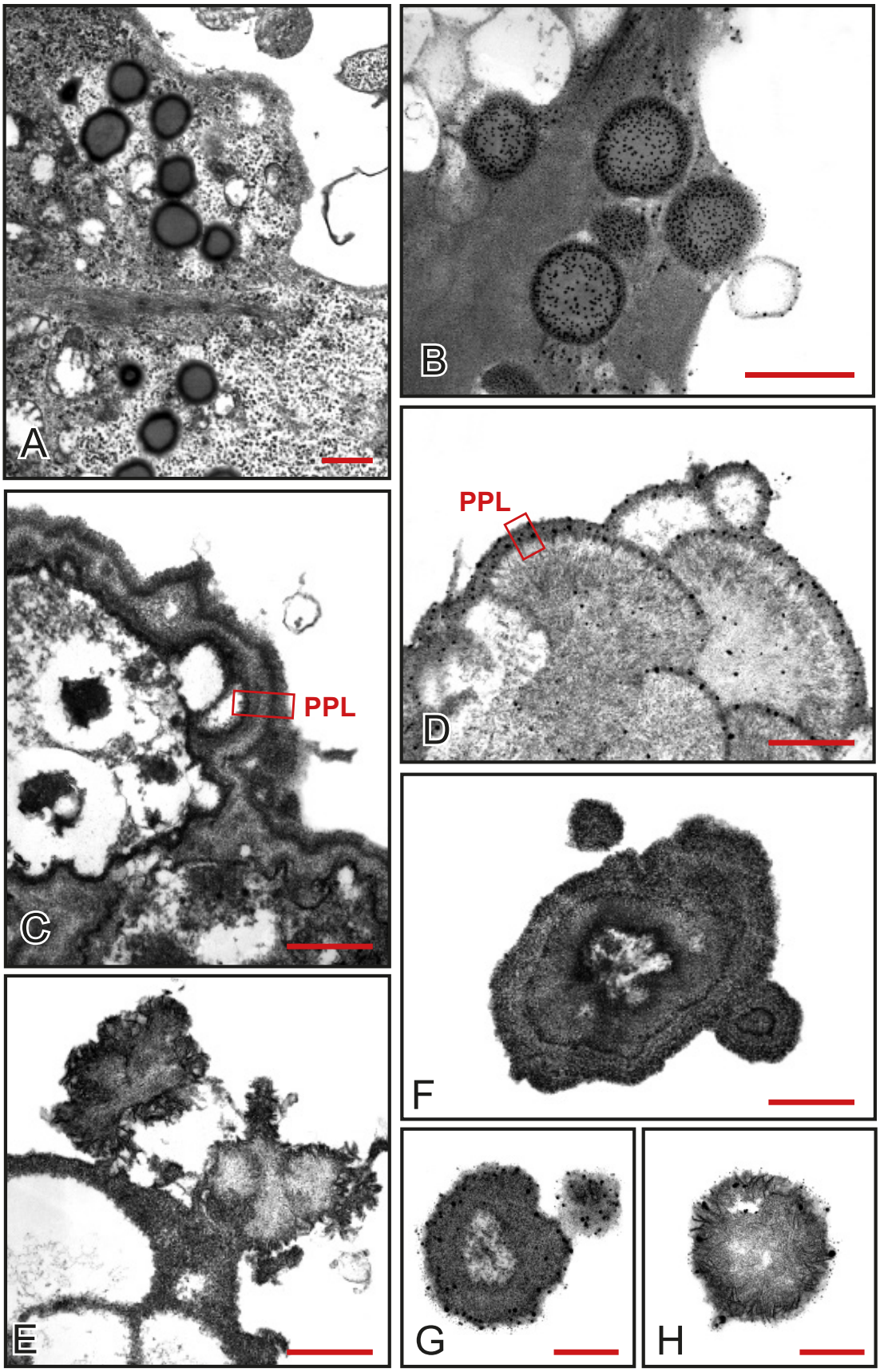

Figure 4.13. 2.0-Pi-LPS-bCM-cultures at different days of stimulation. Cytoplasm enriched in lipid droplets at day 9 (A and B). PPM peripheral exudation forming phthalocyanin-positive layer (PPL) at days 21-28 (C, D). CDPs and CDP-derived paracrystalline *calcospherulae* at day 28 (E-H). Silver staining of calcium binding sites within lipid droplets (B), plasmamembranes (D), and *calcospherulae* (G, H). Scale bars: 0,5 µm (A-E); 0,25 µm (G, H).

Control AVICs exhibited well-preserved organelles with co-existent numbers of autophagic vacuoles (Figs. 4.14 A, B). Compared to controls, AVICs from 0.8-Pi-cultures and 1.3-Pi-cultures showed mild time-dependent changes, whereas those from 0.8-Pi-LPS-bCM-cultures and 1.3-Pi-LPS-bCM-cultures (Figs. 4.14 B, C) exhibited shared patterns of more marked changes. Namely, earlier mild modifications were apparently decreased distribution of autophagic vacuoles. Subsequent changes consisted in on going organule alterations and increasing hypertrophy of rough endoplasmic reticulum (RER), so lining discrete cytoplasm regions occupied by more or less degraded organules (Figs. 4.14 C, D). Further RER overgrowth resulted in multiplication of cytoplasm compartments concurrently with a reduction of their size, up to envelope single mitochondria or their remnants (Figs. 4.14 D, F; 4.15 A, C).

In addition, Gomori's ultracytochemical reactions revealed acid phosphatase activity to be present within RER lumen, at RER membrane, and even at level of the degrading mitochondria enveloped by this abnormally grown organule (Figs. 4.15 B, D), in contrast with control-cultures in which very low enzyme activity was exhibited by RER (not shown). Since the samples derived from all AVIC cultures were subjected to pre-embedding reaction CuB, enhanced electrondensity was exhibited by nuclear chromatin, lysosomes, and autophagic vacuoles, as expected. However, it is noteworthy that additional positivity to this phthalocyanin was occasionally encountered for 1.3-Pi-LPS-bCM-cultures, which was exhibited by cell degradation products similar to those characterizing the early degenerative features exhibited by AVICs from both 2.0-Pi-cultures and 2.0-Pi-LPS-bCM-cultures, i.e. lipid droplets and intracytoplasmic electrondense material (PPM), as described above.

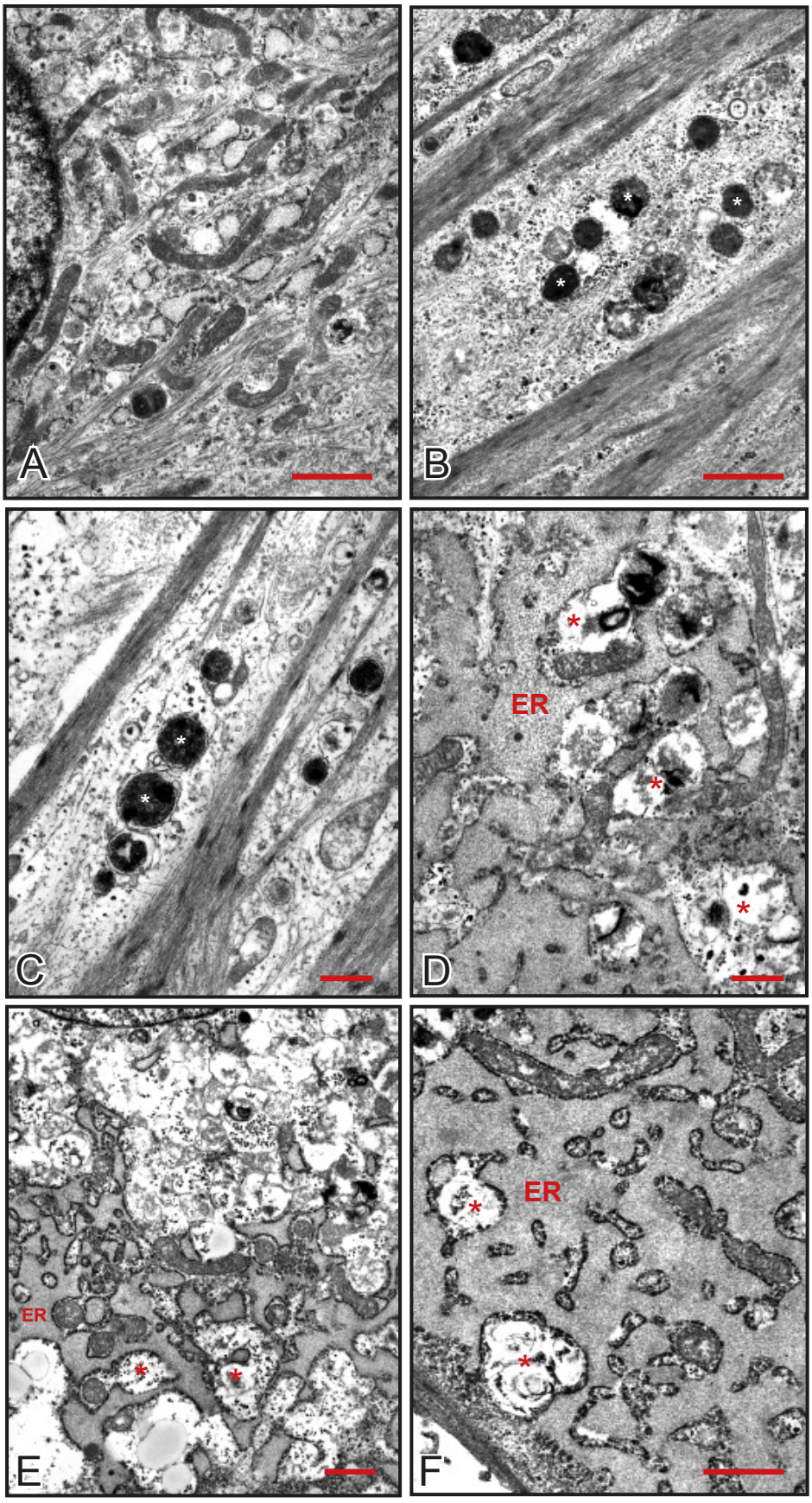

Figure 4.14. Thin sections showing features in AVICs from control-cultures (A and B), with autophagosomes (B; white asterisks); and from 1.3-Pi-LPS-bCM-cultures (C and D) with autophagosomes (C) and abnormal enlargement of rough endoplasmic reticulum (ER) enveloping degraded organule-containing compartments (D-F, red asterisks). Scale bars: 1 µm (A,B); 0,5 µm (C, D); 0,5 µm (E, F).

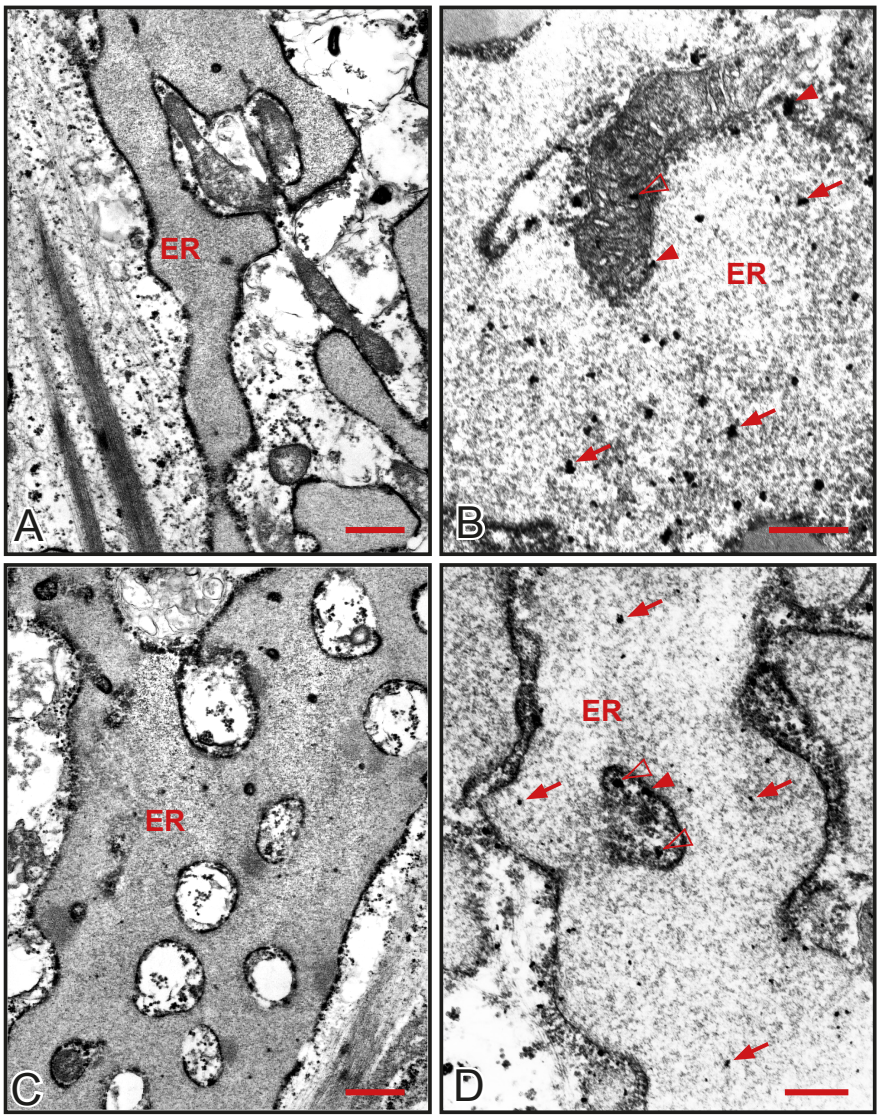

Figure 4.15. Electron micrographs of 1.3 mM-Pi-LPS-bCM cultured AVICs. Increasing cytoplasm compartmentalization by enlarging endoplasmic reticulum (ER). Positivity to acid phosphatase activity indicated by lead-containing black particles, at level of (i) ER lumen (B, D: arrows), (ii) ER-mitochondria contact sites (solid arrowheads) and (iii) enveloped degrading organules or organule residues (B, D: empty arrowheads). Scale bars: 0,5 µm (A); 0,25 µm (B); 0,5 µm (C); 0,25 µm (D).

To explore whether the described AVIC responses to the addition of Pi and the other stimuli correlate with macroautophagocytosis, additional immunocytochemical detection of marker MAP1LC3A was applied to control-cultures, 1.3-Pi-LPS-bCM-cultures, and 2.0-Pi-LPS-bCM-cultures and summarized in Figure 4.16 G. The achieved data were consistent with those obtained with electron microscopy (Figs. 4.14 and 4.15) since marked reactivity after 3-day-long incubation and its drastic decrease within 9 days of treatment, being still negligible after longer times, resulted for control-cultures (Fig. 4.16 A, B) and 1.3-Pi-LPS-bCM-cultures (Fig. 4.16 C, D). In contrast, there was minor positivity, besides its time-related decrease, for 2.0-Pi-LPS-bCM-cultures (Fig. 4.16 E, F).

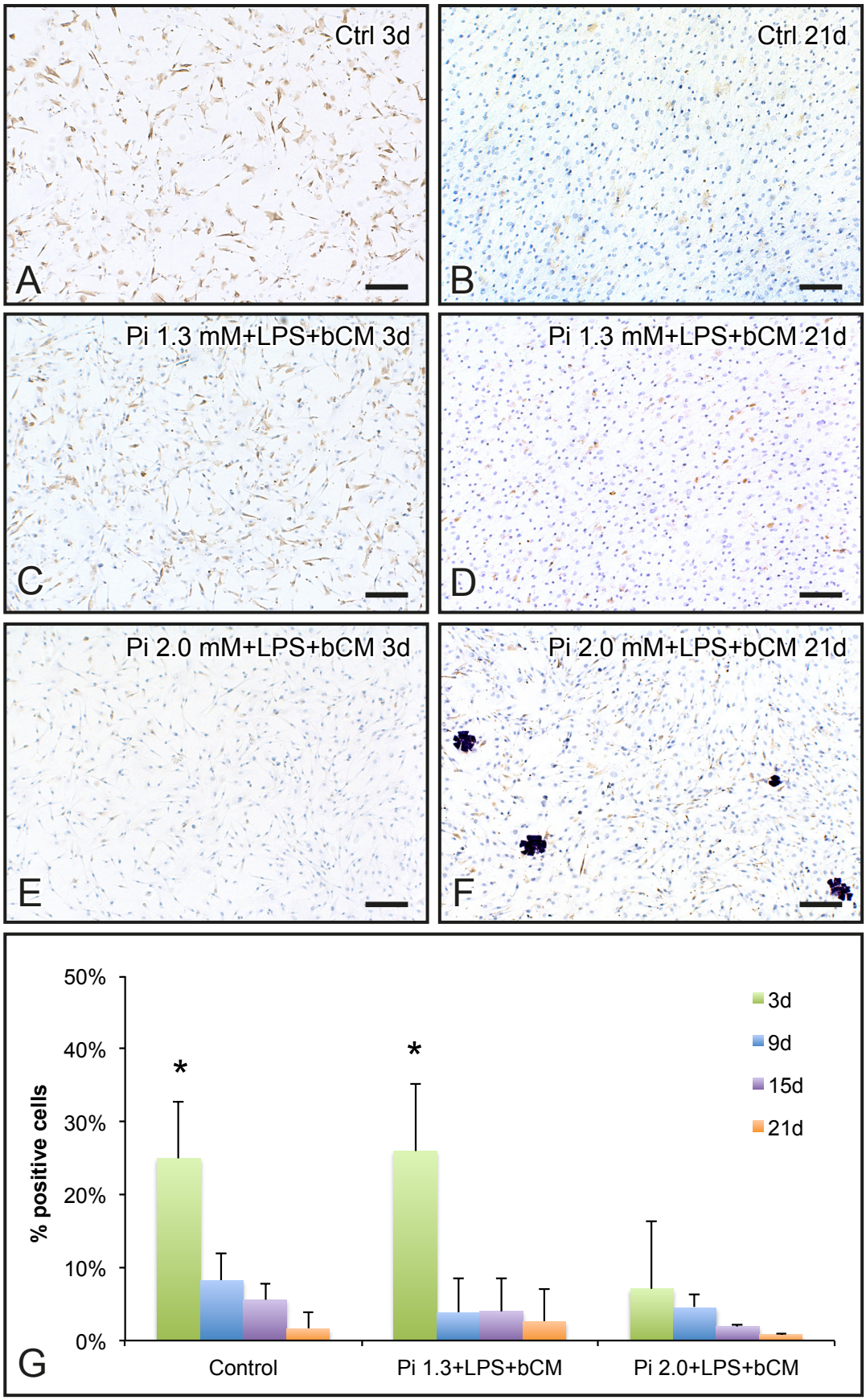

Figure 4.16. A-F: Immunocytochemical localization of MAP1LC3A on cultured AVICs stimulated with pro-calcific stimuli and different concentrations of inorganic phosphate (Pi). Scale bar: 100 µm. G: Histogram of MAP1LC3A-reactive AVICs at different incubation times in the above cultures. The values are reported as mean ± SD. Asterisk indicates $p < 0.001$.

To assess possible involvement of apoptosis, other control-cultures, 1.3-Pi-LPS-bCM-cultures, and 2.0-Pi-LPS-bCM-cultures were lysed and subjected to immunoblot detection of downstream marker caspase-3 to check the presence of the 17 kDa cleaved form of the enzyme, which is known to be required for this cell death program execution. Absence of cleaved caspase-3 even after the longest incubation times was assessed (Fig. 4.17).

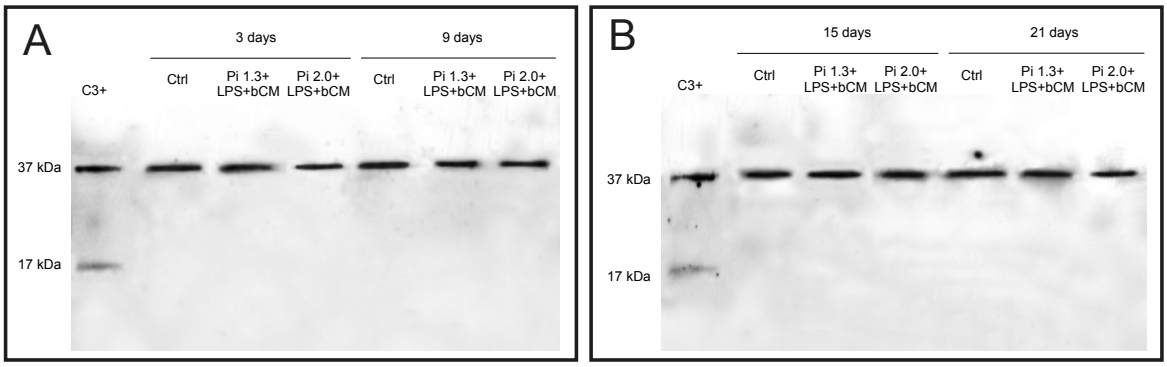

Figure 4.17. Western blotting showing absence of cleaved form of Caspase 3 in cell lysates obtained from AVICs cultured with pro-inflammatory stimuli (LPS + bCM) combined with inorganic phosphate (Pi) at two different concentrations with a time course of 3 to 21 days.

Additional immunocytochemical detection of late marker annexin-V revealed weak immunoreactivity irrespectively from culture conditions and incubation timing (Fig. 4.18). Percentages of immunopositive cells are summarized in Figure 4.18 D.

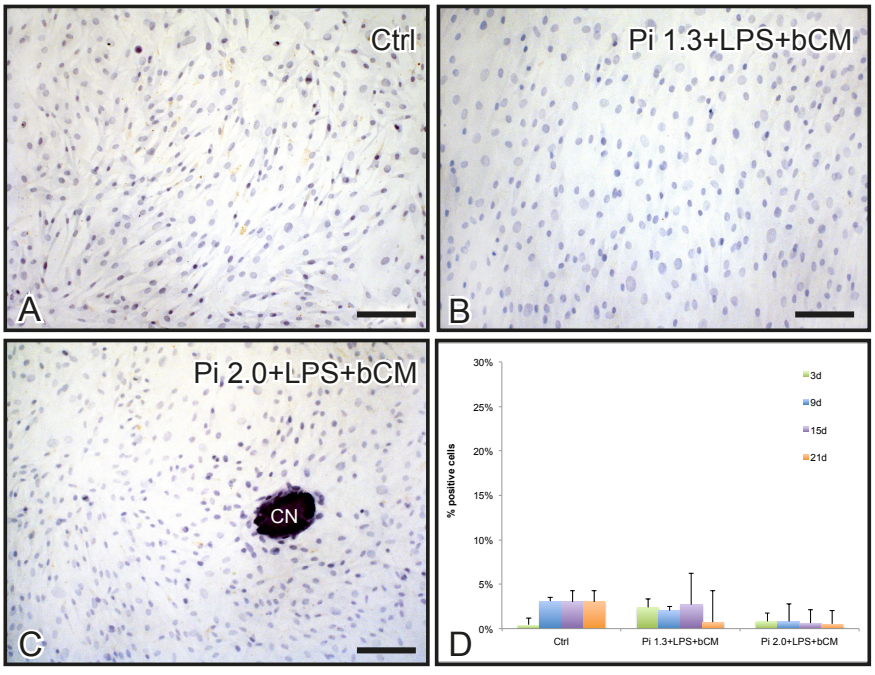

Figure 4.18. Exemplificative pictures showing scarce immunopositivity of AVICs to Annexin V (brown stained) in control cultures (Ctrl; A); 1.3-Pi-LPS-bCM-cultures (B); and 2.0-Pi-LPS-bCM-cultures (C), with only these latter showing calcific nodules (CN) after hematoxylin counter-staining. Scale bar: 50 µm. D: Histogram of Annexin-V-reactive incubated AVICsat different incubation times in the above cultures.

Moreover, treatment of 2.0-Pi-LPS-bCM-cultures with pancaspase inhibitor Boc-D-FMK did not prevent nodule formation and showed degenerative patterns like cultures not subjected to caspase inhibition (Figs. 4.19 and 4.20).

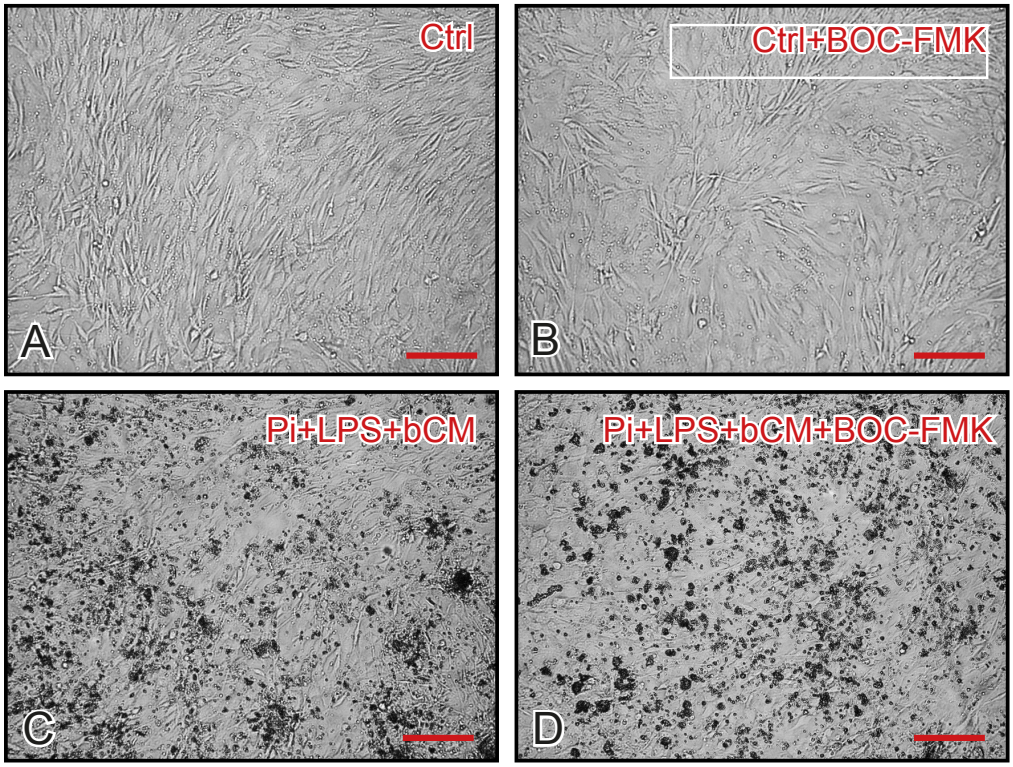

Figure 4.19. Inverted microscope micrographs of unstained AVIC monolayers at 21 days showing absence of calcium precipitation in control cultures (A) and cultures treated with pancaspase inhibitor BOC-FMK (B) and mineral precipitation in 2.0-Pi-LPS-bCM-cultures (C) and 2.0-Pi-LPS-bCM-cultures plus BOC-FMK (D). Scale bar: 50 µm.

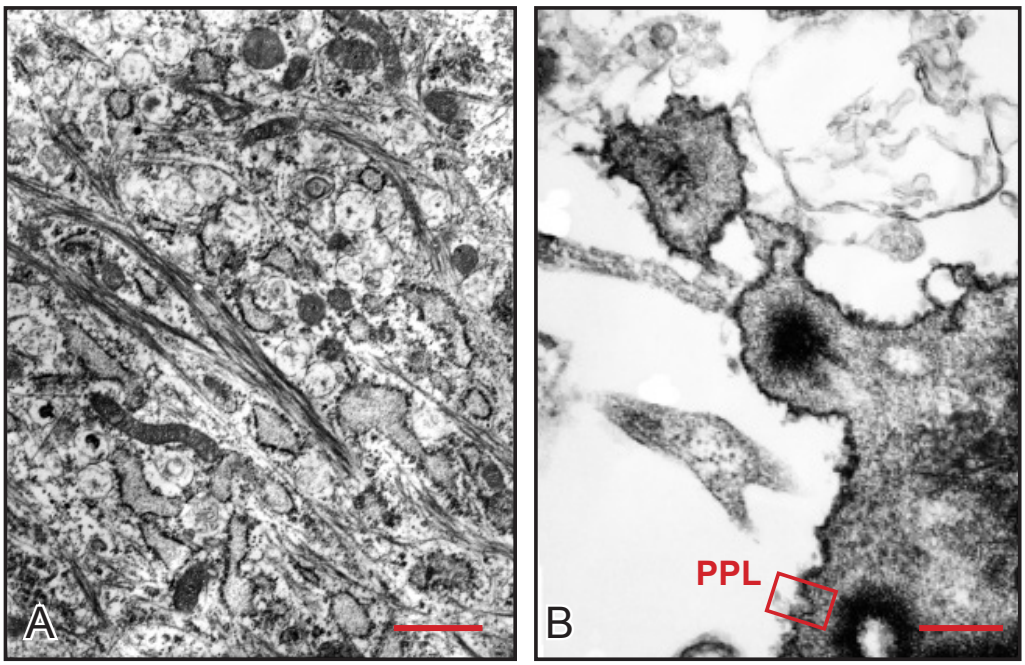

Figure 4.20. Ultrastructual pictures of AVIC cultures plus pancaspase inhibitor BOC-FMK (A), and 2.0-Pi-LPS-bCM-cultures plus BOC-FMK, showing the appearance of phthalocyanin positive layer (PPL) and CDP formation (B). Scale bars: 1 µm (A) 0.5 µm (B).

4.3 STENOTIC VALVES

Ultrastructural examination of surgically excised aortic valve leaflets from patients affected by CAVS revealed the presence of a heterogeneous repertoire of altered features, including the presence in AVIC cytoplasm of (i) electronlucent non-membrane bound lipid droplets which were reminiscent of esteryl-cholesterol droplets (Fig. 4.21 A), (ii) dark CuB-positive droplets likely formed by anionic lipids (Fig. 4.21 B), (iii) heterogeneous droplets dervived from merging of both (Fig. 4.21 A, B), (iv) cholesterol clefts within merged electron-lucent droplets (Fig. 4.21 C), and (v) extracellular electronlucent cholesterol clefts interspersed within heterogeneous drifts of dark lipid material and cell debris (Fig. 4.21 D).

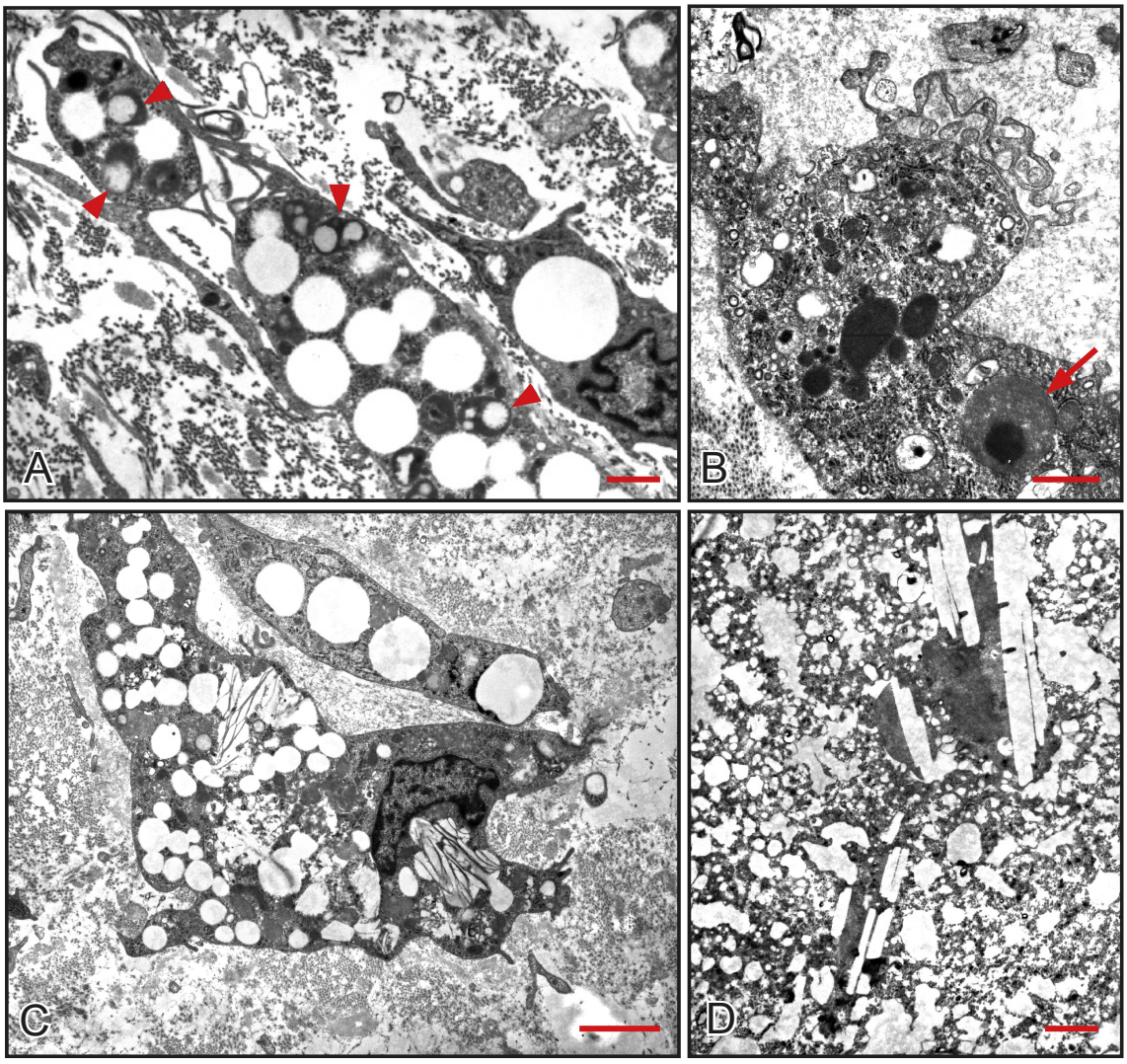

Figure 4.21. Pre-embedding reactions with Cuprolinic Blue on samples from para-nodular calcifiyng areasfigure in stenotic human valve leaflets. A: Electronlucent droplets and their fusion with dark droplets (arrowheads) in an AVIC. B: dark lipid droplets includind one with heterogeneous content (arrow) in a magrophage-like cell. C: Foam cells with intracytoplasmic cholesterol droplets and clefts. D: Cholesterol clefts in residual cell debris. Scale bars: 1 µm (A, B); 2 µm (C); 1 µm (D).

As for *in vitro* model, Raman technique was used for chemical estimations on cryosections of samples from CAVS-affected aortic valve leaflets, which were compared with von-Kossa reacted histological sections. These latter showed heterogeneously sized dark calcific nodules randomly distributed along the outer side of cusp *fibrosa* layer (Fig. 4.22 A). Each nodule was surrounded by a lot of von-Kossa-positive AVICs and a lot of equally dark, irregular microprecipitates, which were even scattered throughout the entire *fibrosa* layer. This latter still exhibited its native feature including eosinophilia and a dense fibrous texture, which was subjected to increasing alterations moving toward the calcific nodules. At level of this interstitial *tunica*, native-type dense fibrous texture was subjected to increasing alterations in parallel with eosinophilia decrease, consistently with prominent collagen degradation, moving toward the calcific nodules.

Figure 4.22 G shows the mean normalized Raman spectrum of the map of a paraserial cryosection on respect to the von Kossa stained one (Fig. 4.22 A). The spectrum shows characteristic peaks for HA at 959 cm^{-1}, for phospholipids/ triglycerides at 719 and 1738 cm^{-1}, for cholesterol at 700 and 741 cm^{-1}, for carotenoids at 1158 and 1525 cm^{-1}, for collagen at 877, 922 and 939 cm^{-1} (van de Poll S.W. *et al.*, 2003; De Gelder J. *et al.* 2007). The presence of unsaturated lipids can be inferred from the small but still distinguishable peak at 1660 cm^{-1}, superimposed to the broad amide-I protein peak (1500-1700 cm^{-1}), whereas the peaks at 1064 and 1128 cm^{-1} indicate the presence of saturated fatty acid chains as well. The corresponding Raman maps indicate localization and concentration of HA, collagen, elastin, phospholipids/triglycerides, cholesterol, and carotenoids. HA distribution of (Fig. 4.22 B) coincided with the calcified areas as revealed by von Kossa staining in the histological cryosection (Fig. 4.22 A).

Collagen distribution (Fig. 4.22 C) spanning the entire valve leaflet roughly correlated with the structure characterizing native valves.

The distribution of phospholipids/triglycerides as observed in the Raman images correlated with that of HA as well as the von Kossa silver staining patterns (Fig. 4.22 D). Intensity of these lipid bands was very low in the area corresponding to the calcific nodule, likely because in this area they are masked by the overwhelming intensity of the precipitated HA. Additional co-localization patterns were shared by both cholesterol and carotenoids (Fig. 4.22 E and F).

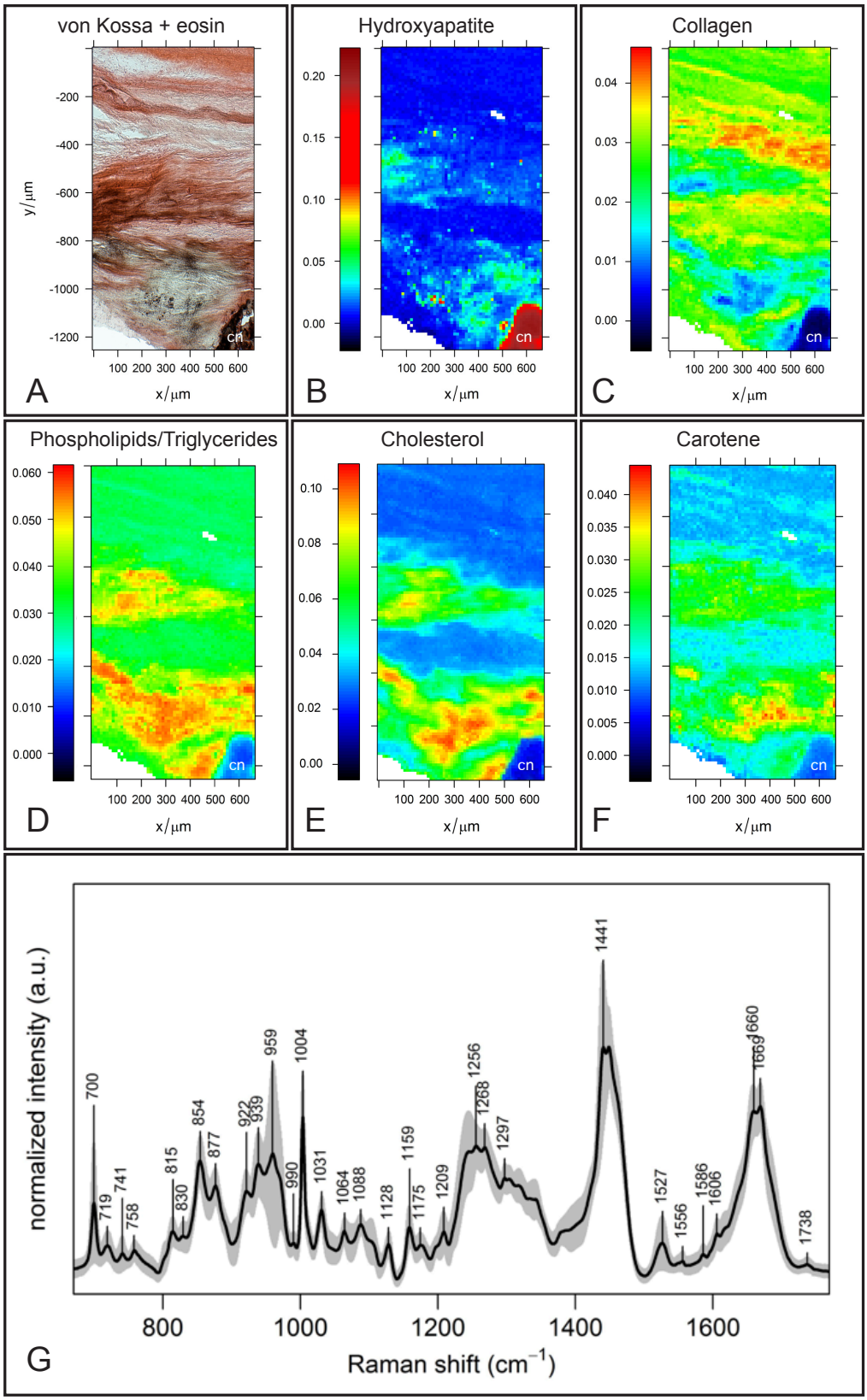

Figure 4.22. A: von Kossa stained cryosection showing metallic Ag deposition on calcific sites (brown precipitates). B-F: Raman images of a para-serial cryosection with respect to that in A showing the distribution of hydroxyapatite (B), collagen (C), phospholipid/triglycerides (D), cholesterol (E), and carotenoids (F) with colours indicating the relative amounts as displayed in the chromatic scales on the left. Note that hydroxyapatite maximum coincides with a calcific nodule (cn) and co-localization of phospholipids/triglycerides, cholesterol and carotene at decreasing rates. G: Mean Raman spectrum of the Raman map, averaged over all the 5708 spectra. Intensity standard deviation, showing the spectral variability, is shown in light grey. For all spectra, excitation wavelength was at 785 nm, laser power was 170 mW and acquisition time was 10 s. Magnification 5 x.

4.4 TREATMENTS WITH LIPOPROTEINS

Since both electron microscopy and Raman microspectroscopy revealed the presence of cholesterol with assumable derivation from LDLs, the pro-calcific role of these lipoproteins was investigated by combining *in vitro* model used above with an atherosclerotic one in both metastatic and dystrophic conditions.

AVICs were cultured with combinations of pro-calcific stimuli (Pi, LPS and bCM) and/or native LDLs (nLDLs) and aggregated LDLs (agLDLs), two forms which have been shown to exert distinct effects on cultured smooth muscle cells, e.g. intracellular cholesteryl ester accumulation (Llorente-Cortés V. *et al.*, 1998).

Figure 4.23 shows changes in intracellular esterified cholesterol (EC) and triglycerides (TG) contents assessed with thin layer chromatography (TLC) in a time course spanning 3-9 days.

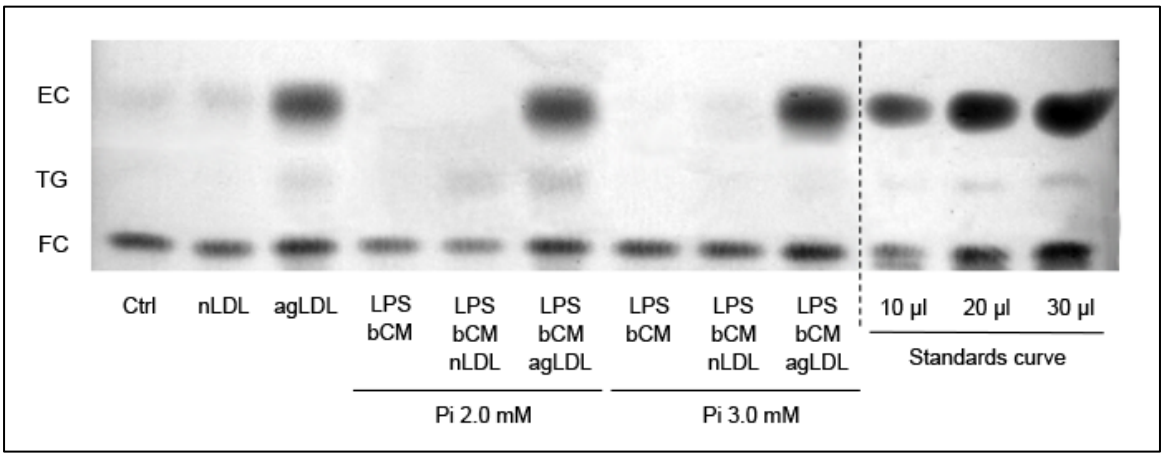

Figure 4.23. Thin layer chromatography after 6-day-long administration to cultured AVICs of native (nLDL) or aggregated LDL (agLDL) alone or combined with pro-calcific stimuli (Pi, LPS and bCM) in metastatic (Pi 3.0 mM) conditions. Bands showing the content of esterified cholesterol (EC), triglycerides (TG) and free cholesterol (FC) are displayed.

Densitometric analysis of EC and TG bands is reported in Figure 4.24 A and B, respectively. All values were normalized on respect with amounts of free cholesterol (FC), which is stable, because it is maintained in a critical concentration range in living cells (Small D.M., 1988).

Compared to control cultures (Pi 0.7 mM), negligible changes in EC amounts resulted after stimulation with pro-calcific stimuli alone, in both dystrophic and metastatic conditions.

After treatment with LDL solely, nLDL-cultures showed significant increase of EC at 3 days, compared to control cultures. Additionally these cultures showed mild, progressive decrease of EC content over time. Conversely, the same parameter did not changed significantly after addition of both pro-calcific stimuli and nLDL (2.0- and 3.0-Pi-LPS-bCM-nLDL-cultures), even if a weak increase of EC was found in 3.0-Pi-LPS-bCM-nLDLcultures at day 6 and in 2.0-Pi-LPS-bCM-nLDL-cultures at day 9, possibly in some relation with Pi concentration.

Concerning cultures added with agLDLs (agLDL-, 2.0-Pi-LPS-bCM-agLDL and 3.0-Pi-LPS-bCM-agLDL-cultures), EC values were very higher than those in control cultures and other treated cultures.

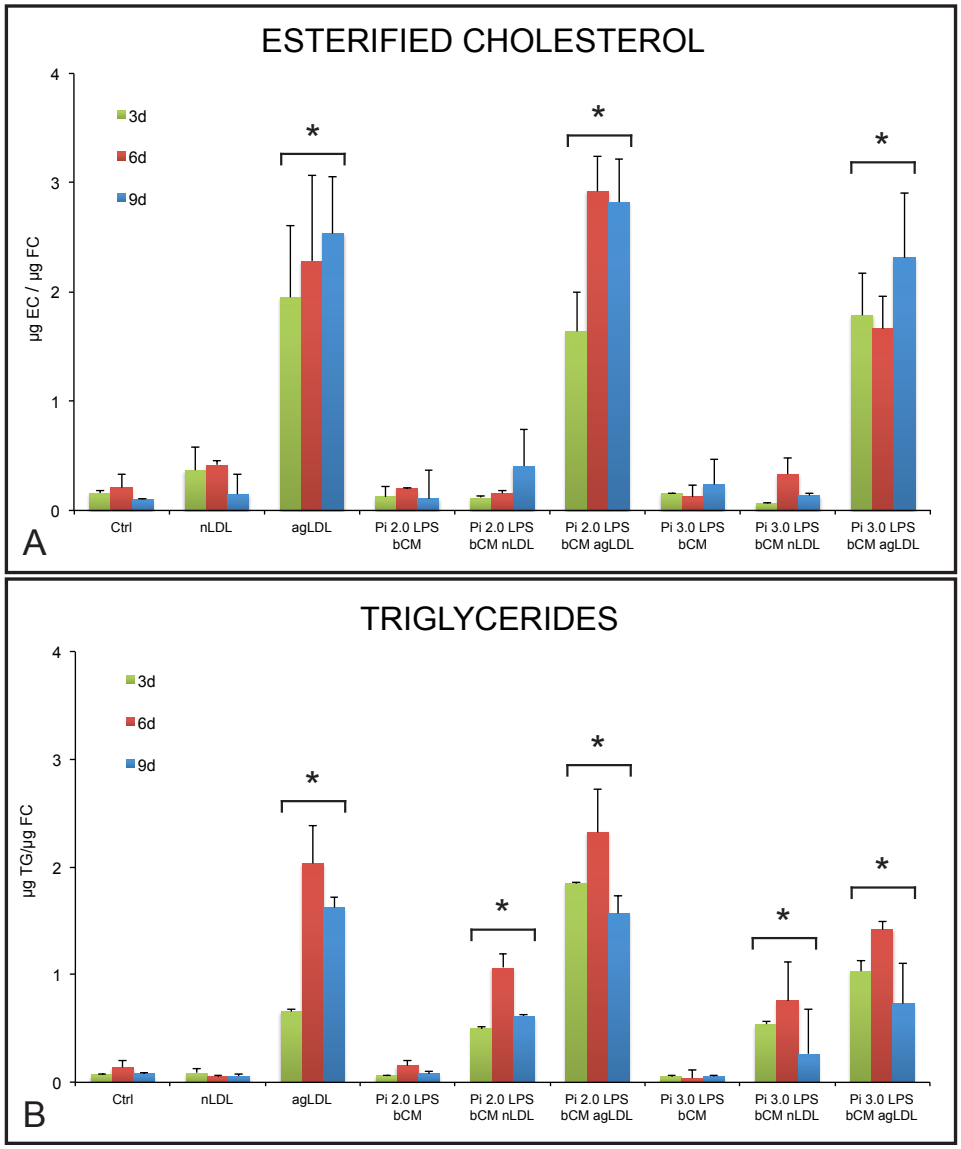

Figure 4.24. Thin layer chromatography quantification of esterified cholesterol (EC) content (A) and triglycerides (TG) content (B) normalized on free cholesterol (FC) content, after administration of n- or agLDL alone or combined with pro-calcific stimuli, at 3, 6 and 9 days. Asterisk indicates $p < 0.01$.

No changes in TG content were found in control-, nLDL-, 2.0-Pi-LPS-bCM- and 3.0-Pi-LPS-bCM-cultures (Fig. 4.24 B).

Significant increases were evident for all other cultures which showed maximum values at the intermediate incubation time, i.e. day 6. Of these, lower values resulted for metastatic-like conditions, i.e. 3.0-Pi-LPS-bCM-nLDL-cultures and 3.0-Pi-LPS-bCM-agLDL-cultures.

First spectrophotometrical estimations of calcium amounts were performed fro metastatic-like conditions (Fig. 4.25).

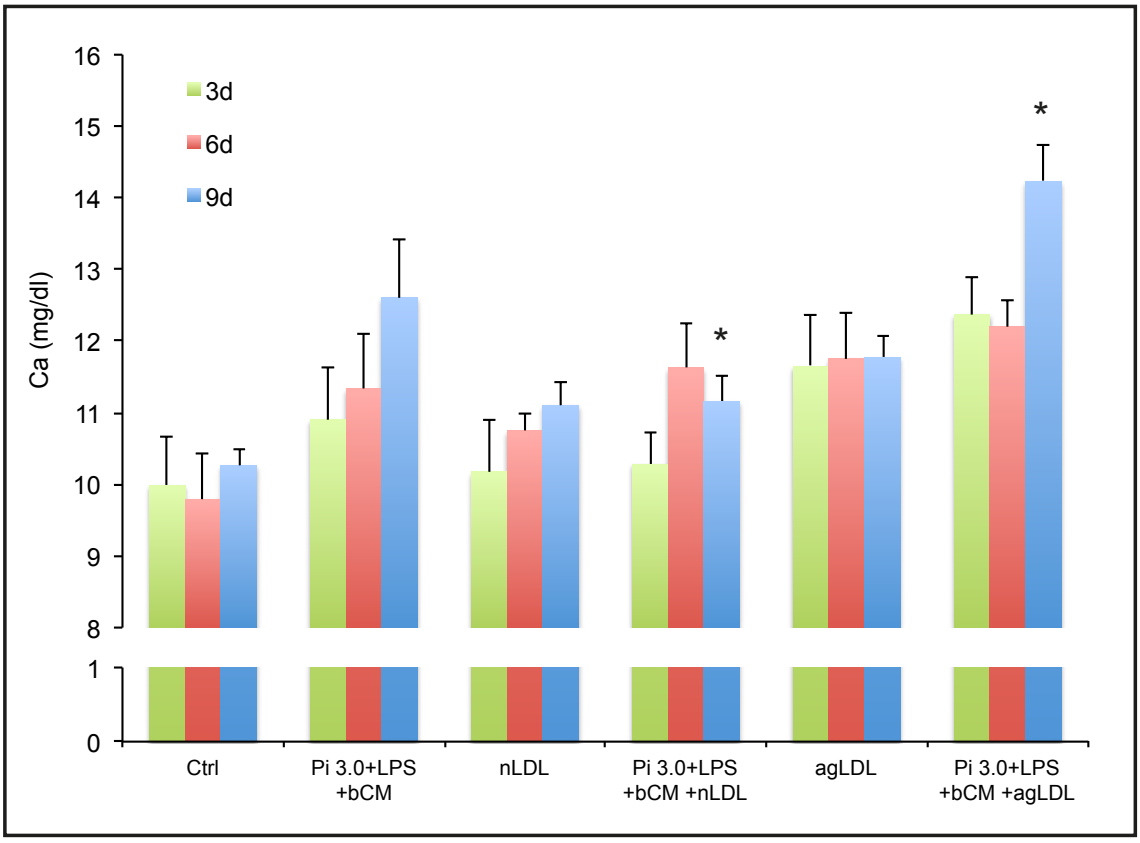

Figure 4.25. Spectrophotometric estimation of calcium amounts considering 3- to 9-day-time-course for bovine AVIC cultures after treatments with nLDL or agLDL, alone or combined with pro-calcific stimuli in metastatic conditions. The values are reported as mean + SD. Asterisks insicate the values concerning 3.0-Pi-LPS-bCM-nLDL- and 3.0-Pi-LPS-bCM-nLDL-cultures at 9 days of stimulation significantly different from 3.0-Pi-LPS-bCM-cultures; $p < 0.01$.

In detail, 3.0-Pi-LPS-bCM-cultures showed a time-dependent increase in calcium levels. Treatment with nLDLs showed mild pro-calcific effect, being calcium levels augmented at day 9, whereas there was a significant increase in calcium after treatment with agLDLs starting from day 3, remaining constant along the time course. Moreover, combination of nLDL with pro-calcific stimuli caused calcium levels to reach a maximum level at day 6, with subsequent weak decrease at day 9. Finally, 3.0-Pi-LPS-bCM-agLDL-cultures showed not only a rapid increase of calcium levels at day 3, which was comparable with those of 3.0-Pi-

LPS-bCM-cultures at day 9, but also a further increase at day 9, reaching the highest level concerning all treatments. Thus a major pro-calcific role appeared to be played by agLDLs.

In order to compare metastatic calcification with dystrophic one, the effects of nLDL and agLDL on calcium amounts were assessed in AVICs also in normophosphatemic-like conditions (Fig 4.26). In this experimental stage, culture time course was prolonged because calcium precipitation is less prominent than for metastatic-like conditions and longer adhesivity of AVICs to Petri dish is allowed.

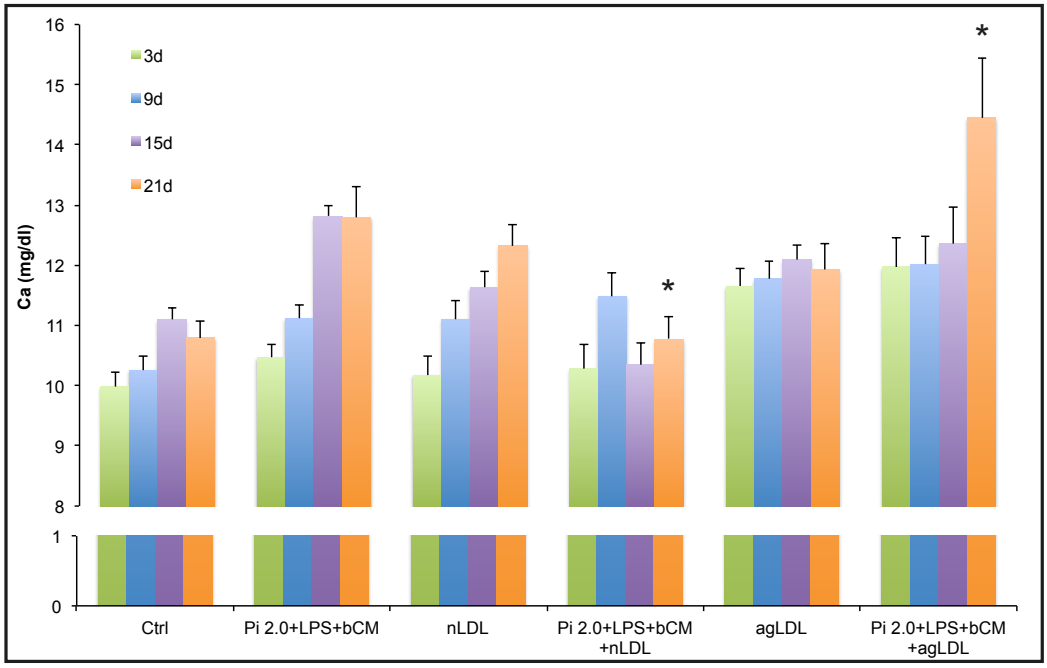

Figure 4.26. Spectrophotometric estimation of calcium amounts considering a time course spanning 3-21 days for bovine AVIC cultures after treatments with nLDL or agLDL, alone or combined with pro-calcific stimuli in metastatic conditions. The values are reported as mean + SD. Asterisks insicate the values concerning 2.0-Pi-LPS-bCM-nLDL- and 2.0-Pi-LPS-bCM-nLDL-cultures at 21 days of stimulation significantly different from 2.0-Pi-LPS-bCM-cultures; $p < 0.01$.

As for metastatic-like calcification, a significant increase in calcium levels was found for 2.0-Pi-LPS-bCM-cultures at the longest incubation times (15 and 21 days). Compared to control cultures, a progressive calcium increase was observed for nLDL-ones, indicating their possible pro-calcific effects. This was confirmed by ultrastructural patterns showing AVICs with several suffering features, such as the atypical enlargement of endoplasmic reticulum, that circumscribes discrete cytoplasm regions occupied by more or less degraded organules (Fig. 4.27 A and B). These patterns were superimposable to those described for mild normophosphatemic-like pro-calcific stimulation (Figs. 4.14 D-F and 4.15).

Interestingly, a paradoxical effect of nLDLs was found in 2.0-Pi-LPS-bCM-nLDL-cultures, because calcium levels were comparable to control cultures, at days 15 and 21. Also these data were confirmed by electron microscopy since 3.0-Pi-LPS-bCM-nLDL-cultured AVICs exhibited well-preserved organules, long stress fibres, unaltered cytoplasm and no evident features of cell degeneration even after long-time stimulation (Fig. 4.27 D).

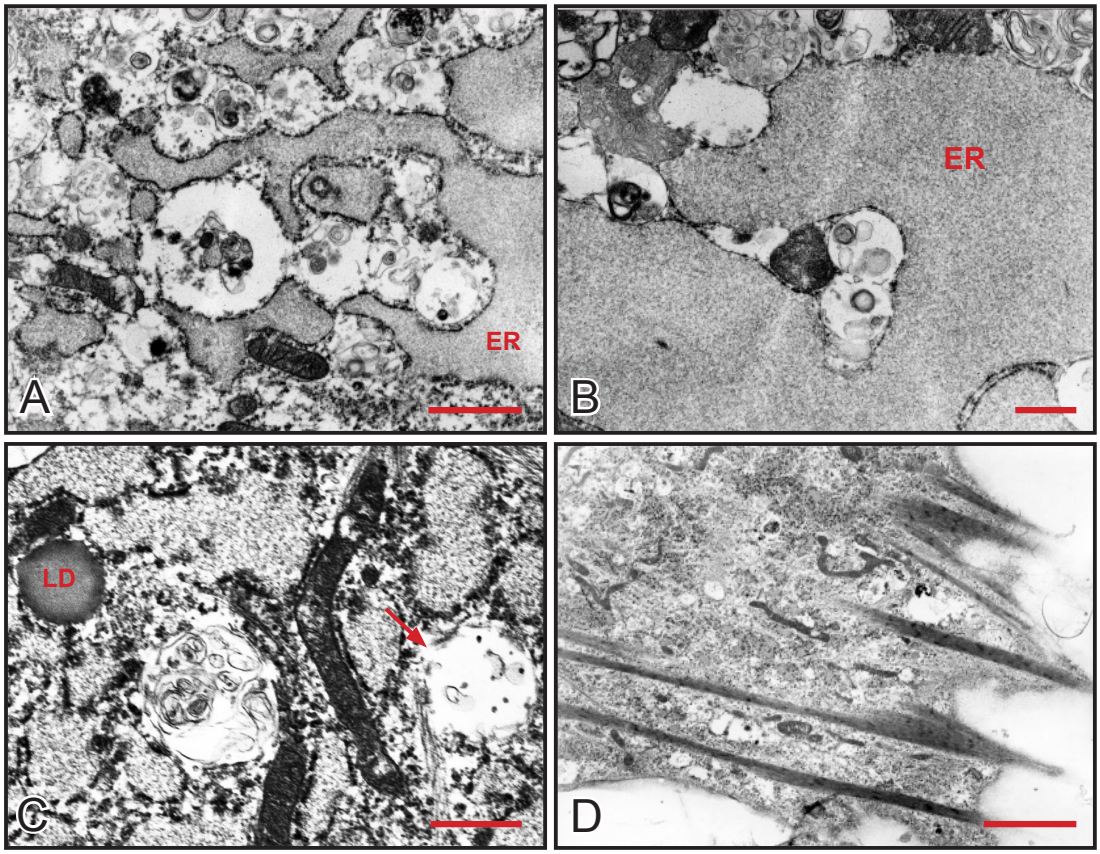

Figure 4.27. AVICs treated with nLDL solely (in A and B) showing abnormally dilated endoplasmic reticulum (ER), or combined with pro-calcific stimuli showing endocytosis vacuoles containing nLDLs (arrow), lipid droplets (LD) (in C) and stress fibers (in D). Scale bars: 1 µm (A); 0,5 µm (B, C); 2 µm (D).

As for metastatic calcification, internalized agLDL (Fig. 4.28 A and B) correlated with increasing calcium levels starting from day 3, and its subsequent unchanging with time. Interestingly, agLDL-treated AVICs did not exhibit suffering features being similar to control ones (Fig. 4.28 A and B). By contrast, agLDL treatment combined with Pi and pro-inflammatory stimulation exacerbated the pro-calcific effect resulting in higher levels of calcium with respect to 2.0-Pi-LPS-bCM-cultures, at 21 days.

In fact, distinct patterns of typical pro-calcific degeneration were found in 3.0-Pi-LPS-bCM-agLDL-cultures, as previously described, being included (i) CuB-reactive acid lipid droplets (Fig. 4.28 C) and the degenerative modifications culminating in the formation of (ii) PPL-lined irregular CDP and roundish *calcospherulae* (Fig. 4.28 D).

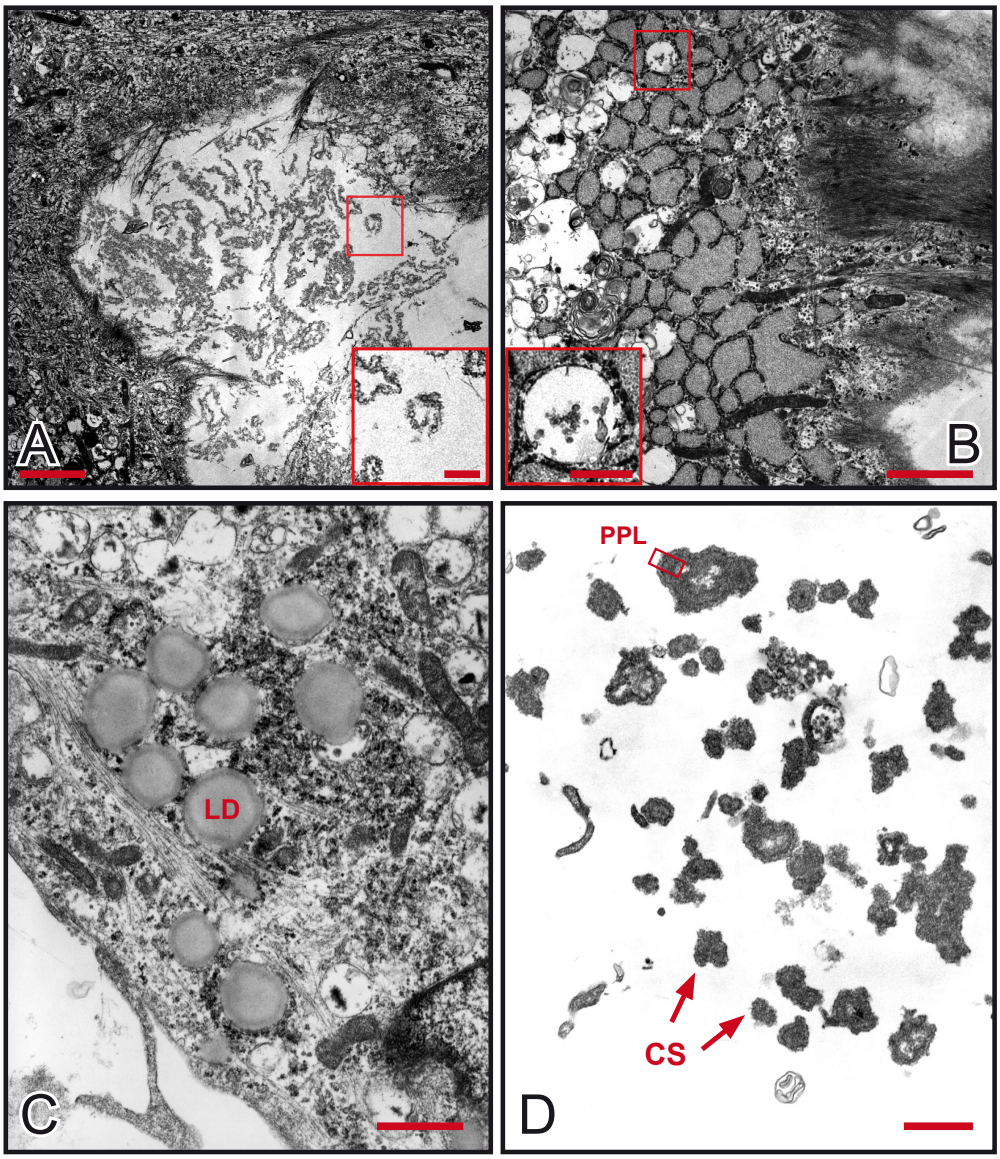

Figure 4.28. Cultured AVIC treated with agLDL solely (A and B) or combined with pro-calcific stimuli (C and D). A: Clusters of agLDLs in the medium. The agLDLs squared are magnified in the inset below-right. B: agLDLs internalized within an AVIC vacuole (squared) which is magnified in the inset below-left. C and D: Patterns of pro-calcific degeneration in 3.0-Pi-LPS-bCM-agLDL-cultures. Cytoplasm Initial degeneration represented by formation of cytoplasmic lipid droplets (LD) and final degenerative products, represented by PPL-lined *calcospherulae* (CS). Scale bars: 2 μm (A, B) 0.5 μm (inset A, inset B); 1 μm (C, D).

5. DISCUSSION

In the present investigation, calcific aortic valve stenosis (CAVS) was mimicked using *in vitro* models, assessing the effects of several pathologic agents, such as inorganic phosphate (Pi), pro-inflammatory stimuli (bacterial LPS and macrophage-derived inflammatory mediators) and subjecting the cultured aortic valve interstitial cells (AVICs) to pro-atherosclerotic stimuli (LDLs).

The AVICs cultured at elevated Pi concentration, consistently with the hyper-phosphatemic conditions in organisms, allowed to shed light on the crucial involvement of this inorganic element in a context reproducing metastatic calcification, since prominent calcific events occurred in all cultures containing elevated Pi (3.0 mM). As a matter, such a condition resulted to be capable of inducing ectopic calcification *per se*, consistently with the concept that elevated Ca x P product represents the most predictive parameter for cardiac valve calcification in hemodialysis patients (Ribeiro S. *et al.*, 1998; Block G.A., 2000; Tarrass F. *et al.*, 2006). Compared to Pi-cultures, additional increase in calcium amount resulted for Pi-LPS-bCM cultures exclusively. Absence of increase in calcium amounts after stimulation of 9-day-cultured AVICs with endotoxin LPS is not consistent with a previous report of marked mineralization occurring in Pi-LPS treated AVIC cultures (Rattazzi M. *et al.*, 2008), although those results concerned longer incubation times. Conversely, in the present work the highest alkaline phosphatase (ALP) activity resulted for Pi-LPS treatment. Of note, direct pro-calcific effects by LPS, including ALP activity enhancement, were shown to occur for cultured AVICs with the involvement of specific LPS Toll-like receptors (TLRs) (Babu A.N. *et al.*, 2008; Meng X. *et al.*, 2008; Yang X. *et al.*, 2009). Thus, it seems likely that this bacterial endotoxin can exert some pro-calcific effect on AVICs, superimposing to that exerted by elevated Pi. Additional stimulations with conditioned media derived from cultures of monocytes/macrophages in their turn stimulated with LPS, were accomplished with the rationale of simulating inflammatory conditions due to bacterial infection in the organism. Treatment with conditioned medium from LPS-stimulated monocytes/macrophages on a subset of bovine aorta-wall-derived smooth muscle cells (Tintut Y. *et al.*, 2002) named calcific vascular cells (CVCs) (Watson K.E. *et al.*, 1994), elicited TNF-α secretion and associated ALP activity increasing. Moreover, specific interaction of LPS with TLR-4 was reported to activate murine RAW264.7 macrophages, suggesting their contribution in

mineralizing processes (Hume D.A. *et al.*, 2001; Wu T.T. *et al.*, 2009). In this study, conditioned media from cultures of LPS-activated RAW264.7 macrophages did not cause increase in mineralization, whereas clear calcific overgrowth occurred by using conditioned media from cultures of allogeneic primary macrophages. Taking into account that macrophage activation by bacterial wall components correlates with secretion of species-specific chemo/cytokines (Nagao S. *et al.*, 1992) and that equal pathogen doses can trigger different inflammatory cell responses (Munford R.S., 2010; Warren H.S. *et al.*, 2010), it is suggested that species-specificity of macrophage-derived cytokines is essential to enhance calcific responses by AVICs.

Together, the above results are in line with the concept that products derived from Gram-negative bacteria may contribute in triggering cardiac valve calcification via inflammatory reactions, as suggested by the detection of *Chlamydia pneumoniae* in both stenotic and sclerotic semilunar valves (Juvonen J. *et al.*, 1997; Nyström-Rosander C. *et al.*, 1997), as well as the experimental demonstration that animal aortic valves undergo mineralizing effects after inoculation with oral bacteria (Cohen D.J. *et al.*, 2004).

Concerning ALP activity in 9-day-long cultures, prominent increases were restricted to the three cultures subjected to stimulation with LPS and LPS plus conditioned media. Since prominent increase in calcium amount was a response shared by AVIC cultures with elevated Pi concentration, analogous sharing was expected to exist for ALP activity. Unpredictably, Pi- and Pi-bCM-cultures showed lower enzyme activity. However, on extending the estimation of ALP activity to 3-day and 6-day long cultures, similar increase was shared by all four culture types up to 6 incubation days, with a marked drop in Pi- and Pi-bCM-cultures between the sixth and the ninth day, in contrast with further increase occurring for the other three treatments. This was consistent with the reported finding of lower enzymatic activity for AVIC Pi-cultures *versus* Pi-LPS cultures (Rattazzi M. *et al.*, 2008). Thus, it is reasonable that ALP activity may be involved in mineralization but without acting as exclusive driving factor. In addition, it cannot be excluded that in Pi-LPS-bCM-cultures increased cell degeneration entails lower ALP synthesis.

Of interest, pro-inflammatory cytokines such as TNF-α were reported to induce over-expression of type III sodium-dependent Pi cotransporter PiT-1 (Li X. and Giachelli C.M., 2007), with a possible increase in Pi uptake by cultured mineralizing vascular smooth muscle cells (Lau W.L. *et al.*, 2010). Putatively, a differential cytokine-induced overexpression of PiT-1 by AVICs and subsequent massive Pi uptake might enhance calcium phosphate formation, thereby eliciting greater HA precipitation at the edges of AVICs and AVIC-

derived products in Pi-LPS-bCM cultures, independently from the rate of ALP activity. It is noteworthy that increases in ALP activity were never associated with signs suggesting some AVIC trans-differentiation into osteoblast-like cells, being the progression of calcific processes exclusively accompanied by advancing of the described pro-calcific degenerative patterns showed by the dying/died cultured AVICs. Although apoptosis was reported to occur for cultured ovine calcifying AVICs stimulated with transforming growth factor beta (TGF-β) (Jian B. *et al.*, 2003) as well as a specific clone of bovine AVICs after stimulation with LPS (Rattazzi M. *et al.*, 2008). Rather, the observation of frequent autophagic figures at the early treatment stages might suggest that autophagic cell death might be primed, as reported for CAVS (Somers P. *et al.*, 2006), with the occurrence of unusually extensive lipolytic processes, possibly resulting in a prominent release of phospholipids and free fatty acids, consistently with the observed reactivity to cationic dye cuprolinic blue (CuB).

Size and number of calcific nodules displayed by light inverted microscope for Pi-containing cultures were morphological parameters fitting with the treatment-dependent increases in calcium amounts estimated by means of spectrophotometry. Consistently, ultrastructural analysis clearly indicated that all treated AVICs underwent dramatic breakdown including intracellular release/accumulation of CuB-reactive and silver-reactive material as well as its outcropping with formation of the pericellular dark layers named PPLs (phthalocyanin-positive-layers). A similar cell degradation process was already described for experimental *in vivo* calcification consisting in xenogenic subdermal implantation of glutaraldehyde-treated aortic valve cusps, with PPLs resulting to be largely formed by lipidic moieties including phospholipids and to contain calcium-binding sites (Ortolani F. *et al.*, 2002a; Ortolani F. *et al.*, 2002b; Ortolani F. *et al.*, 2003; Ortolani F. *et al.*, 2007), as well as experimental *in vitro* models of ectopic calcification (Ortolani F. *et al.*, 2010). Of interest, PPLs are comparable to the alcianophylic envelopes outlining so called "thick walled cell derived products" (CDPs), described for calcific aortic valves and other soft tissues affected by ectopic calcification (Kim K.M. and Huang S.N., 1971; Kim K.M., 1976; Boskey A.L. *et al.*, 1988; Kim K.M., 1995).

Since the production of the PPL precursor named PPM (phthalocyanin-positive-material) paralleled a progressive disappearance of all cytomembrane-bounded organelles, derived membranous residues and nuclear chromatin, it ensues that such a substance results from a complete colliquation of all these components. This was also confirmed by the observation of a lot of transitional patterns showing disrupting organelles or their ghosts to merge with PPM or to be embedded within such a material.

The role of these cell-derived products as major HA nucleators was supported by co-localization of calcium binding sites, as revealed by the selective precipitation of metallic silver after von Kossa staining, as well as effective superimposition of HA crystals. A further significant outcome was the identification of multilayered PPLs and concentrically laminated *calcospherulae*, these latter being closely reminiscent of the typical "porous particles in concentric layering" described for calcific aortic valves and other tissues affected by ectopic calcification (Kim K.M., 1995) as well as failed calcific valve bioprostheses (Valente M. *et al.*, 1985).

Because of affinity to von Kossa silver staining and superimposition by HA crystals, the *calcospherulae* seem to act as mineralization enhancers in the most advanced calcific stages, providing a widespread dissemination of supernumerary nucleation sites. This role is analogous to that played by matrix vesicles and/or apoptotic bodies in both physiological calcification and pathological one (Anderson H.C., 1983; Kirsch T., 2006), although being quite different cell-derived structures. Indeed, *calcospherulae* appeared to result from passive budding of PPLs and lack in cytoplasm, showing a roughly shared para-crystalline structure because of the presumable rearrangement of the pre-existent array of the lipid moiety at the level of the PPL-forming layers. Conversely, matrix vesicles and apoptotic bodies are described to result from distinct regulated mechanisms, contain organized cytoplasm, and are outlined by membranes with specific molecular architectures, including either inner location of phospholipids (Wu L.N. *et al.*, 1997) or outer location (Bratton D.L. *et al.*, 1997), respectively.

Consistently with electron microscopy, Raman analysis of stimulated calcifying cells revealed a peripheral distribution of type B carbonate HA, as revealed by the presence of the band at 959 cm^{-1}, which was prevoiusly shown to correspond to such a salt (Penel G. *et al.*, 1998). Moreover, degenerating cells exhibited a target-like configuration of Raman clusters, with progressive HA increase toward external clusters. Paralleling a prominent decrease in protein amounts up to disappearcance, there was weaker decrease with persistence in the amount of lipids, predominantly the unsaturated ones, indicating their possible role as HA nucleators consistently with their ionic nature. This data fit with the histochemical reactivity of PPLs to phospholipid-specific malachite green staining at the ultrastructural level previously demonstrated using the subdermal model (Ortolani F. *et al.*, 2003).

Concerning the AVICs cultured with Pi concentrations spanning the normophosphatemic range in organism, the dystrophic-like mineralization processes provoked modifications that are consistent with priming of compensatory mechanisms of cell function preservation for the

two lowest Pi levels (0.8 mM and 1.3 mM). The cell responces correlated with the appearance of an unusually prominent RER-dependent organelle segregation and removal. In contrast, after treatment with the highest (2.0 mM) Pi concentration, the cultured cells underwent the described lipid-release-associated pro-calcific death and disruption, confirming the critical role played by Pi concentration in triggering the AVIC-dependent mineralization besides this process starting and advancing in similar manner as that previously described for *in vitro* AVIC experimental calcification (Ortolani F. *et al.*, 2010; Bonetti A. *et al.*, 2012), *in vivo* calcific subdermal models (Ortolani F. *et al.*, 2002a; Ortolani F. *et al.*, 2002b; Ortolani F. *et al.*, 2003; Ortolani F. *et al.*, 2007), and actual aortic valve stenosis (Ortolani F. *et al.*, 2010; paper in preparation). Of interest, increased risk of cardiac dysfunction, with adverse outcomes including coronary calcification, has been reported in human observational studies on individuals with Pi serum levels just below the upper limit of the conventional normophosphatemic range (Tonelli M. *et al.*, 2005; Foley R.N., 2009; van Kuijk J.P. *et al.*, 2010; Ellam T.J. and Chico T.J., 2012; Osuka S. and Razzaque M.S., 2012).

Taking in account that there were enhanced mineralizing effects exerted by the additional treatment with LPS and medium derived from LPS-stimulated macrophage cultures only for AVICs exposed to the highest Pi level, inflammation could be conceivably regarded as an effective exacerbating factor in dystrophic calcification for subjects with the highest normophosphatemic values at least for the short-term period. Actually, for 2.0-Pi-LPS-bCM-cultures spectrophotometrically estimated calcium amounts showed to increase linearly starting from 21 days of treatment, consistently with the formation of von-Kossa-positive intracytoplasmatic PPM and pericellular PPLs clearly appearing as major HA nucleators in increasing numbers of mineralizing cells and cell debris. Likely, in the same cultures cell mineralization may be sustained by the progressive increase in ALP activity, ensuring the continuous production of Pi and concurrent removal of mineralization inhibitor pyrophosphate, which could result from direct effects of bacterial LPS on cultured AVICs, as previously reported (Babu A.N. *et al.*, 2008; Meng X. *et al.* 2008; Yang X. *et al.*, 2009).

However, ALP activity was found drastically to increase during the last three days of treatment also for 2.0-Pi-cultures, which were free from bacterial LPS, consistently with the idea that the extracellular Pi concentration is the most critical factor for cell mineralization (Jono S. *et al.*, 2000; Kirsch T., 2006; Giachelli C.M., 2009). As a matter, interplay seems to exist between Pi concentration and ALP activity in such a way that Pi generated by enzymatic activity can act as a self-upregulating molecule through a positive feedback mechanism thereby sustaining cell mineralization (Kirsch T., 2006). Consistently, absence of calcification

resulted for all AVIC cultures containing 0.8 mM Pi as well as 1.3 mM Pi, in which both calcium amounts and ALP activities were lower than those estimated for cultures containing 2.0 mM Pi. Moreover, these two parameters were similar comparing AVIC cultures treated with low Pi solely and those stimulated with bacterial LPS and macrophage-derived conditioned medium, strengthening the concept that pro-inflammatory mediators require a high-Pi-containing milieu to exert pro-calcific effects exacerbating those elicited by Pi.

Despite the estimated increases in ALP activity, it is noteworthy that, as for metastatic-like *in vitro* calcification, no cell osteoblastic trans-differentiation was observed, being AVICs subjected to the calcification process primed by the above described cell-death-associated lipid moiety release. In such a context, the CB-reactivity and positivity to von Kossa reaction starting from the periphery of the early new-formed lipid droplets correlate with an initial lipid acidification (Ortolani F. *et al.*, 2002a; Ortolani F. *et al.*, 2002b) which may depend on oxidative effects exerted by endogenous reactive oxygen species (ROS) released by degenerating mitochondria (Li X. *et al.*, 2013), with the additional macrophage-derived ROS contained in the conditioned medium (Wu T.T. *et al.*, 2009) possibly reinforcing these deleterious effects. Such an assumption is supported by the evidence that melting of lipids within these droplets and their subsequent release result in the formation of CB-reactive and von-Kossa-positive PPM and PPLs, i.e. the major HA nucleator in actual aortic valve calcification (Kim K.M. and Huang S.N., 1971; Kim K.M. and Trump B.F., 1975; Kim K.M., 1976; Kim K.M. *et al.*, 1976) as well as *in vivo* experimental one (Ortolani F. *et al.*, 2002a; Ortolani F. *et al.*, 2002b; Ortolani F. *et al.*, 2003; Ortolani F. *et al.*, 2007).

Additionally, oxidized phospholipids could result in membrane destabilization leading to organelle swelling, as observed for mineralizing cells from 2.0-Pi-LPS-bCM-cultures. Taking in account that also lysosomes can be subjected to oxidative-stress-dependent membrane permeabilization, it is likely that intracytoplasmatic release of lysosomal acid hydrolases is reasonably responsible for the autolytic organelle colliquation occurring in mineralizing cells. Moreover, phospholipid disarray affecting membranes of mitochondria and RER might elicit intracytoplasmatic calcium leakage from these two calcium storing organules, thereby activating intracellular calcium-dependent enzymes, so contributing to the observed membrane colliquation. Likewise, increased intracytoplasmatic calcium concentration might trigger cytoskeleton disintegration (Smith M.W. *et al.*, 1991) so facilitating plasmamembrane blebbing and pinching off of cell-derived products, as observed for mineralizing AVICs from 2.0-Pi-cultures and, at greater extent, 2.0-Pi-LPS-bCM-cultures after longer incubation times. However, the identification of some degenerating cells accumulating CuB-positive lipid

droplets and/or PPM also in 1.3-Pi-LPS-bCM-cultures suggests that such a Pi level can be permissive at some extent to cell mineralization thus representing a critical threshold for augmented risk of this disease in humans, consistently with clinical reports (Tonelli M. *et al.*, 2005; Foley R.N., 2009; van Kuijk J.P. *et al.*, 2010).

In order to ascertain if the observed degeneration patterns depend on a sudden unregulated cell breakdown or are the final steps of an aborted orthodox type of cell death. Distinct cell fates, that is autophagocytosis survival in opposition to death-associated mineralization, were found to take place and mainly to depend on Pi concentration, with the added inflammation mediators being potential enhancing agents.

Of note, exposure of cells to oxidative stress was also reported to contribute to RER stress, leading to the activation of the signalling pathway called unfolded protein response (UPR) (Malhotra J.D. and Kaufman R.J., 2007; Malhotra J.D. *et al.*, 2008). Since the execution of UPR requires RER expansion (Schröder M., 2008), it ensues that the abnormal RER hypertrophy observed for 0.8- and 1.3-Pi-LPS-bCM-cultures and, to a less extent, 0.8- and 1.3-Pi-cultures may depend on toxic effects exerted by oxidative stress at low Pi concentrations, thereby enabling the activation of transient compensatory mechanisms. Consistently, no mineralization took place in the AVIC cultures containing low Pi and disappearance of RER hypertrophy was observed for the same cultures once standard culture medium was restored. By contrast, the only occasional identification of RER hypertrophy in 2.0-Pi-cultures and 2.0-Pi-LPS-bCM-cultures suggests that elevated Pi might lead to cell death because causing excessive toxication, so compromising the activation of compensatory responses by the stressed cells. Being mitochondria especially found to undergo selective segregation into the cytoplasmic lacunae delimited by the hypertrophic RER, it is likely that sequestration of damaged mitochondria may ensure prompt buffering of increasing intracytoplasmatic calcium *via* its direct uptake by RER, thereby mitigating the deleterious effects of calcium overload, consistently with possibility of direct communication between RER and mitochondria, as previously reported (de Brito O.M. and Scorrano L., 2008; Giorgi C. *et al.*, 2009). Referring to the seemingly unaltered mitochondria entrapped by RER, such communications might represent a way to facilitate calcium transfer from RER to mitochondria, so implementing their bioenergetic response and improving cell adaptation to stressing conditions, as reported for HeLa cell cultures subjected to RER stress (Bravo R. *et al.*, 2011).

Notably, the identification of acid phosphatase activity at level of hypertrophic RER membranes as well as its increasing *versus* controls strongly suggests that an alternative, non-

lysosomal mechanism of organelle digestion is activated by the treated AVICs, as ultracytochemically shown for other cell types (Borgers M. and Thoné F., 1976; Griffiths G.W., 1979; Jones G.W. and Bowen I.D., 1979; Noda T. and Farquhar M.G., 1992). Such RER degrading activity may somehow represent a time-saving process, providing more rapid recovery of homeostatic conditions by stressed cells than activation of orthodox autophagic machinery can do, consistently with the apparent scarcity of autophagic vacuoles and the decrease in immunoreactivity to autophagosome marker MAP1LC3A observed for 1.3-Pi-LPS-bCM-cultures.

On the other hand, excessive autophagic activity has been reported to lead to cell death in various cell types (Debnath J. *et al.*, 2005; Levine B. and Yuan J., 2005), including AVICs for which associated production of calcium-binding matrix vesicles was reported (Somers P. *et al.*, 2006). In the present study, marked immunopositivity to MAP1LC3A restricted to both 3-day-long control-cultures and 1.3-Pi-LPS-bCM-cultures is consistent with the observed ultrastructural features, which are accepted to represent the most reliable parameter to recognize this cell response (Klionsky D.J. et al., 2012), so supporting the concept of autophagocytosis priming. Since also controls-cultures are included in this process, an autophagy will be present under form of orthodox constitutive house-keeping process (Mizushima N., 2005) enabling an adaptive cell response to the culture environment, so representing a mere epiphenomenon which can acquire the role of extreme survival mechanism by RER overgrowing and associated autolytic activity. Later, this cell response might transform from pre-calcific survival process into potentially pro-calcific one once the first activity fails, leading to cell death.

Rather than autophagy-associated cell death, apoptotic cell death is considered to be involved in cardiovascular tissue calcification *via* release of pro-calcific apoptotic bodies by dying cells (Lee Y.S. and Chou Y.Y., 1998; Proudfoot D. *et al.*, 2000; Jian B. *et al.*, 2003; Clarke M.C.H. *et al.*, 2008). Immunocytochemical data revealed only sporadic immuno-positivity to late marker annexin-V. Such an assumption was further supported by the finding that both 1.3-Pi-LPS-bCM-cultures and 2.0-Pi-LPS-bCM-cultures were lacking in the 17 kDa cleaved form of caspase-3, which is an apoptosis executioner. Additionally, absence of apoptotic cascade activation in mineralizing AVICs was confirmed by (i) complete absence of typical apoptosis features, such as cell shrinkage and chromatin condensation/fragmentation, and (ii) occurrence of the described lipid-release-associated pro-calcific cell degeneration also in 2.0-Pi-LPS-bCM-cultures after treatment with pancaspase inhibitor BOC-D-FMK. This latter result also confirmed a previous finding that another apoptosis inhibitor (Z-VAD-FMK)

prevented *in vitro* cultured sheep AVICs from apoptosis without affecting calcific nodules formation (Jian B. *et al.*, 2003). All these data suggested that apoptosis is not involved in AVIC degeneration.

Since no main features characterizing oncosis, such as cell swelling with cytoplasm loss, were observed too, an alternative, still unclassified type of cell death could be assumed to take place in calcific AVICs, putatively characterized by a distinct regulated process resulting in the lipid-releasing-associated cell degeneration which was actually observed in the present conditions as well as in others referring to valve calcification (Ortolani F. *et al.*, 2002a; Ortolani F. *et al.*, 2002b; Ortolani F. *et al.*, 2003; Ortolani F. *et al.*, 2007; Ortolani F. *et al.*, 2010; Bonetti A. *et al.*, 2012).

Raman microspectroscopy and Raman imaging allowed to achieve the identification of accumulated lipid moieties as well as their distinct topographical distribution also within CAVS-affected aortic valves. The Raman maps achieved specifically correlated with the histological pattern, proving that Raman microspectroscopy can represent a reliable technique in addiing information on the calcific process underlying this calcific disease.

In particular, HA maps revealed the highest intensity of mineral there where calcific nodules were histologically displayed and minor intense areas corresponded to those containing von Kossa reactive particles. Silver staining showed a distribution closely correlating with that displayed by the Raman map for HA, except for the zones occupied by calcific nodules, in which excessive mineral accumulation masked the underlying/mingled material.

Consistently with *in vitro* data, Raman microspectroscopy provided the additional information that the precipitated material was type B carbonate HA, as inferred from the presence of Raman band at 959 cm^{-1} (Penel G. *et al.*, 1998). This chemical species was previously identified as the most abundant form of HA in young bone tissue (Burnell J.M. *et al.*, 1980; Rey C. *et al.*, 1989). Although this identification could be consistent with the view of valve calcification being a form of heterotopic ossification, it must be stressed that effective bone metaplasia was reported but being restricted to less than 13% of hundreds of aortic valves and dozens of mitral valves affected by dystrophic calcification (Mohler E.R. 3rd *et al.*, 2001; Steiner I. *et al.*, 2007) and no osteogenetic features resulted from the present histologic and ultrastructural examinations as well.

Notably, complete overlapping between reactivity to von Kossa reaction and HA Raman map was found to be extended to the map patterns revealing the deposition of

phospholipid/triglyceride moieties, whereas those of cholesterol and carotenoids were restricted to the areas in which phospholipids/triglycerides showed the highest intensities.

A first indication supplied by these results is that a direct role in calcification is played by phospholipid/triglyceride moieties with restriction to phospholipids because of their ionic nature. In addition, the lacking of cholesterol and carotenoids in the areas containing minor concentrations of HA leads to exclude that these lipids are essential at least for early mineralizing process. Thus calcification priming would have to be restricted to phospholipids alone, supporting the concept of these amphiphilic molecules being major HA nucleators (Kim K.M. and Huang S.N., 1971; Kim K.M. and Trump B.F., 1975; Kim K.M., 1976; Kim K.M. *et al.*, 1976). Consistently with this assumption, the CuB-reacted thin sections showed release and accumulation of a material which likely contains abundant phospholipids in that (i) it must be anionic, because of their strong affinity for CuB which is a basic phthalocyanin, and (ii) it clearly appears in parallel with disappearance of plasmamembranes and organule membranes. Interestingly, analogous deposition of CuB-reacting pro-calcific material was found to represent one of the degenerative events involving dying AVICs in experimental calcification induced using both *in vivo* (Ortolani F. *et al.*, 2002a; Ortolani F. *et al.*, 2002b; Ortolani F. *et al.*, 2003; Ortolani F. *et al.*, 2007) and *in vitro* models colocalizing with early HA crystallization (Ortolani F. *et al.*, 2010; Bonetti A. *et al.*, 2012).

It is noteworthy that HA deposition at level of calcific nodules was so prominent that the underlying chemical components were not detectable at all because of complete masking effect.

With the exception of calcific nuclei, the presence of abundant cholesterol at level of valve the other calcific foci resulted from Raman microspectrometry consistently with the reports that cholesterol deposition is a hallmark of CAVS (Otto C.M.*et al.*, 1994; O'Brien K.D. *et al.*, 1996; Pohle K. *et al.*, 2001) as well as the concept that CAVS is a kind of valve atherosclerosis (Agmon Y. *et al.*, 2001; Branch K.R. *et al.*, 2002; Novaro G.M. and Griffin B.P., 2003; Kuusisto J. *et al.*, 2005). Additionally, overabundance of phospholipids/ triglycerides is not quantitatively reliable to cell degeneration only, suggesting that an exogenous uptake of these molecules occurs *via* LDL endocytosis. This concept is strengthened by Raman detection of carotenoids, as discussed below.

Although the major HA nucleating role is played by phospholipids, it cannot be excluded that also cholesterol contained within LDLs might contribute to mineralization once these lipoproteins undergo oxidation thereby exerting toxic effects on AVICs and concurrent transformation of macrophages into foam cells followed by pro-calcific cell death, as reported

to occur for CAVS (Olsson M. *et al.*, 1999; Mohty D. *et al.*, 2008). Consistently, effective formation of oxysterols was reported to occur in atherosclerotic lesions (Carpenter K.L. *et al.*, 1995; Brown A.J. and Jessup W., 1999).

Additional result gained for the first time was the identification of carotenoids accumulated within the calcific areas of CAVS-affected valves, so exhibiting close co-localization with cholesterol. Of interest, Raman microspectroscopy already revealed the presence of carotenoids, as well as their co-localization with lipid/cholesterol deposits, at level of atherosclerotic plaques (Redd D.C. *et al.*, 1991; Baraga J.J. *et al.*, 1992; Römer T.J. *et al.*, 1998; van de Poll S.W. *et al.*, 2003). This further corroborates the concept of CAVS to represent valve atherosclerosis.

Since it is well known that these lipophilic molecules are mostly transported in the human plasma by LDLs in addition to cholesterol and phospholipids (Parker R.S., 1996), it ensues that their presence correlates with an uptake of lipoprotein-cholesterol-carotenoid complexes by lipid-loading macrophages and/or AVICs *via* their native LDL-receptors, at the early stages of CAVS disease. Subsequently, these complexes could merge with the membrane-derived phospholipids/cholesterol released during initial cell degeneration and then retained in dying cells and cell-derived products.

Concerning collagen detection with Raman microspectroscopy, its presence generally appeared in areas coinciding with those showing eosinophilia in their counterpart on adjacent cryosections undergone histological staining and von-Kossa reaction, without allowing a discrimination between those still containing collagen fibers and those occupied by unarrayed collagen because of fiber dissociation/degeneration (Kaden J.J. *et al.*, 2003). In addition, the areas in which Raman maps revealed collagen absence roughly to correspond to those completely lacking in eosinophilia in their counterparts. Both results lead to assume ongoing collagen degeneration to result in protein denaturation and these areas to represent the most aged foci affected by the pro-calcific degenerative processes.

Electron microscopy pictures of CAVS-affected human valves revealed the presence of foam cells and monohydrate cholesterol clefts, consistently with previous findings (Olsson M. *et al.*, 1999). It is noteworthy the observation of mixing between neutral lipid formed light droplets and acidic lipid containing CuB-reactive droplets, suggesting foam cells to undergo analogous pro-calcific degeneration, with the difference that CuB-reactive lipid droplets will contain greater moieties of neutral lipids, possibly destined to undergo subsequent acidification by oxidative processes.

Uptake of subendothelial LDLs and cytosolic accumulation of LDL-derived lipids represent a critical step in foam cell formation. Most of the LDL in atherosclerotic plaques is aggregated and avidly bound to the subendothelial matrix (Smith E.B. *et al*., 1976; Tabas I., 1999; Boren J. *et al*., 2000). Aggregated lipoproteins require different uptake than those used for endocytosis of monomeric lipoproteins, as described below.

The possible involvement of LDL suggested by the obtained Raman data led to investigate possible pro-calcific AVIC responses by combining for the first time pro-calcific models with a pro-atherosclerotic model already used to study vascular smooth muscle cells (Llorente-Cortés V. *et al*., 1998), which includes the subministration of native low density lipoproteins (nLDL) and aggregated ones (agLDL) to the cultured cells.

Consistently with the identification of specific LDL receptor 5 (Lrp5) reported for AVICs (Rajamannan N.M. *et al*., 2005), effective LDL uptake was directly shown by the ultrastructural visualization of intracellular vacuoles containing either nLDL or agLDLs and indirectly by the chromatographically detected changes in LDL-related lipid contents, i.e. accumulated esterified cholesterol (EC) and triglycerides (TG), these latter resulting from intracytoplasmic phospholipid processing and storage.

Treatments with nLDLs were chromatographically found to result in no or negligible increases in intracellular EC and TGs, except for 2.0-Pi-LPS-bCM-nLDL-cultures and 3.0-Pi-LPS-bCM-nLDL-cultures.

In contrast, increased amounts of intracellular both CE and TGs were detected after treatments with agLDLs. The datum concerning CE agrees with previous finding concerning VSMCs (Llorente-Cortés V. *et al*., 1998) besides being consistent with the ultrastructural visualization of many vacuoles containing beaded elongated structures.

The above different changes in lipid amounts indicate different internalization rates by AVICs to exist, comparing nLDLs to agLDLs. These results can be explained taking in account that distinct pathways are elicited, since specific Lrp5 is involved for nLDLs and LDL-receptor-related-protein-1 (LRP1) for agLDLs, as shown for cultured human VSMCs (Llorente-Cortés V. *et al*., 2000). Additionally, it is noteworthy that opposite cell responses are triggered by intracellular cholesterol since it downregulates Lrp5 and upregulates LRP1 (Llorente-Cortés V. *et al*., 2002a; 2002b).

In addition, the constant unchanging of CE content in all nLDL-treated cultures as well as its constant marked increase in all agLDL-treated ones, lead to argue that neither Pi concentration nor the presence of pro-inflammatory factors can influence AVIC capability to uptake LDLs for both cases.

The estimations of TGs seem to be not consistent with such a conclusion, since these lipids increased in 2.0-Pi-LPS-bCM-nLDL-cultures and 3.0-Pi-LPS-bCM-nLDL-cultures and there was a lesser increase in 3.0-Pi-LPS-bCM-agLDL-cultures compared to the increases estimated for agLDL-cultures and 2.0-Pi-LPS-bCM-agLDL-cultures.

At first glance, these results seem to be inconsistent with the LDL-uptake propensity assumed above. However, several speculations could explain these discrepancies. First, TG increasing in 2.0-Pi-LPS-bCM-nLDL-cultures and 3.0-Pi-LPS-bCM-nLDL-cultures might depend on endogenous mechanisms someway evocated by the pro-inflammatory agents involved in the superstimulation, i.e. added LPS and/or cytokines derived from LPS-stimulated macrophages, which might exert endogenous TG synthesis. As a matter, it was found that stimulation with IL-1β increases intracellular TGs in von Kupffer cells and hepatic stellate cells (Miura K. *et al*., 2010). Second thing, the lesser TG increase in 3.0-Pi-LPS-bCM-agLDL-cultures may be explained by the fact that not all the internalized agLDL-derived PLs are converted into TGs because of their ongoing degeneration, implying diminished activity of the inherent enzymatical machinery, with not converted PLs being degraded and contributing to generate the heterogeneously electrondense lipid droplets revealed by electron microscopy.

Spectrophotometric assays revealed that agLDL-treatment resulted in increased calcium levels at greater extent and earlier than nLDLs did, i.e. at three day of incubation instead of nine. Of note, agLDLs have been reported to represent the main character in the atherogenic process (Haka A.S. *et al*., 2009).

Moreover, calcium increases provoked by the basical pro-calcific stimulations (2.0-Pi-LPS-bCM-cultures and 3.0-Pi-LPS-bCM-cultures) were distinctly modified by the addition of nLDLs or agLDLs. Namely, significantly higher Ca content resulted after agLDL administration, whereas it was significantly lower after nLDL administration.

Of note, the opposite effect exerted by nLDLs is consistent with several *in vivo* and *in vitro* findings that nLDLs bind LPS *via* a mechanism involving apolipoprotein B-100, thus neutralizing the effects of this bacterial endotoxin (Van Lenten B.J. *et al*., 1986; Flegel W.A. *et al*., 1989; Victorov A.V. *et al*., 1989; Feingold K.R. *et al*., 1995; Netea M.G. *et al*., 1996; Netea M.G. *et al*., 1998). Thus the decrease of Ca levels observed in 2.0-Pi-LPS-bCM-nLDL-cultures and 3.0-Pi-LPS-bCM-nLDL-cultures might be postulated that the potential pro-calcific effect of LPS was inhibited by binding between endotoxin and lipoprotein.

Electron microscopy showed that treatments with nLDL solely correlated with features of cell suffering as in AVICs cultured at low Pi concentrations, mainly consisting in the

described abnormal enlargement of endoplasmic reticulum. These ER-stress patterns can be correlated with the finding that oxidized LDLs increase cytosolic calcium concentration in cultured porcine AVICs, thereby alterating ER capability to promote protein folding (Cai Z. *et al*., 2013) resulting in the accumulation of unfolded or misfolded proteins (Xu C. *et al*., 2005; Marciniak S.J. and Ron D., 2006; Ron D. and Walter P., 2007).

Conversely, combination of nLDL treatment with pro-calcific one resulted in no evident suffering features at ultrastructural level, indicating a possible anti-calcific role played by nLDL, consistently with the above mentioned spectrophotometrical calcium estimations.

Administration of agLDLs alone was not associated with appearance of evident features of cell suffering, suggesting increased calcium levels in AVICs to occur *via* a different mechanism, maybe involving LRP1. This is consistent with the finding that such a receptor protein is overexpressed in presence of agLDLs (Llorente-Cortés V. *et al*., 2002b), thereby increasing the number of its cytoplasmic domains, which are characterized by capability to retain calcium (Bacskai B.J., *et al*., 2000; Andersen O.M. *et al*., 2003).

Conversely, agLDL combined with Pi, LPS and bCM exacerbated pro-calcific AVIC degeneration, culminating in the formation of the same final mineralization products described above, i.e. CDPs and *calcospherulae*.

Taken together, the obtained results lead to the conclusion that in both *in vitro* metastatic-like and dystrophic-like conditions as well as in actual CAVS, AVICs calcification (i) depends on the described peculiar cell degeneration, being (ii) Pi concentration the major determinant, (iii) pro-inflammatory agents potential enhancing factors, and (iv) agLDLs additional exacerbating factors.

6. REFERENCES

- Abreo K., Adlakha A., Kilpatrick S., Flanagan R., Webb R., Shakamuri S. 1993. The milk-alkali syndrome. A reversible form of acute renal failure. *Arch. Intern. Med.* 153 (8): 1005-1010.
- Agmon Y., Khandheria B.K., Miessner I., Sicks J.R., O'Fallon W.M., Wiebers D.O., Whisnant J.P., Seward J.B., Tajik A.J. 2001. Aortic valve sclerosis and aortic atherosclerosis: different manifestations of the same disease? Insights from a population-based study. *J. Am. Coll. Cardiol.* 38: 827-834.
- Aikawa E., Nahrendorf M., Sosnovik D., Lok V.M., Jaffer F.A., Aikawa M., Weissleder R. 2007. Multimodality molecular imaging identifies proteolytic and osteogenic activities in early aortic valve disease. *Circulation*. 115(3): 377-386.
- Alexandraki K., Piperi C., Kalofoutis C., Singh J., Alaveras A., Kalofoutis A., 2006. Inflammatory process in type 2 diabetes: The role of cytokines. *Ann. N. Y. Acad. Sci.* 1084: 89-117.
- Anber V., Griffin B.A., McConnell M., Packard C.J., Shepherd J. 1996. Influence of plasma lipid and LDL-subfraction profile on the interaction between low density lipoprotein with human arterial wall proteoglycans. *Atherosclerosis*. 124: 261-71.
- Andersen O.M., Vorum H., Honoré B., Thøgersen H.C. 2003 Ca2+ binding to complement-type repeat domains 5 and 6 from the low-density lipoprotein receptor-related protein. *BMC Biochem*. 18: 4-7.
- Anderson H.C. 1967. Electron microscopic studies of induced cartilage development and calcification. *J. Cell Biol*. 35: 81-101.
- Anderson H.C. 1969. Vesicles associated with calcification in the matrix of epiphyseal cartilage. *J. Cell Biol*. 41: 57-72.
- Anderson H.C. 1976. Matrix vesicle calcification. *Fed. Proc*. 35 (2): 104.
- Anderson H.C., Sajdera S.W. 1976. Calcification of rachitic cartilage to study matrix vesicle function. *Fed. Proc*. 35 (2): 148-153.
- Anderson H.C. 1980. Calcification processes. *Pathol. Annu*. 15 (Pt 2): 45-75.
- Anderson H.C. 1983. Calcific diseases. A concept. *Arch. Pathol. Lab. Med*. 107 (7): 341-348.

- Anderson H.C., Morris D.C. 1993. Mineralization. Physiology and Pharmacology of Bone. *Handbook of Experimental Pharmacology*. 107: 267-298
- Anderson HC. 1995. Molecular biology of matrix vesicles. *Clin. Orthop. Relat. Res*. 314: 266-280.
- Anderson H.C., Sipe J.B., Hessle L., Dhanyamraju R., Atti E., Camacho N.P., Millán J.L. 2004. Impaired calcification around matrix vesicles of growth plate and bone in alkaline phosphatase-deficient mice. *Am. J. Pathol*. 164 (3): 841-847.
- Arsenault A.L., Frankland B.W., Ottensmeyer F.P. Vectorial sequence of mineralization in the turkey leg tendon determined by electron microscopic imaging. *Calcif. Tissue Int.* 48 (1): 46-55.
- Babu A.N., Meng X., Zou N., Yang X., Wang M., Song Y., Cleveland J.C., Weyant M., Banerjee A., Fullerton D.A. 2008. Lipopolysaccharide stimulation of human aortic valve interstitial cells activates inflammation and osteogenesis. *Ann. Thorac. Surg*. 86: 71-76.
- Bacskai B.J., Xia M.Q., Strickland D.K., Rebeck G.W., Hyman B.T. 2000. The endocytic receptor protein LRP also mediates neuronal calcium signaling via N-methyl-D-aspartate receptors. *Proc. Natl. Acad. Sci. USA*. 97: 11551-11556.
- Baraga J.J., Feld M.S., Rava R.P. 1992. In situ optical histochemistry of human artery using near infrared Fourier transform Raman spectroscopy. *Proc. Natl. Acad. Sci. U. S. A.* 89: 3473-3477.
- Baughman R.P., Janovcik J., Ray Et Al M. 2013. Calcium and vitamin D metabolism in sarcoidosis. *Sarcoidosis Vasc. Diffuse Lung Dis*. 30 (2): 113-120.
- Beadenkopf W.G., Daoud A.S., Love B.M. 1964. Calcification in the coronary arteries and its relationship to arteriosclerosis and myocardial infarction. *Am. J. Roentgenol. Radium Ther. Nucl. Med.* 92: 865-871.
- Beleites C and Sergo V. HyperSpec: a package to handle hyperspectral data sets in R. R package version 0.98-20120923. http://hyperspec.r-forge.r-project.org
- Bernard G.W. 1972. Ultrastructural observations of initial calcification in dentine and enamel. *J. Ultrastruct. Res*. 41 (1): 1-17.
- Bligh E.G., Dyer W.J. 1959. A rapid method of total lipid extraction and purification. *Can. J. Biochem. Physiol.* 37 (8): 911-917.
- Binkert C., Demetriou M., Sukhu B., Szweras M., Tenenbaum H.C., Dennis J.W. 1999. Regulation of osteogenesis by fetuin. J Biol Chem. 274 (40): 28514-28520.
- Block G.A. 2000. Prevalence and clinical consequences of elevated Ca x P product in hemodialysis patients. *Clin. Nephrol*. 54: 318-324.

- Boesten L.S., Zadelaar A.S., Van Nieuwkoop A., Gijbels M.J., De Winther M.P., Havekes L.M., Van Vlijmen B.J. 2005. Tumor necrosis factor-alpha promotes atherosclerotic lesion progression in APOE*3-leiden transgenic mice. *Cardiovasc. Res*. 66 (1): 179-85.
- Bonetti A., Della Mora A., Contin M., Tubaro F., Marchini M., Ortolani F. 2012. Ultrastructural and spectrophotometric study on the effects of putative triggers on aortic valve interstitial cells in in vitro models simulating metastatic calcification. *Anat. Rec.* 295: 1117-1127.
- Bonucci E. 1967. Fine structure of early cartilage calcification. *J. Ultrastruct. Res*. 20: 33-50.
- Bonucci E. 1971. The locus of initial calcification in cartilage and bone. *Clin. Orthop*. 78: 108-139.
- Bonucci E. 1984. The structural basis of calcification. In: "Ultrastructure of connective tissue", A. Ruggeri and P.M. Motta, eds., Martinus Nijhoff Publ., Boston, The Hague, Dordrecht, Lancaster.
- Boren J., Gustafsson M., Skalen K., Flood C., Innerarity T.L. 2000. Role of extracellular retention of low density lipoproteins in atherosclerosis. *Curr. Opin. Lipidol*. 11: 451-456.
- Borgers M., Thoné F. 1976. Further characterization of phosphatase activities using non-specific substrates. *Histochem. J.* 8: 301-317.
- Boskey A.L., Posner A.S. 1976. Extraction of a calcium-phospholipid-phosphate complex from bone. *Calcif. Tissue Res*. 19 (4): 273-283.
- Boskey A.L., Goldberg M.R., Posner A.S. 1977. Calcium-phopholipid-phosphate complexes in mineralizing tissue. *Proc. Soc. Exp. Biol. Med*. 157: 588-591.
- Boskey A.L., Wians F.H. Jr, Hauschka P.V. 1985. The effect of osteocalcin on in vitro lipid-induced hydroxyapatite formation and seeded hydroxyapatite growth. *Calcif. Tissue Int*. 37 (1): 57-62.
- Boskey A.L., Bullough P.G., Vigorita V., Di Carlo E. 1988. Calcium acidic phospholipid-phosphate complexes in human hydroxyapatite containing pathologic deposits. *Am. J. Pathol*. 133: 22-29.
- Boström K., Watson K.E., Horn S., Wortham C., Herman I.M., Demer L.L. 1993. Bone morphogenetic protein expression in human atherosclerotic lesions. *J. Clin. Invest*. 91 (4): 1800-1809.
- Boyan B.D., Boskey A.L. 1984. Co-isolation of proteolipids and calcium-phospholipid-phosphate complexes. *Calcif. Tissue Int.* 36 (2): 214-218.

- Branch K.R., O'Brien K.D., Otto C.M. 2002. Aortic valve sclerosis as a marker of active atherosclerosis. *Curr. Cardiol. Rep.* 4: 111-117.
- Bratton D.L., Fadok V.A., Richter D.A., Kailey J.M., Guthrie L.A., Henson P.M. 1997. Appearance of phosphatidylserine on apoptotic cells requires calcium-mediated nonspecific flip-flop and is enhanced by loss of the aminophospholipid translocase. *J. Biol. Chem*. 272: 26159-26165.
- Bravo R., Vicencio J.M., Parra V., Troncoso R., Munoz J.P., Bui M., Quiroga C., Rodriguez A.E., Verdejo H.E., Ferreira J., Iglewski M., Chiong M., Simmen T., Zorzano A., Hill J.A., Rothermel B.A., Szabadkai G., Lavandero S. 2011. Increased ER-mitochondrial coupling promotes mitochondrial respiration and bioenergetics during early phases of ER stress. *J. Cell. Sci.* 124: 2143-2152.
- Briand M., Lemieux I., Dumesnil J.G., Mathieu P., Cartier A., Després J.P., Arsenault M. Couet J., Pibarot P. 2006. Metabolic syndrome negatively influences disease progression and prognosis in aortic stenosis. *J. Am. Coll. Cardiol*. 47 (11): 2229-2236.
- Brown A.J., Jessup W. 1999. Oxysterols and atherosclerosis. *Atherosclerosis.* 142: 1-28.
- Bucay N., Sarosi I., Dunstan C.R., Morony S., Tarpley J., Capparelli C., Scully S., Tan H.L., Xu W., Lacey D.L., Boyle W.J., Simonet W.S. 1998. Osteoprotegerin-deficient mice develop early onset osteoporosis and arterial calcification. *Genes Dev*. 12 (9): 1260-1268.
- Burke A.P., Kolodgie F.D., Virmani R. 2007. Fetuin-A, valve calcification, and diabetes: what do we understand? *Circulation*. 115 (19): 2464-2467.
- Burnell J.M., Teubner E.J., Miller A.G. 1980. Norman maturational changes in bone matrix, mineral, and crystal size in the rat. *Calcif. Tissue Int.* 31: 13-19.
- Cai Z., Li F., Gong W., Liu W., Duan Q., Chen C., Ni L., Xia Y., Cianflone K., Dong N., Wang D.W. 2013. Endoplasmic reticulum stress participates in aortic valve calcification in hypercholesterolemic animals. *Arterioscler. Thromb. Vasc. Biol*. 33 (10): 2345-2354.
- Calara F., Dimayuga P., Niemann A., Thyberg J., Diczfalusy U., Witztum J.L., Palinski W., Shah P.K., Cercek B., Nilsson J., Regnström J. 1998. An animal model to study local oxidation of LDL and its biological effects in the arterial wall. *Arterioscler. Thromb. Vasc. Biol*. 18 (6): 884-893.
- Carpenter K.L., Taylor S.E., van der Veen C., Williamson B.K., Ballantine J.A., Mitchinson M.J. 1995. Lipids and oxidised lipids in human atherosclerotic lesions at different stages of development. *Biochim. Biophys. Acta.* 1256: 141-150.
- Cecil R.N.A., Anderson H.C. 1978. Freeze-fracture studies of matrix vesicle calcification in epiphyseal growth plate. *Metabolic Bone Disease and Related Research*. 1 (2): 89-95.

- Chantelau E., Lee K.M., Jungblut R. 1997. Distal arterial occlusive disease in diabetes is related to medial arterial calcification. *Exp. Clin. Endocrinol. Diabetes*. 105 (2): 11-13.
- Chen N.X., O'Neill K.D., Duan D., Moe S.M. 2002. Phosphorus and uremic serum up-regulate osteopontin expression in vascular smooth muscle cells. *Kidney Int*. 62 (5): 1724-1731.
- Cimini M., Boughner D.R., Ronald J.A., Aldington L., Rogers K.A. 2005. Development of aortic valve sclerosis in a rabbit model of atherosclerosis: an immunohistochemical and histological study. *J. Heart Valve Dis*. 14 (3): 365-375.
- Clark-Greuel J.N., Connolly J.M., Sorichillo E., Narula N.R., Rapoport H.S., Mohler E.R. 3rd, Gorman J.H. 3rd, Gorman R.C., Levy R.J. 2007. Transforming growth factor-beta1 mechanisms in aortic valve calcification: increased alkaline phosphatase and related events. *Ann Thorac Surg*. 83 (3): 946-953.
- Clarke M.C.H., Littlewood T.D., Figg N., Maguire J.J., Davenport A.P., Goddard M., Bennett M.R. 2008. Chronic apoptosis of vascular smooth muscle cells accelerates atherosclerosis and promotes calcification and medial degeneration. *Circ. Res.* 102: 1529-1538.
- Cohen D.J., Malave D., Ghidoni J.J., Iakovidis P., Everett M.M., You S., Liu Y., Boyan B.D. 2004. Role of oral bacterial flora in calcific aortic stenosis: an animal model. *Ann. Thorac. Surg*. 77: 537-543.
- Dean D.D., Schwartz Z.V., Muniz O.E., Gomez R., Swain L.D., Howell D.S., Boyan B.D. 1992. Matrix vesicles contain metalloproteinases that degrade proteoglycans. *Bone Miner*. 17 (2): 172-176.
- Debnath J., Baehrecke E.H., Kroemer G. 2005. Does autophagy contribute to cell death? *Autophagy*. 1: 66-74.
- de Brito O.M., Scorrano L. 2008. Mitofusin 2 tethers endoplasmic reticulum to mitochondria. *Nature*. 456: 605-610.
- De Gelder J., De Gussem K., Vandenabeele P., Vancanneyt M., De Vos P., Moens L. 2007. Methods for extracting biochemical information from bacterial Raman spectra: focus on a group of structurally similar biomolecules--fatty acids. *Anal. Chim. Acta*. 603 (2): 167-175.
- Della Rocca F., Sartore S., Guidolin D., Bertiplaglia B., Gerosa G., Casarotto D., Pauletto P. 2000. Cell composition of the human pulmonary valve: a comparative study with the aortic valve. The VESALIO Project. Vitalitate Exornatum Succedaneum Aorticum labore Ingegnoso Obtinebitur. *Ann. Thorac. Surg*. 70 (5): 1594-1600.

- Demer L.L. 1991. Effect of calcification on in vivo mechanical response of rabbit arteries to balloon dilation. *Circulation*. 83 (6): 2083-2093.
- Demer L.L. 2002. Vascular calcification and osteoporosis: inflammatory responses to oxidized lipids. *Int. J. Epidemiol*. 31 (4): 737-741.
- Dhingra R., Sullivan L.M., Fox C.S., Wang T.J., D'Agostino R.B. Sr, Gaziano J.M., Vasan R.S. 2007. Relations of serum phosphorus and calcium levels to the incidence of cardiovascular disease in the community. *Arch. Intern. Med*. 167 (9): 879-885.
- Dmitrovsky E., Boskey A.L. 1985. Calcium-acidic phospholipid-phosphate complexes in human atherosclerotic aortas. *Calcif. Tissue Int*. 37 (2): 121-125.
- Doherty T.M., Detrano R.C. 1994. Coronary arterial calcification as an active process: a new perspective on an old problem. *Calcif. Tissue Int*. 54 (3): 224-230.
- Doherty T.M., Fitzpatrick L.A., Inoue D., Qiao J.H., Fishbein M.C., Detrano R.C., Shah P.K., Rajavashisth T.B. 2004. Molecular, endocrine, and genetic mechanisms of arterial calcification. *Endocr. Rev.* 25 (4): 629-672.
- Drolet M.C., Arsenault M., Couet J. 2003. Experimental aortic valve stenosis in rabbits. *J. Am. Coll. Cardiol*. 41 (7): 1211-1217.
- Drolet M.C., Roussel E., Deshaies Y., Couet J., Arsenault M. 2006. A high fat/high carbohydrate diet induces aortic valve disease in C57BL/6J mice. *J. Am. Coll. Cardiol*. 47 (4): 850-855.
- Edep M.E., Shirani J., Wolf P., Brown D.L. 2000. Matrix metalloproteinase expression in nonrheumatic aortic stenosis. *Cardiovasc. Pathol*. 9 (5): 281-286.
- Edmonds M.E., Morrison N., Laws J.W., Watkins P.J. 1982. Medial arterial calcification and diabetic neuropathy. *Br. Med. J. Clin. Res.* 284: 928-930.
- Edmonds M.E. 2000. Medial arterial calcification and diabetes mellitus. Z. Kardiol. 89 Suppl 2: 101-104.
- Eisenmann D.R., Glick P.L. 1972. Ultrastructure of initial crystal formation in dentin. *J. Ultrastruct. Res.* 41 (1): 18-28.
- Ellam T.J., Chico T.J. 2012. Phosphate: the new cholesterol? The role of the phosphate axis in non-uremic vascular disease. *Atherosclerosis*. 220 (2): 310-318.
- Elliott R.J., McGrath L.T. 1994. Calcification of the human thoracic aorta during aging. *Calcif. Tissue Int.* 54 (4): 268-273.
- Esterbauer H., Gebicki J., Puhl H., Jürgens G. 1992. The role of lipid peroxidation and antioxidants in oxidative modification of LDL. *Free Radic. Biol. Med*. 13 (4): 341-390.

- Everhart J.E., Pettitt D.J., Knowler W.C., Rose F.A., Bennett P.H. 1988. Medial arterial calcification and its association with mortality and complications of diabetes. *Diabetologia*. 31 (1): 16-23.
- Farb A., Burke A.P., Tang A.L., Liang T.Y., Mannan P., Smialek J., Virmani R. 1996. Coronary plaque erosion without rupture into a lipid core. A frequent cause of coronary thrombosis in sudden coronary death. *Circulation*. 93 (7): 1354-1363.
- Farrow E.G., Imel E.A., White K.E. 2011. Miscellaneous non-inflammatory musculoskeletal conditions. Hyperphosphatemic familial tumoral calcinosis (FGF23, GALNT3 and αKlotho). *Best Pract. Res. Clin. Rheumatol*. 25 (5): 735-747.
- Feingold K.R., Funk J.L., Moser A.H., Shigenaga J.K., Rapp J.H., Grunfeld C. 1995. Role for circulating lipoproteins in protection from endotoxin toxicity. *Infect. Immun*. 52: 1930-1935.
- Fishbein M.C., Levy R.J., Ferrans V.J., Dearden L.C., Nashef A., Goodman A.P., Carpentier A. 1982. Calcifications of cardiac valve bioprostheses. Biochemical, histologic, and ultrastructural observations in a subcutaneous implantation model system. *J. Thorac. Cardiovasc. Surg*. 83(4): 602-609.
- Fitzpatrick L.A., Severson A., Edwards W.D., Ingram R.T. 1994. Diffuse calcification in human coronary arteries. Association of osteopontin with atherosclerosis. *J. Clin. Invest*. 94 (4): 1597-1604.
- Flegel W.A., Wolpl A., Mannel D.N., Northoff H. 1989. Inhibition of endotoxin-induced activation of human monocytes by human lipoproteins. *Infect. Immun*. 57: 2237-2245.
- Fleisch H., Russell R.G., Straumann F. 1966. Effect of pyrophosphate on hydroxyapatite and its implications in calcium homeostasis. *Nature*. 212 (5065): 901-903.
- Foley R.N., Parfrey P.S., Sarnak M.J. 1998. Clinical epidemiology of cardiovascular disease in chronic renal disease. *Am. J. Kidney Dis*. 32 (5 Suppl 3): S112-119.
- Foley R.N. 2009. Phosphate levels and cardiovascular disease in the general population. *Clin. J. Am. Soc. Nephrol*. 4: 1136-1139.
- Freeman R.V., Otto C.M. 2005. Spectrum of calcific aortic valve disease: pathogenesis, disease progression, and treatment strategies. *Circulation*. 111 (24): 3316-3326.
- Frostergård J., Ulfgren A.K., Nyberg P., Hedin U., Swedenborg J., Ulf Andersson U., Hansson G.K. 1999. Cytokine expression in advanced human atherosclerotic plaques: dominance of pro-inflammatory (Th1) and macrophage-stimulating cytokines. *Atherosclerosis*. 145: 33-43.

- Fukumoto S. 2005. Post-translational modification of Fibroblast Growth Factor 23. *Ther. Apher. Dial*. 9 (4): 319-322.
- Genge B.R., Sauer G.R., Wu L.N., McLean F.M., Wuthier R.E. 1988. Correlation between loss of alkaline phosphatase activity and accumulation of calcium during matrix vesicle-mediated mineralization. *J. Biol. Chem*. 263 (34): 18513-18519.
- Gentile S., Bizzarro A., Marmo R., de Bellis A., Orlando C. 1990. Medial arterial calcification and diabetic neuropathy. *Acta Diabetol. Lat*. 27 (3): 243-253.
- Giachelli C.M., Bae N., Almeida M., Denhardt D.T., Alpers C.E., Schwartz S.M. 1993. Osteopontin is elevated during neointima formation in rat arteries and is a novel component of human atherosclerotic plaques. *J. Clin. Invest*. 92 (4): 1686-1696.
- Giachelli C.M. 1999. Ectopic calcification: gathering hard facts about soft tissue mineralization. *Am. J. Pathol*. 154 (3): 671-675.
- Giachelli C.M. 2005. Inducers and inhibitors of biomineralization: lessons from pathological calcification. *Orthod. Craniofac. Res.* 8 (4): 229-231.
- Giachelli C.M., Speer M.Y., Li X., Rajachar R.M., Yang H. 2005. Regulation of vascular calcification: roles of phosphate and osteopontin. *Circ. Res*. 96 (7): 717-722.
- Giachelli C.M. 2009. The emerging role of phosphate in vascular calcification. *Kidney Int*. 75: 890-897.
- Giorgi C., De Stefani D., Bononi A., Rizzuto R., Pinton P. 2009. Structural and functional link between the mitochondrial network and the endoplasmic reticulum. *Int. J. Biochem. Cell. Biol*. 41: 1817-1827.
- Girardot M.N., Torrianni M., Dillehay D., Girardot J.M. 1995. Role of glutaraldehyde in calcification of porcine heart valves: Comparing cusp and wall. *J. Biomed. Mat. Res*. 29: 793-801.
- Glimcher M.J. 1981. On the form and function of bone: From molecules to organs: Wolff's law revisited. In: The Chemistry and Biology of Mineralized Connective Tissues. Veis A. Ed., New York, Elsevier-North-Holland. 617-673.
- Goldbarg S.H., Elmariah S., Miller M.A., Fuster V. 2007. Insights into degenerative aortic valve disease. *J. Am. Coll. Cardiol*. 50 (13): 1205-1213.
- Goulinet S., Chapman M.J. 1997. Plasma LDL and HDL subspecies are heterogenous in particle content of tocopherols and oxygenated and hydrocarbon carotenoids. Relevance to oxidative resistance and atherogenesis. *Arterioscler. Thromb. Vasc. Biol*. 17: 786-96.
- Griffiths G.W. 1979. Transport of glial cell acid phosphatase by endoplasmic reticulum into damaged axons. *J. Cell. Sci*. 36: 361-389.

- Guzik T.J., Mangalat D., Korbut R. 2006. Adipocytokines - novel link between inflammation and vascular function? *J. Physiol. Pharmacol.* 57 (4): 505-528.
- Haka A.S., Grosheva I., Chiang E., Buxbaum A.R. Baird B.A., Pierini L.M., Maxfield F.R. 2009. Macrophages create an acidic extracellular hydrolytic compartment to digest aggregated lipoproteins. *Mol. Biol. Cell.* 20: 4932-4940.
- Harmey D., Hessle L., Narisawa S., Johnson K.A., Terkeltaub R., Millán J.L. 2004. Concerted regulation of inorganic pyrophosphate and osteopontin by akp2, enpp1, and ank: an integrated model of the pathogenesis of mineralization disorders. *Am. J. Pathol*. 164 (4): 1199-1209.
- Hauschka P.V., Lian J.B., Gallop P.M. 1975. Direct identification of the calcium-binding amino acid, gamma-carboxyglutamate, in mineralized tissue. *Proc. Natl. Acad. Sci. U. S. A*. 72 (10): 3925-3929.
- Heiss A., DuChesne A., Denecke B., Grötzinger J., Yamamoto K., Renné T., Jahnen-Dechent W. 2003. Structural basis of calcification inhibition by alpha 2-HS glycoprotein/ fetuin-A. Formation of colloidal calciprotein particles. *J. Biol. Chem*. 278 (15): 13333-13341.
- Helske S., Oksjoki R., Lindstedt K.A., Lommi J., Turto H., Werkkala K., Kupari M., Kovanen P.T. 2008. Complement system is activated in stenotic aortic valves. *Atherosclerosis*. 196 (1): 190-200.
- Hessle L., Johnson K.A., Anderson H.C., Narisawa S., Sali A., Goding J.W., Terkeltaub R., Millan J.L. 2002. Tissue-nonspecific alkaline phosphatase and plasma cell membrane glycoprotein-1 are central antagonistic regulators of bone mineralization. *Proc. Natl. Acad. Sci. USA*. 99 (14): 9445-9449.
- Hoff H.F., O'Neil J. 1991. Lesion-derived low density lipoprotein and oxidized low density lipoprotein share a lability for aggregation, leading to enhanced macrophage degradation. *Arterioscler. Thromb*. 11 (5): 1209-1222.
- Hoshino T., Chow L.A., Hsu J.J., Perlowski A.A., Abedin M., Tobis J., Tintut Y., Mal A.K., Klug W.S., Demer L.L. 2009. Mechanical stress analysis of a rigid inclusion in distensible material: a model of atherosclerotic calcification and plaque vulnerability. *Am. J. Physiol. Heart. Circ. Physiol.* 297 (2): H802-810.
- Hume D.A., Underhill D.M., Sweet M.J., Ozinsky A.O., Liew F.Y., Aderem A. 2001. Macrophages exposed continuously to lipopolysaccharide and other agonists that act via toll-like receptors exhibit a sustained and additive activation state. BMC *Immunol*. 2: 11.

- Jahnen-Dechent W., Schäfer C., Ketteler M., McKee M.D. 2009. Mineral chaperones: a role for fetuin-A and osteopontin in the inhibition and regression of pathologic calcification. *J. Mol. Med*. 86 (4): 379-389.
- Jahnen-Dechent W., Heiss A., Schäfer C., Ketteler M. 2011. Fetuin-A Regulation of Calcified Matrix Metabolism. *Circ. Res*. 108: 1494-1509.
- Jian B., Narula N., Li Q.Y., Mohler E.R. 3rd, Levy R.J. 2003. Progression of aortic valve stenosis: TGF-beta1 is present in calcified aortic valve cusps and promotes aortic valve interstitial cell calcification via apoptosis. *Ann. Thorac. Surg*. 75 (2): 457-465.
- Johnson K., Goding J., Van Etten D., Sali A., Hu S.I., Farley D., Krug H., Hessle L., Millán J.L., Terkeltaub R. 2003. Linked deficiencies in extracellular PP(i) and osteopontin mediate pathologic calcification associated with defective PC-1 and ANK expression. *J. Bone Miner. Res.* 18 (6): 994-1004.
- Johnson K., Polewski M., van Etten D., Terkeltaub R. 2005. Chondrogenesis mediated by PPi depletion promotes spontaneous aortic calcification in NPP1-/- mice. *Arterioscler. Thromb. Vasc. Biol*. 25: 686-691.
- Jones G.W., Bowen I.D. 1979. The fine structural localization of acid phosphatase in pore cells of embryonic and newly hatched Deroceras reticulatum (Pulmonata: Stylommatophora). *Cell. Tissue Res*. 204: 253-265.
- Jono S., McKee M.D., Murry C.E., Shioi A., Nishizawa Y., Mori K., Morii H., Giachelli C.M. 2000. Phosphate regulation of vascular smooth muscle cell calcification. *Circ. Res*. 87: e10-e17.
- Jorge-Herrero E., Gutierrez M., Casillo-Olivares J.L. 1991. Calcification of soft tissue employed in the construction of heart valve bioprostheses: Study of different chemical treatments. *Biomaterials*. 12: 249-251.
- Jorge-Herrero E., Fernandez P., De La Torre N., Escudero C., Garcia-Paez J.M., Bujan J., Casillo-Olivares J.L. 1994. Inhibition of the calcification of porcine valve tissue by selective lipid removal. *Biomaterials*. 15: 815-820.
- Jovinge S., Ares M.P., Kallin B., Nilsson J. 1996. Human monocytes/macrophages release TNF-alpha in response to Ox-LDL. *Arterioscler. Thromb. Vasc. Biol.* 16 (12): 1573-1579.
- Juvonen J., Laurila A., Juvonen T., Aläkarppä H., Surcel H.M., Lounatmaa K., Kuusisto J., Saikku P. 1997. Detection of Chlamydia pneumoniae in human nonrheumatic stenotic aortic valves. *J. Am. Coll. Cardiol*. 29: 1054-1059.
- Kaden J.J., Dempfle C.E., Grobholz R., Tran H.T., Kiliç R., Sarikoç A., Brueckmann M., Vahl C., Hagl S., Haase K.K., Borggrefe M. 2003. Interleukin-1 beta promotes matrix

metalloproteinase expression and cell proliferation in calcific aortic valve stenosis. *Atherosclerosis*. 170 (2): 205-211.

- Kaden J.J., Dempfle C.E., Grobholz R., Fischer C.S., Vocke D.C., Kiliç R., Sarikoç A., Piñol R., Hagl S., Lang S., Brueckmann M., Borggrefe M. 2005a. Inflammatory regulation of extracellular matrix remodeling in calcific aortic valve stenosis. *Cardiovasc. Pathol*. 14 (2): 80-87.
- Kaden J.J., Kiliç R., Sarikoç A., Hagl S., Lang S., Hoffmann U., Brueckmann M., Borggrefe M. 2005b. Tumor necrosis factor alpha promotes an osteoblast-like phenotype in human aortic valve myofibroblasts: a potential regulatory mechanism of valvular calcification. *Int. J. Mol. Med*. 16 (5): 869-872.
- Khoo J.C., Miller E., McLoughlin P., Steinberg D. 1988. Enhanced macrophage uptake of low density lipoprotein after self-aggregation. *Arteriosclerosis*. 8 (4): 348-358.
- Kiechl S., Werner P., Knoflach M., Furtner M., Willeit J., Schett G. 2006. The osteoprotegerin/RANK/RANKL system: a bone key to vascular disease. *Expert Rev. Cardiovasc. Ther*. 4 (6): 801-811.
- Kim K.M., Huang S.N. 1971. Ultrastructural study of calcification of human aortic valve. *Lab. Invest.* 25 (5): 357-366.
- Kim K.M., Trump B.F. 1975. Amorphous calcium precipitates in human aortic valve. *Calcif. Tiss. Res*. 18: 155-160.
- Kim K.M. 1976. Calcification of matrix vesicles in human aortic valve and aortic media. *Federation Proc*. 35: 156-162.
- Kim K.M., Valigorsky J.M., Mergner W.J., Jones R.T., Pendergrass R.F., Trump B.F. 1976. Aging changes in the human aortic valve in relation to dystrophic calcification. *Hum. Pathol.* 7: 47-60.
- Kim K.M. 1995. Apoptosis and calcification. *Scanning Microsc*. 9: 1137-1175.
- Kirsch T., Ishikawa Y., Mwale F., Wuthier R.E. 1994. Roles of the nucleational core complex and collagens (types II and x) in calcification of growth plate cartilage matrix vesicles. *J. Biol. Chem*. 269: 20103-20109.
- Kirsch T., Wuthier R.E. 1994. Stimulation of calcification of growth plate cartilage matrix vesicles by binding to type II and X collagens. *J. Biol. Chem*. 269 (15): 11462-11469.
- Kirsch T., Nah H.D., Demuth D.R., Harrison G., Golub E.E., Adams S.L., Pacifici M. 1997. Annexin V-mediated calcium flux across membranes is dependent on the lipid composition: implications for cartilage mineralization. *Biochemistry*. 36 (11): 3359-3367.

- Kirsch T. 2006. Determinants of pathological mineralization. *Curr. Opin. Rheumatol.* 18: 174-180.
- Klionsky D.J., Abdalla F.C., Abeliovich H., Abraham R.T., *et al*. 2012 Guidelines for the use and interpretation of assays for monitoring autophagy. *Autophagy*. 8 (4): 445-544.
- Kockx M.M., De Meyer G.R., Muhring J., Jacob W., Bult H., Herman A.G. 1998. Apoptosis and related proteins in different stages of human atherosclerotic plaques. *Circulation*. 97 (23): 2307-2315.
- Kuusisto J., Räsänen K., Särkioja T., Alarakkola E., Kosma V.M. 2005. Atherosclerosis-like lesions of the aortic valve are common in adults of all ages: a necropsy study. *Heart.* 91: 576-582.
- Laemmli U.K., 1970. Cleavage of structural proteins during the assembly of the head of bacteriophage T4. *Nature*. 227 (5259): 680-685.
- Larsson T.E., Olauson H., Hagström E., Ingelsson E., Arnlöv J., Lind L., Sundström J. 2010. Conjoint effects of serum calcium and phosphate on risk of total, cardiovascular, and noncardiovascular mortality in the community. *Arterioscler. Thromb. Vasc. Biol*. 30 (2): 333-339.
- Lau W.L., Festing M.H., Giachelli C.M. 2010. Phosphate and vascular calcification: emerging role of the sodium-dependent phosphate cotransporter PiT-1. *Thromb. Haemost.* 104: 464-470.
- Lau W.L., Ix J.H. 2013. Clinical detection, risk factors, and cardiovascular consequences of medial arterial calcification: a pattern of vascular injury associated with aberrant mineral metabolism. *Semin. Nephrol*. 33 (2): 93-105.
- Lee Y.S., Chou Y.Y. 1998. Pathogenetic mechanism of senile calcific aortic stenosis: the role of apoptosis. *Chin Med J (Engl)*. 111: 934-939.
- Lehto S., Niskanen L., Suhonen M., Rönnemaa T., Laakso M. 1996. Medial artery calcification. A neglected harbinger of cardiovascular complications in non-insulin-dependent diabetes mellitus. *Arterioscler. Thromb. Vasc. Biol*. 16 (8): 978-983.
- Levine B., Yuan J. 2005. Autophagy in cell death: an innocent convict? *J. Clin. Invest.* 115: 2679-2688.
- Levy R.J., Lian J.B., Gallop P. 1979. Atherocalcin, a gamma-carboxyglutamic acid containing protein from atherosclerotic plaque. *Biochem. Biophys. Res. Commun*. 91 (1): 41-49.
- Levy R.J., Zenker J.A., Lian J.B. 1980. Vitamin K-dependent calcium-binding proteins in aortic valve calcification. *J. Clin. Invest*. 65: 563-566.

- Levy R.J., Gundberg C., Scheinman R. 1983a. The identification of the vitamin K-dependent bone protein, osteocalcin, as one of the γ-carboxyglutamic acid containing proteins present in calcified atherosclerotic plaque and mineralized heart valves. *Atherosclerosis*. 46: 49-56.
- Levy R.J., Zenker J.A., Bernhard W.F. 1983b. Porcine bioprosthetic valve calcification in bovine left ventricle-aorta shunts: studies of the deposition of vitamin K-dependent proteins. *Ann. Thorac. Surg*. 36: 187-192.
- Levy R.J., Schoen F.J., Levy J.T., Nelson A.C., Howard S.L., Oshry L.J. 1983c. Biologic determinants of distrophic calcification and osteocalcin deposition in glutaraldehyde-preserved porcine aortic valve leaflets implanted subcutaneosly in rats. *Am. J. Pathol.* 113: 143-155.
- Levy R.J., Schoen F.J., Flowers W.B., Staelin S.T. 1991. Initiation of mineralization in bioprosthetic heart valves studies of alkaline phosphatase activity and its inhibition by $AlCl_3$ or $FeCl_3$ preincubation. *J. Biomed. Mater. Res*. 25: 905-935.
- Li X., Giachelli C.M. 2004. The role of type III sodium-dependent phosphate cotransporter Pit-1in smooth muscle cell calcification. *Cardiovasc. Pathol*. 13 (Suppl 1): 185.
- Li X, Yang HY, Giachelli CM. 2006. Role of the sodium-dependent phosphate cotransporter, Pit-1, in vascular smooth muscle cell calcification. *Circ. Res*. 98 (7): 905-912.
- Li X., Giachelli C.M. 2007. Sodium-dependent phosphate cotransporters and vascular calcification. *Curr. Opin. Nephrol. Hypertens*. 16: 325-328.
- Li X., Fang P., Mai J., Choi E.T., Wang H., Yang X.F. 2013. Targeting mitochondrial reactive oxygen species as novel therapy for inflammatory diseases and cancers. *J. Hematol. Oncol.* 6: 19.
- Lian J.B., Skinner M., Glimcher M.J., Gallop P. 1976. The presence of gamma-carboxyglutamic acid in the proteins associated with ectopic calcification. *Biochem. Biophys. Res. Commun*. 73 (2): 349-355.
- Liberman M., Pesaro A.E., Carmo L.S., Serrano Jr C.V. 2013. Vascular calcification: pathophysiology and clinical implications. *Einstein (Sao Paulo)*. 11 (3): 376-382.
- Lin T.C., Tintut Y., Lyman A., Mack W., Demer L.L., Hsiai T.K., 2006. Mechanical response of a calcified plaque model to fluid shear force. *Ann. Biomed. Eng.* 34 (10): 1535-1541.
- Liu A.C., Gotlieb A.I. 2008. Transforming growth factor-beta regulates in vitro heart valve repair by activated valve interstitial cells. *Am. J. Pathol.* 173 (5): 1275-1285.

- Llorente-Cortés V., Martínez-González J., Badimon L. 1998. Esterified cholesterol accumulation induced by aggregated LDL uptake in human vascular smooth muscle cells is reduced by HMG-CoA reductase inhibitors. *Arterioscler. Thromb. Vasc. Biol*. 18 (5): 738-746.
- Llorente-Cortés V., Martínez-González J., Badimon L. 2000. LDL receptor-related protein mediates uptake of aggregated LDL in human vascular smooth muscle cells. *Arterioscler. Thromb. Vasc. Biol*. 20 (6): 1572-1579.
- Llorente-Cortés V., Otero-Viñas M., Hurt-Camejo E., Martínez-González J., Badimon L. 2002a. Human coronary smooth muscle cells internalize versican modified LDL through LDL receptor-related protein and LDL receptors. *Arterioscler. Thromb. Vasc. Biol*. 22: 387-393.
- Llorente-Cortés V., Otero-Viñas M., Sánchez S., Rodríguez C., Badimon L. 2002b. Low density lipoprotein upregulates low density lipoprotein receptor related protein expression in vascular smooth muscle cells. *Circulation*. 106: 3104-3110.
- Llorente-Cortés V., Otero-Viñas M., Camino-López S., Costales P., Badimon L. 2006. Cholesteryl esters of aggregated LDL are internalized by selective uptake in human vascular smooth muscle cells. *Arterioscler. Thromb. Vasc. Biol*. 26 (1): 117-123.
- Lomashvili K.A., Cobbs S., Hennigar R.A., Hardcastle K.I., O'Neill W.C. 2004. Phosphate-induced vascular calcification: role of pyrophosphate and osteopontin. *J. Am. Soc. Nephrol*. 15 (6): 1392-1401.
- Lomashvili K.A., Garg P., Narisawa S., Millan J.L., O'Neill W.C. 2008. Upregulation of alkaline phosphatase and pyrophosphate hydrolysis: potential mechanism for uremic vascular calcification. *Kidney Int.* 73 (9): 1024-1030.
- Lumachi F., Brunello A., Roma A., Basso U. 2009. Cancer-induced hypercalcemia. *Anticancer Res.* 29 (5): 1551-1555.
- Luo G., Ducy P., McKee M.D., Pinero G.J., Loyer E., Behringer R.R., Karsenty G. 1997. Spontaneous calcification of arteries and cartilage in mice lacking matrix GLA protein. *Nature*. 386 (6620): 78-81.
- Maeda S.S., Fortes E.M., Oliveira U.M., Borba V.C., Lazaretti-Castro M. 2006. Hypoparathyroidism and pseudohypoparathyroidism. *Arq. Bras. Endocrinol. Metabol*. 50 (4): 664-673.
- Malhotra J.D., Kaufman R.J. 2007. Endoplasmic reticulum stress and oxidative stress: a vicious cycle or a double-edged sword? *Antioxid. Redox Signal.* 12: 2277-2293.

- Malhotra J.D., Miao H., Zhang K., Wolfson A., Pennathur S., Pipe S.W., Kaufman R.J. 2008. Antioxidants reduce endoplasmic reticulum stress and improve protein secretion. *Proc. Natl. Acad. Sci. USA* 105: 18525-18530.
- Mallick N.P., Berlyne G.M. 1968. Arterial calcification after vitamin-D therapy in hyperphosphatemic renal failure. *Lancet.* 2 (7582): 1316-1320.
- Maranto A.R., Schoen F.J. 1988. Alkaline phosphatase activity of glutaraldehyde-treated bovine pericardium used in bioprosthetic cardiac valves. *Circ. Res*. 63 (4): 844-848.
- Marciniak S.J., Ron D. 2006. Endoplasmic reticulum stress signaling in disease. *Physiol. Rev*. 86: 1133-1149.
- Marcocci C., Cetani F. 2011. Clinical practice. Primary hyperparathyroidism. *N. Engl. J. Med*. 365 (25): 2389-2397.
- Martinet W., De Bie M., Schrijvers D.M., De Meyer G.R.Y., Herman A.G., Kockx M.M. 2004. 7-Ketocholesterol induces protein ubiquitination, myelin figure formation, and light chain 3 processing in vascular smooth muscle cells. *Arterioscler. Thromb. Vasc. Biol*. 24: 2296-2301.
- Mathews S.T., Rakhade S., Zhou X., Parker G.C., Coscina D.V., Grunberger G. 2006. Fetuin-null mice are protected against obesity and insulin resistance associated with aging. *Biochem Biophys Res Commun*. 350 (2): 437-443.
- Mathieu P., Voisine P., Pépin A., Shetty R., Savard N., Dagenais F. 2005. Calcification of human valve interstitial cells is dependent on alkaline phosphatase activity. *J. Heart Valve Dis*. 14 (3): 353-357.
- Mattjus P., Slotte J.P. 1996. Does cholesterol discriminate between sphingomyelin and phosphatidylcholine in mixed monolayers containing both phospholipids? *Chem. Phys. Lipids.* 81 (1): 69-80.
- Mazzone A., Venneri L., Berti S. 2007. Aortic valve stenosis and coronary artery disease: pathophysiological and clinical links. *J. Cardiovasc. Med*. 8 (12): 983-989.
- Meng X., Ao L., Song Y., Babu A.N., Yang X., Wang M., Weyant M.J., Dinarello C.A., Cleveland J.C. Jr, Fullerton D.A. 2008. Expression of functional Toll-like receptors 2 and 4 in human aortic valve interstitial cells: potential roles in aortic valve inflammation and stenosis. *Am. J. Physiol. Cell Physiol*. 294 (1): C29-35.
- Messika-Zeitoun D., Bielak L.F., Peyser P.A., Sheedy P.F., Turner S.T., Nkomo V.T., Breen J.F., Maalouf J., Scott C., Tajik A.J., Enriquez-Sarano M. 2007. Aortic valve calcification: determinants and progression in the population. *Arterioscler. Thromb. Vasc. Biol.* 27 (3): 642-648.

- Min H., Morony S., Sarosi I., Dunstan C.R., Capparelli C., Scully S., Van G., Kaufman S., Kostenuik P.J., Lacey D.L., Boyle W.J., Simonet W.S. 2000. Osteoprotegerin reverses osteoporosis by inhibiting endosteal osteoclasts and prevents vascular calcification by blocking a process resembling osteoclastogenesis. *J. Exp. Med.* 192 (4): 463-474.
- Miura K., Kodama Y., Inokuchi S., Schnabl B., Aoyama T., Ohnishi H., Olefsky J.M., Brenner D.A., Seki E. 2010. Toll-like receptor 9 promotes steatohepatitis by induction of interleukin-1β in mice. *Gastroenterology*. 139: 323-334.
- Mizushima N. 2005. The pleiotropic role of autophagy: from protein metabolism to bactericide. *Cell Death Differ*. 12: 1535-1541.
- Mohler E.R. 3rd, Chawla M.K., Chang A.W., Vyavahare N., Levy R.J., Graham L., Gannon F.H. 1999. Identification and characterization of calcifying valve cells from human and canine aortic valves. *J. Heart Valve Dis*. 8 (3): 254-260.
- Mohler E.R. 3rd, Gannon F., Reynolds C., Zimmerman R., Keane M.G., Kaplan F.S. 2001. Bone formation and inflammation in cardiac valves. *Circulation.* 103: 1522-1528.
- Mohler E.R. 3rd. 2004. Mechanisms of aortic valve calcification. *Am. J. Cardiol*. 94 (11): 1396-1402.
- Mohty D., Pibarot P., Després J.P, Côté C., Arsenault B., Cartier A., Cosnay P., Couture C., Mathieu P. 2008. Association between plasma LDL particle size, valvular accumulation of oxidized LDL, and inflammation in patients with aortic stenosis. *Arterioscler. Thromb. Vasc. Biol.* 28: 187-193.
- Mönckeberg J.C., 1904. The histological structure of normal and sclerotic aortic valves. *Virchows Arch. Path. Anat*. 176: 472-513.
- Mori H., Yamaguchi K., Fukushima H., Oribe Y., Kato N., Wakamatsu T., Uzawa H. 1992. Extensive arterial calcification of unknown etiology in a 29-year-old male. *Heart Vessels*. 7 (4): 211-214.
- Müller A.M., Cronen C., Kupferwasser L.I., Oelert H., Müller K.M., Kirkpatrick C.J. 2000. Expression of endothelial cell adhesion molecules on heart valves: up-regulation in degeneration as well as acute endocarditis. *J. Pathol*. 191 (1): 54-60.
- Munford R.S. 2010. Murine responses to endotoxin: another dirty little secret? *J. Infect. Dis*. 201: 175-177.
- Murphy H.C., Ala-Korpela M., White J.J., Raoof A., Bell J.D., Barnard M.L., Burns S.P., Iles R.A. 1997. Evidence for distinct behaviour of phosphatidylcholine and sphingomyelin at the low density lipoprotein surface. *Biochem. Biophys. Res. Commun*. 234 (3): 733-737.

- Murshed M., Schinke T., McKee M.D., Karsenty G. 2004. Extracellular matrix mineralization is regulated locally; different roles of two gla-containing proteins. *J. Cell. Biol*. 165 (5): 625-630.
- Nabeshima Y. 2008. The discovery of alpha-Klotho and FGF23 unveiled new insight into calcium and phosphate homeostasis. *Cell. Mol. Life Sci.* 65 (20): 3218-3230.
- Nakagawa N., Kinosaki M., Yamaguchi K., Shima N., Yasuda H., Yano K., Morinaga T., Higashio K. 1998. RANK is the essential signaling receptor for osteoclast differentiation factor in osteoclastogenesis. *Biochem. Biophys. Res. Commun*. 253 (2): 395-400.
- Nakamura S., Ishibashi-Ueda H., Niizuma S., Yoshihara F., Horio T., Kawano Y. 2009. Coronary calcification in patients with chronic kidney disease and coronary artery disease. *Clin. J. Am. Soc. Nephrol*. 4 (12): 1892-1900.
- Nagao S., Akagawa K.S., Okada F., Harada Y., Yagawa K., Kato K., Tanigawa Y. 1992. Species dependency of in vitro macrophage activation by bacterial peptidoglycans. *Microbiol. Immunol*. 36: 1155-1171.
- Netea M.G., Demacker P.N.M., Kullberg B.J., Boerman O.C., Verschueren I., Stalenhoef A.F.H., Van der Meer J.W.M. 1996.Low-density lipoprotein receptor-deficient mice are protected against lethal endotoxemia and severe Gram-negative infections. *J. Clin. Invest*. 97: 1366-1372.
- Netea M.G., Demacker P.N., Kullberg B.J., Jacobs L.E., Verver-Jansen T.J., Boerman O.C., Stalenhoef A.F., Van der Meer J.W. 1998. Bacterial lipopolysaccharide binds and stimulates cytokine-producing cells before neutralization by endogenous lipoproteins can occur. *Cytokine*. 10 (10): 766-772.
- Ng A.T., Peng D.H. 2011. Calciphylaxis. *Dermatol. Ther*. 24 (2): 256-262.
- Nievelstein-Post P., Mottino G., Fogelman A., Frank J. 1994. An ultrastructural study of lipoprotein accumulation in cardiac valves of the rabbit. *Arterioscler. Thromb*. 14 (7): 1151-1161.
- Nkomo V.T., Gardin J.M., Skelton T.N., Gottdiener J.S., Scott C.G., Enriquez-Sarano M. 2006. Burden of valvular heart diseases: a population-based study. *Lancet*. 368 (9540): 1005-1011.
- Noda T., Farquhar M.G. 1992. A non-autophagic pathway for diversion of ER secretory proteins to lysosomes. *J. Cell. Biol* 119: 85-97.
- Novaro G.M., Griffin B.P. 2003. Calcific aortic stenosis: another face of atherosclerosis? *Cleve. Clin. J. Med.* 70: 471-477.

- Nyström-Rosander C., Thelin S., Hjelm E., Lindquist O., Pahlson C., Friman G. 1997. High incidence of Chlamydia pneumoniae in sclerotic heart valves of patients undergoing aortic valve replacement. *Scand. J. Infect. Dis*. 29: 361-365.
- O'Brien K.D., Kuusisto J., Reichenbach D.D., Ferguson M., Giachelli C.M., Alpers C.E., Otto C.M. 1995. Osteopontin is expressed in human aortic valvular lesions. *Circulation*. 92 (8): 2163-2168.
- O'Brien K.D., Reichenbach D.D., Marcovina S.M., Kuusisto J., Alpers C.E., Otto C.M. 1996. Apolipoproteins B, (a), and E accumulate in the morphologically early lesion of 'degenerative' valvular aortic stenosis. *Arterioscler. Thromb. Vasc. Biol*. 16 (4): 523-532.
- Odutuga A.A., Prout R.E.S., Hoare R.J. 1975. Hydroxyapatite precipitation in vitro by lipids extracted from mammalian hard and soft tissues. *Arch. Oral Biol*. 20: 311-316.
- Olsson M., Dalsgaard C.J., Haegerstrand A., Rosenqvist M., Rydén L., Nilsson J. 1994. Accumulation of T lymphocytes and expression of interleukin-2 receptors in nonrheumatic stenotic aortic valves. *J. Am. Coll. Cardiol.* 23 (5): 1162-1170.
- Olsson M., Thyberg J., Nilsson J. 1999. Presence of oxidized low density lipoprotein in nonrheumatic stenotic aortic valves. *Arterioscler. Thromb. Vasc. Biol.* 19 (5): 1218-1222.
- Olsson U., Camejo G., Hurt-Camejo E., Elfsber K., Wiklund O., Bondjers G. 1997. Possible functional interactions of apolipoprotein B-100 segments that associate with cell proteoglycans and the ApoB/E receptor. *Arterioscler. Thromb. Vasc. Biol*. 17 (1): 149-155.
- Oörni K., Hakala J.K., Annila A., Ala-Korpela M., Kovanen P.T. 1998. Sphingomyelinase induces aggregation and fusion, but phospholipase A2 only aggregation, of low density lipoprotein (LDL) particles. Two distinct mechanisms leading to increased binding strength of LDL to human aortic proteoglycans. *J. Biol. Chem*. 273 (44): 29127-29134.
- Oörni K., Pentikäinen., Ala-Korpela M., Kovanen P.T. 2000. Aggregation, fusion and vesicle formation of modified low density lipoprotein particles: molecular mechanisms and effects on matrix interactions. *J. Lipid Res*. 41: 1703-1714.
- Ortolani F., Petrelli L., Tubaro F., Spina M., Marchini M. 2002a. Novel ultrastructural features as revealed by phthalocyanin reactions indicate cell priming for calcification in subdermally implanted aortic valves. *Connect. Tissue Res.* 43: 44-55.
- Ortolani F., Tubaro F., Petrelli L., Gandaglia A., Spina M., Marchini M. 2002b. Specific relation between mineralization and cuprolinic blue uptake as revealed by copper retention in calcified aortic valves and ultrastructural evidences. *Histochem. J.* 34: 41-50.

- Ortolani F., Petrelli L., Nori S.L., Spina M., Marchini M. 2003. Malachite green and phthalocyanin-silver reactions reveal acidic phospholipid involvement in calcification of porcine aortic valves in rat subdermal model. *Histol. Histopathol.* 18: 1131-1140.
- Ortolani F., Bonetti A., Tubaro F., Petrelli L., Contin M., Nori S.L., Spina M., Marchini M. 2007. Ultrastructural characterization of calcification onset and progression in subdermally implanted aortic valves. Histochemical and spectrometric data. *Histol. Histopathol.* 22: 261-272.
- Ortolani F., Rigonat L., Bonetti A., Contin M., Tubaro F., Rattazzi M., Marchini M. 2010. Pro-calcific responses by aortic valve interstitial cells in a novel in vitro model simulating dystrophic calcification. *Ital. J. Anat. Embryol.* 115: 135-139.
- Osman L., Chester A.H., Sarathchandra P., Latif N., Meng W., Taylor P.M., Yacoub M.H. 2007. A novel role of the sympatho-adrenergic system in regulating valve calcification. *Circulation*. 116 (11 Suppl): I282-287.
- Osuka S., Razzaque M.S. 2012. Can features of phosphate toxicity appear in normophosphatemia? *J. Bone Miner. Metab*. 30: 10-18.
- Otto C.M., Kuusisto J., Reichenbach D.D., Gown A.M., O'Brien K.D. 1994. Characterization of the early lesion of 'degenerative' valvular aortic stenosis. Histological and immunohistochemical studies. *Circulation*. 90 (2): 844-853.
- Otto C.M., Burwash I.G., Legget M.E., Munt B.I., Fujioka M., Healy N.L., Kraft C.D., Miyake-Hull C.Y., Schwaegler R.G. 1997. Prospective study of asymptomatic valvular aortic stenosis. Clinical, echocardiographic, and exercise predictors of outcome. *Circulation*. 95 (9): 2262-2270.
- Otto C.M., Lind B.K., Kitzman D.W., Gersh B.J., Siscovick D.S. 1999. Association of aortic-valve sclerosis with cardiovascular mortality and morbidity in the elderly. *N. Engl. J. Med*. 341 (3): 142-147.
- Packard C., Caslake M., Shepherd J. 2000. The role of small, dense low density lipoprotein (LDL): a new look. *Int. J. Cardiol*. 74 (Suppl. 1): S17-22.
- Palumbo C. 1986. A three-dimensional ultrastructural study of osteoid-osteocytes in the tibia of chick embryos. *Cell Tissue Res.* 246 (1): 125-131.
- Panizo S., Cardus A., Encinas M., Parisi E., Valcheva P., López-Ongil S., Coll B., Fernandez E., Valdivielso J.M. 2009. RANKL increases vascular smooth muscle cell calcification through a RANK-BMP4-dependent pathway. *Circ. Res.* 104 (9): 1041-1048.
- Parhami F., Morrow A.D., Balucan J., Leitinger N., Watson A.D., Tintut Y., Berliner J.A., Demer L.L. 1997. Lipid oxidation products have opposite effects on calcifying vascular

cell and bone cell differentiation. A possible explanation for the paradox of arterial calcification in osteoporotic patients. *Arterioscler. Thromb. Vasc. Biol*. 17 (4): 680-687.

- Parker R.S. 1996. Absorption, metabolism, and transport of carotenoids. *FASEB J.* 10: 542-551.
- Peltier M., Trojette F., Sarano M.E., Grigioni F., Slama M.A., Tribouilloy C.M. 2003. Relation between cardiovascular risk factors and nonrheumatic severe calcific aortic stenosis among patients with a three-cuspid aortic valve. *Am. J. Cardiol*. 91(1): 97-99.
- Penel G., Leroy G., Rey C., Bres E. 1998. MicroRaman spectral study of the PO4 and CO3 vibrational modes in synthetic and biological apatites. *Calcif. Tissue Int*. 63 (6): 475-481.
- Pentikäinen M.O., Lehtonen E.M., Kovanen P.T. 1996. Aggregation and fusion of modified low density lipoprotein. *J. Lipid Res*. 37 (12): 2638-2649.
- Pohle K., Mäffert R., Ropers D., Moshage W., Stilianakis N., Daniel W.G., Achenbach S. 2001. Progression of aortic valve calcification: association with coronary atherosclerosis and cardiovascular risk factors. *Circulation*. 104 (16): 1927-1932.
- Price P.A., Faus S.A., Williamson M.K. 1998. Warfarin causes rapid calcification of the elastic lamellae in rat arteries and heart valves. *Arterioscler. Thromb. Vasc. Biol*. 18 (9): 1400-1407.
- Proudfoot D., Skepper J.N., Hegyi L., Bennett M.R., Shanahan C.M., Wiessberg P.L. 2000. Apoptosis regulates human vascular calcification in vitro: evidence for initiation of vascular calcification by apoptotic bodies. *Circ. Res*. 87: 1055-1062.
- Proudfoot D., Shanahan C.M. 2006. Molecular mechanisms mediating vascular calcification: role of matrix Gla protein. *Nephrology (Carlton)*. 11 (5): 455-461.
- Qian J., Chen Z., Ge J., Ma J., Chang S., Fan B., Liu X., Ge L. 2010. Relationship between aortic valve calcification and the severity of coronary atherosclerotic disease. *J. Heart Valve Dis*. 19 (4): 466-470.
- Qunibi W.Y., Nolan C.A., Ayus J.C. 2002. Cardiovascular calcification in patients with end-stage renal disease: a century-old phenomenon. Kidney. Int. Suppl. (82): S73-80.
- Rabuş M.B., Kayalar N., Sareyyüpoğlu B., Erkin A., Kirali K., Yakut C. 2009. Hypercholesterolemia association with aortic stenosis of various etiologies. J. Card. Surg. 24 (2): 146-150.
- Rachow JW, Ryan LM. 1988. Inorganic pyrophosphate metabolism in arthritis. *Rheum. Dis. Clin. North. Am*. 14 (2): 289-302.
- Rajamannan N.M., Subramaniam M., Springett M., Sebo T.C., Niekrasz M., McConnell J.P., Singh R.J., Stone N.J., Bonow R.O., Spelsberg T.C. 2002. Atorvastatin inhibits

hypercholesterolemia-induced cellular proliferation and bone matrix production in the rabbit aortic valve. *Circulation*. 105 (22): 2660-2665.

- Rajamannan N.M., Subramaniam M., Rickard D., Stock S.R., Donovan J., Springett M., Orszulak T., Fullerton D.A., Tajik A.J., Bonow R.O., Spelsberg T. 2003. Human aortic valve calcification is associated with an osteoblast phenotype. *Circulation*. 107 (17): 2181-2184.
- Rajamannan N.M., Subramaniam M., Caira F., Stock S.R., Spelsberg T.C. 2005. Atorvastatin inhibits hypercholesterolemia-induced calcification in the aortic valves via Lrp5 receptor pathway. *Circulation*. 112: I-229-I-234.
- Rattazzi M., Iop L., Faggin E., Bertacco E., Zoppellaro G., Baesso I., Puato M., Torregrossa G., Fadini G.P., Agostini C., Gerosa G., Sartore S., Pauletto P. 2008. Clones of interstitial cells from bovine aortic valve exhibit different calcifying potential when exposed to endotoxin and phosphate. *Arterioscler. Thromb. Vasc. Biol.* 28: 2165-2172.
- Redd D.C., Yue K.Y., Martin L.G., Kaufman S.L. 1991. Young Investigator Award. Raman spectroscopy of human atherosclerotic plaque: implications for laser angioplasty. *J. Vasc. Interv. Radiol.* 2: 247-252.
- Reid J.D., Andersen M.E. 1993. Medial calcification (whitlockite) in the aorta. *Atherosclerosis*. 101 (2): 213-224.
- Rey C., Collins B., Goehl T., Dickson I.R., Glimcher M. 1989. The carbonate environment in bone mineral: a resolution-enhanced Fourier transform spectroscopy study. *Calcif. Tissue Int.* 45: 157-164.
- Reynolds J.L., Joannides A.J., Skepper J.N., McNair R., Schurgers L.J., Proudfoot D., Jahnen-Dechent W., Weissberg P.L., Shanahan C.M. 2004. Human vascular smooth muscle cells undergo vesicle-mediated calcification in response to changes in extracellular calcium and phosphate concentrations: a potential mechanism for accelerated vascular calcification in ESRD. *J. Am. Soc. Nephrol*. 15: 2857-2867.
- Reynolds J.L., Skepper J.N., McNair R., Kasama T., Gupta K., Weissberg P.L., Jahnen-Dechent W., Shanahan C.M. 2005. Multifunctional roles for serum protein fetuin-a in inhibition of human vascular smooth muscle cell calcification. *J. Am. Soc. Nephrol*. 16: 2920-2930.
- Ribeiro S., Ramos A., Brandão A., Rebelo J.R., Guerra A., Resina C., Vila-Lobos A., Carvalho F., Remédio F., Ribeiro F. 1998. Cardiac valve calcification in haemodyalisis patients. Role of calcium-phosphate metabolism. *Nephrol. Dial. Transplant.* 13: 2037-2040.

- Richardson P.D., Davies M.J., Born G.V. 1989. Influence of plaque configuration and stress distribution on fissuring of coronary atherosclerotic plaques. *Lancet*. 2 (8669): 941-944.
- Rizzo M., Berneis K. 2006. Low-density lipoprotein size and cardiovascular risk assessment. *QJM*. 99: 1-14.
- Roberts W.C., Ko J.M. 2005. Frequency by decades of unicuspid, bicuspid, and tricuspid aortic valves in adults having isolated aortic valve replacement for aortic stenosis, with or without associated aortic regurgitation. *Circulation*. 111 (7): 920-925.
- Rochette C.N., Rosenfeldt S., Heiss A., Narayanan T., Ballauff M., Jahnen-Dechent W. 2009. A shielding topology stabilizes the early stage protein-mineral complexes of fetuin-A and calcium phosphate: a time-resolved small-angle X-ray study. *Chembiochem.* 10 (4): 735-740.
- Rodriguez-Benot A., Martin-Malo A., Alvarez-Lara A., Rodriguez M., Aljama P. 2005. Mild hyperphosphatemia and mortality in hemodialysis patients. *Am. J. Kidney Dis*. 46: 68-77.
- Römer T.J., Brennan J.F. 3rd, Fitzmaurice M., Feldstein M.L., Deinum G., Myles J.L., Kramer J.R., Lees R.S., Feld M.S. 1998. Histopathology of human coronary atherosclerosis by quantifying its chemical composition with Raman spectroscopy. *Circulation.* 97: 878-885.
- Ron D., Walter P. 2007. Signal integration in the endoplasmic reticulum unfolded protein response. *Nat. Rev. Mol. Cell. Biol*. 8: 519-529.
- Rutsch F., Vaingankar S., Johnson K., Goldfine I., Maddux B., Schauerte P., Kalhoff H., Sano K., Boisvert W.A., Superti-Furga A., Terkeltaub R.. 2001. PC-1 nucleoside triphosphate pyrophosphohydrolase deficiency in idiopathic infantile arterial calcification. *Am. J. Pathol*. 158 (2): 543-554.
- Sage AP, Tintut Y, Demer LL. 2010. Regulatory mechanisms in vascular calcification. *Nat. Rev. Cardiol*. 7 (9): 528-536.
- Schibler D., Russell R.G., Fleisch H. 1968. Inhibition by pyrophosphate and polyphosphate of aortic calcification induced by vitamin D3 in rats. *Clin. Sci*. 35 (2): 363-372.
- Schinke T., Amendt C., Trindl A., Pöschke O., Müller-Esterl W., Jahnen-Dechent W. 1996. The serum protein alpha2-HS glycoprotein/fetuin inhibits apatite formation in vitro and in mineralizing calvaria cells. A possible role in mineralization and calcium homeostasis. *J. Biol. Chem*. 271 (34): 20789-20796.

- Schissel S.L., Tweedie-Hardman J., Rapp J.H., Graham G., Williams K.J., Tabas I. 1996. Rabbit aorta and human atherosclerotic lesions hydrolyze the sphingomyelin of retained low-density lipoprotein. Proposed role for arterial-wall sphingomyelinase in subendothelial retention and aggregation of atherogenic lipoproteins. *J. Clin. Invest*. 98 (6): 1455-1464.
- Schissel S.L., Keesler G.A., Schuchman E.H., Williams K.J., Tabas I. 1998. The cellular trafficking and zinc dependence of secretory and lysosomal sphingomyelinase, two products of the acid sphingomyelinase gene. *J. Biol. Chem*. 273 (29): 18250-18259.
- Schoen F.J., Levy J.R., Nelson A.C., Bernhard W.F, Nashef A., Hawley M. 1985. Onset and progression of experimental bioprosthetic heart valve calcification. *Lab. Invest*. 52: 523-532.
- Schoen F.J., Tsao J.W., Levy R.J. 1986. Calcification of bovine pericardium used in cardiac valve bioprosthesed. Implications for the mechanism of bioprosthetic tissue mineralization. *Am. J. Pathol*. 123: 134-145.
- Schoen F.J, Levy R.J. 1992. Bioprosthetic heart valve calcification: membrane-mediated events and alkaline phosphatase. *Bone Miner*. 17 (2): 129-133.
- Schoppet M., Al-Fakhri N., Franke F.E., Katz N., Barth P.J., Maisch B., Preissner K.T., Hofbauer L.C. 2004. Localization of osteoprotegerin, tumor necrosis factor-related apoptosis-inducing ligand, and receptor activator of nuclear factor-kappaB ligand in Mönckeberg's sclerosis and atherosclerosis. *J. Clin. Endocrinol. Metab*. 89 (8): 4104-4112.
- Schröder M. 2008. Endoplasmic reticulum stress responses. *Cell. Mol. Life Sci.* 65: 862-894.
- Schurgers L.J., Aebert H., Vermeer C., Bültmann B., Janzen J. 2004. Oral anticoagulant treatment: friend or foe in cardiovascular disease? *Blood*. 104 (10): 3231-3232.
- Shao J.S., Cheng S.L., Sadhu J., Towler D.A. 2010. Inflammation and the osteogenic regulation of vascular calcification: a review and perspective. *Hypertension*. 55 (3): 579-592.
- Shen M., Marie P., Farge D., Carpentier S., De Pollak C., Hott M., Chen L., Martinet B., Carpentier A. 1997. Osteopontin is associated with bioprosthetic heart valve calcification in humans. *C. R. Acad. Sci. III*. 320 (1): 49-57.
- Simonet W.S., Lacey D.L., Dunstan C.R., Kelley M., Chang M.S., Lüthy R., Nguyen H.Q., Wooden S., Bennett L., Boone T., Shimamoto G., DeRose M., Elliott R., Colombero A., Tan H.L., Trail G., Sullivan J., Davy E., Bucay N., Renshaw-Gegg L., Hughes T.M., Hill D., Pattison W., Campbell P., Sander S., Van G., Tarpley J., Derby P., Lee R., Boyle W.J.

1997 Osteoprotegerin: a novel secreted protein involved in the regulation of bone density. *Cell*. 89 (2): 309-319.

- Skold B.H., and Getty R. 1961. Spontaneous atherosclerosis of swine. *Amer. Vet. Med. Ass*. 139: 655-660.
- Slavin R.E., Wen J., Barmada A. 2012. Tumoral calcinosis. A pathogenetic overview: a histological and ultrastructural study with a report of two new cases, one in infancy. *Int. J. Surg. Pathol*. 20 (5): 462-473.
- Small D.M. 1988. Mechanisms of reversed cholesterol transport. *Agents Actions Suppl*. 26: 135-146.
- Smith E.B., Massie I.B., Alexander K.M. 1976. The release of an immobilized lipoprotein fraction from atherosclerotic lesions by incubation with plasmin. *Atherosclerosis*. 25: 71-84.
- Smith M.W., Phelps P.C., Trump B.F. 1991. Cytosolic Ca2+ deregulation and blebbing after $HgCl_2$ injury to cultured rabbit proximal tubule cells as determined by digital imaging microscopy. *Proc. Natl. Acad. Sci. USA*. 88: 4926-4930.
- Somers P., Knaapen M., Kockx M., van Cauwelaert P., Bortier H., Mistiaen W. 2006. Histological evaluation of autophagic cell death in calcified aortic valve stenosis. *J. Heart Valve Dis*. 15: 43-48.
- Sommer A., Prenner E., Gorges R., Stütz H., Grillhofer H., Kostner G.M., Paltauf F., Hermetter A. 1992. Organization of phosphatidylcholine and sphingomyelin in the surface monolayer of low density lipoprotein and lipoprotein(a) as determined by time-resolved fluorometry. *J. Biol. Chem*. 267 (34): 24217-24222.
- Speer M.Y., McKee M.D., Guldberg R.E., Liaw L., Yang H.Y., Tung E., Karsenty G., Giachelli C.M. 2002. Inactivation of the osteopontin gene enhances vascular calcification of matrix Gla protein-deficient mice: evidence for osteopontin as an inducible inhibitor of vascular calcification in vivo. *J. Exp. Med*. 196 (8): 1047-1055.
- Steiner I., Kasparová P., Kohout A., Dominik J. 2007. Bone formation in cardiac valves: a histopathological study of 128 cases. *Virchows Arch.* 450: 653-657.
- Steitz S.A., Speer M.Y., Curinga G., Yang H.Y., Haynes P., Aebersold R., Schinke T., Karsenty G., Giachelli C.M. 2001. Smooth muscle cell phenotypic transition associated with calcification: upregulation of Cbfa1 and downregulation of smooth muscle lineage markers. *Circ. Res*. 89 (12): 1147-1154.

- Steitz S.A., Speer M.Y., McKee M.D., Liaw L., Almeida M., Yang H., Giachelli C.M. 2002. Osteopontin inhibits mineral deposition and promotes regression of ectopic calcification. *Am. J. Pathol*. 161 (6): 2035-2046.
- Stewart B.F., Siscovick D., Lind B.K., Gardin J.M., Gottdiener J.S., Smith V.E., Kitzman D.W., Otto C.M. 1997. Clinical factors associated with calcific aortic valve disease. Cardiovascular Health Study. *J. Am. Coll. Cardiol.* 29 (3): 630-634.
- Tabas I. 1999. Nonoxidative modifications of lipoproteins in atherogenesis. *Annu. Rev. Nutr*. 19: 123-139.
- Tanaka K., Sata M., Fukuda D., Suematsu Y., Motomura N., Takamoto S., Hirata Y., Nagai R. 2005. Age-associated aortic stenosis in apolipoprotein E-deficient mice. *J. Am. Coll. Cardiol.* 46 (1): 134-141.
- Tanimura A., McGregor D.H., Anderson H.C. 1983. Matrix vesicles in atherosclerotic calcification. *Proc. Soc. Exp. Biol. Med*. 172: 173-177.
- Tarrass F., Benjelloun M., Zamd M., Medkouri G., Hachim K., Benghanem M.G., Ramdani B. 2006. Heart valve calcifications in patients with end-stage renal disease: Analysis for risk factors. *Nephrology*. 11: 494-496.
- Termine J.D., Belcourt A.B., Conn K.M., Kleinman H.K. 1981. Mineral and collagen-binding proteins of fetal calf bone. *J. Biol. Chem*. 256 (20): 10403-10408.
- Thompson B. and Towler D.A. 2012. Arterial calcification and bone physiology: role of the bone-vascular axis. *Nat. Rev. Endocrinol*. 8 (9): 529-543.
- Tintut Y., Patel J., Parhami F., Demer L.L. 2000. Tumor necrosis factor-alpha promotes in vitro calcification of vascular cells via the cAMP pathway. *Circulation*. 102 (21): 2636-42.
- Tintut Y., Patel J., Territo M., Saini T., Parhami F., Demer L.L. 2002. Monocyte/ macrophage regulation of vascular calcification in vitro. *Circulation.* 105: 650-655.
- Tohno Y., Tohno S., Minami T., Ichii M., Okazaki Y., Utsumi M., Nishiwaki F., Moriwake Y., Yamada M., Araki T. 1996. Age-related change of mineral content in the human thoracic aorta and in the human cerebral artery. *Biol Trace Elem Res*. 54 (1): 23-31.
- Tonelli M., Sacks F., Pfeffer M., Gao Z., Curhan G. 2005. Relation between serum phosphate level and cardiovascular event rate in people with coronary disease. *Circulation.* 112: 2627-2633.
- Top C., Cankir Z., Silit E., Yildirim S., Danaci M. 2002. Mönckeberg's sclerosis: an unusual presentation--a case report. *Angiology*. 53 (4): 483-486.
- Towler D.A. 2008. Vascular Calcification: A perspective on an imminent disease epidemic. *Inter. Bone Miner. Soc*. 5 (2): 41-58.

- Tribble D.L., Rizzo M., Chait A., Lewis D.M., Blanche P.J., Krauss R.M. 2001. Enhanced oxidative susceptibility and reduced antioxidant content of metabolic precursors of small, dense low-density lipoproteins. *Am. J. Med*. 110: 103-10.
- Valente M., Bortolotti U., Thiene G. 1985. Ultrastructural substrates of dystrophic calcification in porcine bioprosthetic valve failure. *Am. J. Pathol*. 119: 12-21.
- van de Poll S.W., Kastelijn K., Bakker Schut T.C., Strijder C., Pasterkamp G., Puppels G.J., van der Laarse A. 2003. On-line detection of cholesterol and calcification by catheter based Raman spectroscopy in human atherosclerotic plaque ex vivo. *Heart*. 89 (9): 1078-1082.
- van Kuijk J.P., Flu W.J., Chonchol M., Valentijn T.M., Verhagen H.J.M., Bax J.J, Poldermans D. 2010. Elevated preoperative phosphorus levels are an independent risk factor for cardiovascular mortality. *Am. J. Nephrol.* 32: 163-168.
- Van Lenten B.J., Fogelman A.M., Haberland M.E., Edwards P.A. 1986. The role of lipoproteins and receptor-mediated endocytosis in the transport of bacterial lipopolysaccharide. *Proc. Natl. Acad. Sci. USA*. 83: 2704-2708.
- Vattikuti R., Towler D.A. 2004. Osteogenic regulation of vascular calcification: an early perspective. *Am. J. Physiol. Endocrinol. Metab*. 286 (5): E686-696.
- Victorov A.V., Medvedeva N.V., Gladkaya E.M., Morozkin A.D., Podrez E.A., Kosykh V.A., Yurkiv V.A. 1989. Composition and structure of lipopolysaccharide-human plasma low density lipoprotein complex. Analytical ultracentrifugation, 31P-NMR, ESR and fluorescence spectroscopy studies. *Biochim. Biophys. Acta*. 984 (1): 119-127.
- Villa-Bellosta R., Bogaert Y.E., Levi M., Sorribas V. 2007. Characterization of phosphate transport in rat vascular smooth muscle cells: implications for vascular calcification. *Arterioscler. Thromb. Vasc. Biol*. 27 (5): 1030-106.
- Villa-Bellosta R., Sorribas V. 2011. Calcium phosphate deposition with normal phosphate concentration. -Role of pyrophosphate-. *Circ. J*. 75 (11): 2705-2710.
- Villa-Bellosta R., Wang X., Millán J.L., Dubyak G.R., O'Neill W.C. 2011. Extracellular pyrophosphate metabolism and calcification in vascular smooth muscle. *Am. J. Physiol. Heart Circ. Physiol*. 301 (1): H61-68.
- Vogel J.J., Boyan-Salyers B.D. 1976 Acidic lipids associated with the local mechanism of calcification: a review. *Clin. Orthop. Relat. Res.* 118: 231-241.
- Wang N., Wang X., Xing C., Sun B., Yu X., Hu J., Liu J., Zeng M., Xiong M., Zhou S., Yang J. 2010. Role of TGF-beta1 in bone matrix production in vascular smooth muscle cells induced by a high-phosphate environment. *Nephron. Exp. Nephrol*. 115 (3): e60-68.

- Warren H.S., Fitting C., Hoff E., Adib-Conquy M., Beasley-Topliffe L., Tesini B., Liang X., Valentine C., Hellman J., Hayden D., Cavaillon J.M. 2010. Resilience of bacterial infection: difference between species could be due to proteins in serum. *J. Infect. Dis*. 201: 223-232.
- Watson K.E., Boström K., Ravindranath R., Lam T., Norton B., Demer L.L. 1994. TGF-beta 1 and 25-hydroxycholesterol stimulate osteoblast-like vascular cells to calcify. *J. Clin. Invest*. 93: 2106-2113.
- Weiss R.M., Ohashi M., Miller J.D., Young S.G., Heistad D.D. 2006. Calcific aortic valve stenosis in old hypercholesterolemic mice. *Circulation*. 114 (19): 2065-2069.
- Westenfeld R., Schäfer C., Krüger T., Haarmann C., Schurgers L.J., Reutelingsperger C., Ivanovski O., Drueke T., Massy Z.A., Ketteler M., Floege J., Jahnen-Dechent W. 2009. Fetuin-A protects against atherosclerotic calcification in CKD. *J. Am. Soc. Nephrol*. 20 (6): 1264-1274.
- Whyte M.P. 2006. Extraskeletal (ectopic) calcification and ossification. *Am. Soc. Bone Miner. Res.* Section XI: 436-437.
- Wu L.N., Genge B.R., Wuthier R.E. 1991. Association between proteoglycans and matrix vesicles in the extracellular matrix of growth plate cartilage. *J. Biol. Chem.* 266: 1187-1194.
- Wu L.N., Yoshimori T., Genge B.R., Sauer G.R., Kirsch T., Ishikawa Y., Wuthier R.E. 1993. Characterization of the nucleational core complex responsible for mineral induction by growth plate cartilage matrix vesicles. *J. Biol. Chem*. 268 (33): 25084-25094.
- Wu L.N., Genge B.R., Sauer G.R., Wuthier R.E. 1996. Characterization and reconstitution of the nucleation complex for mineral formation by growth plate cartilage matrix vesicles. *Connect. Tissue Res.* 35: 309-315.
- Wu L.N., Genge B.R., Dunkelberger D.G., LeGeros R.Z., Concannon B., Wuthier R.E. 1997. Physicochemical characterization of the nucleational core of matrix vesicles. *J. Biol. Chem*. 272: 4404-4411.
- Wu T.T., Chen T.L., Chen R.M. 2009. Lipopolysaccharide triggers macrophage activation of inflammatory cytokine expression, chemotaxis, phagocytosis, and oxidative ability via a toll-like receptor 4-dependent pathway: validated by RNA interference. *Toxicol. Lett*. 191: 195-202.
- Wuthier R.E. 1973. The role of phospholipids in biological calcification: distribution of phospholipase activity in calcifying epiphyseal cartilage. *Clin. Orthop. Relat. Res*. 90: 191-200.

- Wuthier R.E. 1976. Lipids of matrix vesicles. *Fed. Proc*. 35 (2): 117-121.
- Wuthier R.E., Gore S.T., 1977. Partition of inorganic ions and phospholipids in isolated cell, membrane and matrix vesicle fractions: evidence for Ca-Pi-acidic phospholipid complexes. *Calcif. Tissue Res*. 24 (2): 163-171.
- Wuthier R.E., Wians F.H. Jr, Giancola M.S., Dragic S.S. 1978. In vitro biosynthesis of phospholipids by chondrocytes and matrix vesicles of epiphyseal cartilage. *Biochemistry*. 17 (8): 1431-1436.
- Wuthier R.E. 1982. A review of the primary mechanism of the endochondral calcification with special emphasis on the role of cells, mitochondria, and matrix vesicles. *Clin. Orthop*. 169: 219-242.
- Wuthier R.E., Wu L.N., Sauer G.R., Genge B.R., Yoshimori T., Ishikawa Y. 1992. Mechanism of matrix vesicle calcification: characterization of ion channels and the nucleational core of growth plate vesicles. *Bone Miner*. 17 (2): 290-295.
- Xu C., Bailly-Maitre B., Reed J.C. 2005. Endoplasmic reticulum stress: cell life and death decisions. *J. Clin. Invest*. 115: 2656-2664.
- Xu Z., Huang C.X., Li Y., Wang P.Z., Ren G.L., Chen C.S., Shang F.J., Zhang Y., Liu Q.Q., Jia Z.S., Nie Q.H., Sun Y.T., Bai X.F. 2007. Toll-like receptor 4 siRNA attenuates LPS-induced secretion of inflammatory cytokines and chemokines by macrophages. *J. Infect*. 55 (1): e1-e9.
- Yacoub M.H., Takkenberg J.J. 2005. Will heart valve tissue engineering change the world? *Nat. Clin. Pract. Cardiovasc. Med*. 2 (2): 60-61.
- Yang X., Fullerton D.A., Su X., Ao L., Cleveland J.C. jr, Meng X. 2009. Pro-osteogenic phenotype of human aortic valve interstitial cells is associated with higher levels of Toll-like receptors 2 and 4 and enhanced expression of bone morphogenetic protein 2. *J. Am. Coll. Cardiol.* 53: 491-500.
- Ylä-Herttuala S., Palinski W., Rosenfeld M.E., Parthasarathy S., Carew T.E., Butler S., Witztum J.L., Steinberg D. 1989. Evidence for the presence of oxidatively modified low density lipoprotein in atherosclerotic lesions of rabbit and man. *J. Clin. Invest*. 84 (4): 1086-1095.
- Yu Z., Seya K., Daitoku K., Motomura S., Fukuda I., Furukawa K. 2011. Tumor necrosis factor-α accelerates the calcification of human aortic valve interstitial cells obtained from patients with calcific aortic valve stenosis via the BMP2-Dlx5 pathway. *J. Pharmacol. Exp. Ther.* 337 (1): 16-23.

- Zeng Z., Nievelstein-Post P., Yin Y., Jan K.M., Frank J.S., Rumschitzki D.S. 2007. Macromolecular transport in heart valves. III. Experiment and theory for the size distribution of extracellular liposomes in hyperlipidemic rabbits. *Am. J. Physiol. Heart Circ. Physiol*. 292 (6): H2687-2697.

THE ANATOMICAL RECORD 295:1117–1127 (2012)

Ultrastructural and Spectrophotometric Study on the Effects of Putative Triggers on Aortic Valve Interstitial Cells in *In Vitro* Models Simulating Metastatic Calcification

ANTONELLA BONETTI,[1] ALBERTO DELLA MORA,[1] MAGALI CONTIN,[1] FRANCO TUBARO,[2] MAURIZIO MARCHINI,[1] AND FULVIA ORTOLANI[1]*

[1]Department of Experimental Clinical Medicine, University of Udine, Piazzale Kolbe 3, Udine, Italy

[2]Department of Food Sciences, University of Udine, Via delle Scienze 208, Udine, Italy

ABSTRACT

Metastatic calcification of cardiac valves is a common complication in patients affected by chronic renal failure. In this study, primary bovine aortic valve interstitial cells (AVICs) were subjected to pro-calcific treatments consisting in cell stimulation with (i) elevated inorganic phosphate (Pi = 3 mM), to simulate hyperphosphatemic conditions; (ii) bacterial endotoxin lipopolysaccharide (LPS), simulating direct effects by microbial agents; and (iii) conditioned media (CM) derived from cultures of either LPS-stimulated heterogenic macrophages (commercial murine RAW264.7 cells) or LPS-stimulated fresh allogenic monocytes/macrophages (bCM), simulating consequent inflammatory responses, alone or combined. Compared to control cultures, spectrophotometric assays revealed shared treatment-dependent higher values of both calcium amounts and alkaline phosphatase activity for cultures involving the presence of elevated Pi. Ultrastructurally, shared peculiar pro-calcific degeneration patterns were exhibited by AVICs from these latter cultures irrespectively of the additional treatments. Disappearance of all cytomembranes and concurrent formation of material showing positivity to Cuprolinic Blue and co-localizing with silver precipitation were followed by the outcropping of such a material, which transformed in layers outlining the dead cells. Subsequent budding of these layers resulted in the formation of bubbling bodies and concentrically laminated calcospherulae mirroring those in actual soft tissue calcification. In conclusion, the *in vitro* models employed appear to be reliable tools for simulating metastatic calcification and indicate that hyperphosphatemic-like conditions could trigger valve calcification *per se*, with LPS and allogenic macrophage-derived secretory products acting as possible calcific enhancers *via* inflammatory responses. Anat Rec, 295:1117–1127, 2012. ©2012 Wiley Periodicals, Inc.

Key words: aortic valve calcification; metastatic calcification; inflammation; heart valve disease; valve interstitial cells

INTRODUCTION

Cardiovascular mortality still represents the leading cause of death in patients affected by end-stage renal disease. Derangement of divalent ion metabolism with consequent hyperphosphatemia, high calcium load, and increased calcium-phosphorus (Ca x P) product is suggested largely to contribute to the pathogenesis of valve

*Correspondence to: Fulvia Ortolani, Department of Experimental Clinical Medicine, University of Udine, Piazzale Kolbe 3, I-33100 Udine, Italy. E-mail: fulvia.ortolani@uniud.it

Received 30 November 2011; Accepted 29 March 2012.

DOI 10.1002/ar.22494

Published online 23 May 2012 in Wiley Online Library (wileyonlinelibrary.com).

calcification in uraemic patients (Ribeiro et al., 1998; Block, 2000; Tarrass et al., 2006). There is also increasing evidence suggesting that the mineralization of heart valves in dialysis patients shares multiple pathogenetic and clinical aspects with atherosclerosis including inflammation, lipid and lipoprotein deposition, and presence/regulation of bone-related proteins (Torun et al., 2005; Wang, 2009; Montasser et al., 2011).

In the attempt to clarify the mechanisms underlying cardiovascular tissue mineralization, in the last decade several *in vitro* models have been developed, providing a simulation of: (i) metastatic calcification, subjecting cells to high levels ($\geq$2 mmol/L) of either organic phosphate (Mathieu et al., 2005) or inorganic phosphate (Pi; Jono et al., 2000; Steitz et al., 2001; Giachelli et al., 2005); (ii) inflammation, treating cells with conditioned medium from cultures of heterogenic macrophages stimulated with bacterial endotoxin lipopolysaccharide (LPS; Tintut et al., 2002; Babu et al., 2008), which was supposed to contain pro-inflammatory cytokines, as recently confirmed (Xu et al., 2007; Wu et al., 2009); and (iii) co-existence of metastatic calcification and inflammation, stimulating cells cultured under mineralizing conditions with tumor necrosis factor alpha (TNF-α; Kaden et al., 2005) or LPS (Rattazzi et al., 2008).

Using these models, major results were that mineralization of cardiovascular tissues is associated with alkaline phosphatase (ALP) activity increasing as well as the expression of bone-related mediators in vascular smooth muscle cells or in aortic valve interstitial cells (AVICs), in contrast with other findings showing calcification of aortic valves to depend on various types of cell death processes (Kim, 1995; Jian et al., 2003; Somers et al., 2006; Rattazzi et al., 2008).

In previous studies on *in vivo* experimentally induced aortic valve mineralization, the calcific event was shown to depend on a peculiar AVIC degenerative process culminating with a lipid-release-dependent formation of peripheral phthalocyanin-positive layers (PPLs), acting as major hydroxyapatite (HA) nucleation sites at the level of cells and cell-derived vesicular bodies (Ortolani et al., 2002a,b, 2003, 2007). Similar calcific degenerative patterns were also found to take place in cultured AVICs using a novel *in vitro* model simulating dystrophic calcification (Ortolani et al., 2010).

In the present study, different *in vitro* conditions were accomplished to elucidate the possible contributes of putative agents in influencing metastatic calcification. Combined spectrophotometric estimations and ultrastructural analysis revealed how AVICs are responsive to the treatments, with elevated Pi alone a sufficient trigger of mineralization and possible enhancement exerted by LPS and species-specific pro-inflammatory mediators. In addition, calcification was found to correlate with a shared AVIC degeneration pattern as those described previously, which included the generation of final calcifying cell-derived structures superimposable to those existing in actual *in vivo* ectopic calcification.

MATERIALS AND METHODS

Isolation and Culture of Aortic Valve Interstitial Cells

Primary cultures of AVICs were obtained by enzymatic digestion of aortic valve leaflets isolated from hearts of slaughtered healthy bovines (age = 15 months), as previously described (Rattazzi et al., 2008). Namely, excised aortic roots were placed in Dulbecco's Modified Eagle's Medium (DMEM, Sigma) plus 1% penicillin/streptomycin and 1 μg/mL amphotericin B kept cool in ice. Then, aortic valve leaflets were isolated, depleted of endothelial cells by gentle surface scraping, and minced into ~2–3 mm^3 pieces, which were digested with type-I collagenase (125 U/mL; Sigma), elastase (8 U/mL; Sigma), and soybean trypsin inhibitor (0.375 mg/mL; Sigma) for 30 min at 37°C. After digestion, the pieces were transferred into tissue culture Petri dishes (Greiner) and cultured in DMEM plus 20% Fetal Bovine Serum (FBS; Gibco), 1% L-glutamine, and 1% penicillin/streptomycin for 7–10 days. Once drawn from the digested pieces, AVICs were cultured in complete DMEM as above until pre-confluent state and expanded up to 10 folds. Cells from passages 4 to 6 were used. Light microscopy monitoring was made using an Olympus IX70 inverted microscope.

Conditioned Medium from Murine RAW264.7 Macrophages

Murine RAW264.7 macrophages were plated on tissue culture flasks (Falcon) and cultured in DMEM supplemented with 10% FBS, 1% L-glutamine, and 1% penicillin/streptomycin. At pre-confluence, RAW cells (passage 4) were stimulated with LPS (100 ng/mL; Sigma) for 1 hr at 37°C, rinsed twice with DMEM plus 10% FBS, and additionally cultured in complete DMEM for 12 hr achieving macrophage degranulation. After culture medium collection and centrifugation, supernatant was 0.22-μm-filtered, added with 1% polymyxin B (BioChemika) to neutralize residual LPS, and stored at −20°C until use.

Conditioned Medium from Bovine Fresh Macrophages

Fresh lympho/monocytes were collected by Ficoll® (1:2; Sigma) density gradient centrifugation of peripheral blood from healthy bovines (age = 18 months) before slaughtering and then plated on tissue culture flasks and maintained in complete DMEM, prepared as for RAW cells, overnight. After lymphocyte removing by rinsing with DMEM plus 10% FBS, monocytes were cultured in complete DMEM for 3 days to promote cell differentiation. These monocytes/macrophages were then treated like murine RAW264.7 macrophages.

AVIC Treatments

At pre-confluence, AVICs seeded on 35 mm culture plates (Greiner) were cultured in DMEM plus 10% FBS, 1% L-glutamine, and 1% penicillin/streptomycin (i) alone (control-cultures) or supplemented with: (ii) murine RAW264.7 macrophage conditioned medium equal to 1/5 of total supernatant volume (mCM-cultures); (iii) bovine macrophage conditioned medium equal to 1/5 of total supernatant volume (bCM-cultures); (iv) 100 ng/mL LPS (LPS-cultures); (v) 2.6 mM Pi (Pi-cultures); (vi) 2.6 mM Pi and 100 ng/mL LPS (Pi-LPS-cultures); (vii) 2.6 mM Pi, plus 100 ng/mL LPS, plus murine RAW264.7 macrophage conditioned medium equal to 1/5 of total supernatant volume (Pi-LPS-mCM-cultures); (viii) 2.6 mM Pi, plus 100 ng/mL LPS, plus bovine macrophage

conditioned medium equal to 1/5 of total supernatant volume (Pi-LPS-bCM-cultures). In each cell culture supplemented with 2.6 mM Pi, the final concentration of Pi was 3 mM. The treatments were performed for 3, 6, and 9 days, renewing the culture medium every 3 days.

Calcium Quantification

After culture medium recovering, cells were scraped from each culture plate, centrifuged, and treated with an aqueous lysis buffer containing 50 mM TRIS-HCl, 150 mM NaCl, 5 mM EDTA, and 1% Triton X-100, pH 7.4, for 1 hr at 4°C. After micro-centrifugation at 2000 rpm for 5 min, part of supernatant (500 μL) was recovered for ALP activity/protein assay and remaining lysed samples were rejoined to their original culture media and transferred into distinct Teflon vessels. Samples were added with 1 mL of 65% supra-pure grade nitric acid (Merck) and 500 μL of 30% supra-pure hydrogen peroxide (Merck), irradiated using the High Performance Microwave Digestion Unit mls 1200 mega (Milestone; 2 min at 250 W, 2 min at 0 W, 5 min at 300 W, 5 min at 450 W, and 6 min at 650 W), and diluted with ultra-pure water until obtaining 100 mL of total solution. Calcium quantification was assessed using the *o*-cresolphtalein complexone method (Chema Diagnostica) and absorbance was read at 575 nm with a Cary 50 Bio spectrophotometer (Varian). Each estimation came from 10 readings of five distinct experiments.

ALP Activity/Protein Assay

Supernatants (500 μL) obtained from micro-centrifugation of lysed samples were used to determine ALP activity and protein content. ALP activity was assessed using a kinetic method based on measurement of 4-nitrophenol production (Chema Diagnostica) reading the absorbance at 405 nm at 37°C within 5 min of enzymatic activity using the Cary 50 Bio spectrophotometer. Values corresponding to the trend line gradients coming from reading of five distinct experiments were normalized on the basis of protein content, estimated using a Coomassie Plus Protein Assay Reagent (Pierce) with absorbance reading at 595 nm using the spectrophotometer as above.

Ultrastructural Evidentiation of Polyanions with Pre-Embedding Reactions with Phthalocyanin Cuprolinic Blue

After culture medium removal, AVICs adhering to culture plates were washed twice with 0.1 M phosphate buffer and subjected to pre-embedding reaction with 0.05% phthalocyanin Cuprolinic Blue (CB; Electron Microscopy Sciences) dissolved in 25 mM sodium acetate buffer, containing 0.05 M magnesium chloride and 2.5% glutaraldehyde, pH 4.8, overnight, at room temperature and under continuous agitation. After further washing, AVICs were post-fixed with phosphate-buffered 2% osmium tetraoxide (Agar Scientific) for 1 hr at 4°C, washed again, dehydrated in graded ethanols, and embedded in Epon 812 resin. Thin sections were collected on formvar-coated 2 × 1-mm-slot copper grids and contrasted with uranyl acetate and lead citrate. Observations and photographic recordings were made using a Philips CM12/STEM electron microscope.

Ultrastructural Evidentiation of Calcium-Binding Sites with Post-Embedding Von Kossa Silver Staining

Semithin sections of CB-reacted and Epon-embedded AVICs were mounted on glass slides, covered with a drop of an aqueous solution of 1% silver nitrate, and placed on an 80°C warm plate under direct sunlight for 15 min. After washing with distilled water and drying, semithin sections were covered with a drop of an aqueous solution of 5% sodium thiosulfate at 80°C for 5 min for silver reduction. After further washing and drying, these semithin sections were re-embedded. Briefly, conic Beem capsules (Agar Scientific), previously cut at their top, were placed onto the slides encircling each reacted semithin section, glued at their base, and filled with Epon-Araldite fluid. After resin polymerization, the re-embedded sections underwent standard processing.

Statistical Analysis

The values of calcium amounts were reported as mean ± SD. Statistical differences among control and the different AVIC treatments were assessed using the ANOVA test, with Bonferroni correction for multiple comparisons. Values with $P < 0.0001$ were considered to be statistically significant.

RESULTS

To assess whether and how much elevated Pi and/or pro-inflammatory agents promote AVIC-mediated mineralization, spectrophotometric estimations of calcium amounts and ALP activity were carried out on treated primary cultures of cells derived from bovine aortic valve leaflets. ALP activity was tested because it is one of the most representative enzymes implicated in calcification.

In Fig. 1, the values are reported on the amounts of calcium contained in digested samples from AVIC cultures after 9-day-long treatments. The mean values resulted for samples from control-cultures, LPS-cultures, mCM-cultures, and bCM-cultures were similar to one another and collectively lower with respect to those in samples from the cultures supplemented with elevated Pi. Also, these higher mean values were similar to one another, except for the Pi-LPS-bCM-cultures, which contained even more mineral.

The values of ALP activity in the 9-day-long AVIC cultures are reported in Fig. 2. Compared to control-cultures, no change resulted for mCM-cultures and bCM-cultures, a weak increase for LPS-cultures, and a further weak increase for Pi-cultures. A marked increase resulted for the remaining cultures, being the highest value measured for Pi-LPS-cultures, with linearly lower values for Pi-LPS-mCM-cultures and Pi-LPS-bCM-cultures, respectively.

Since the values of calcium content were markedly increased for all four cultures containing elevated Pi, whereas higher ALP activity only resulted for the cultures containing elevated Pi combined with other treatments but not Pi alone, supplementary estimations of this parameter were supplied for all these cultures verifying the time course spanning 3–9 days (Fig. 3). In detail, enzymatic activity reached a maximum at 6-day-

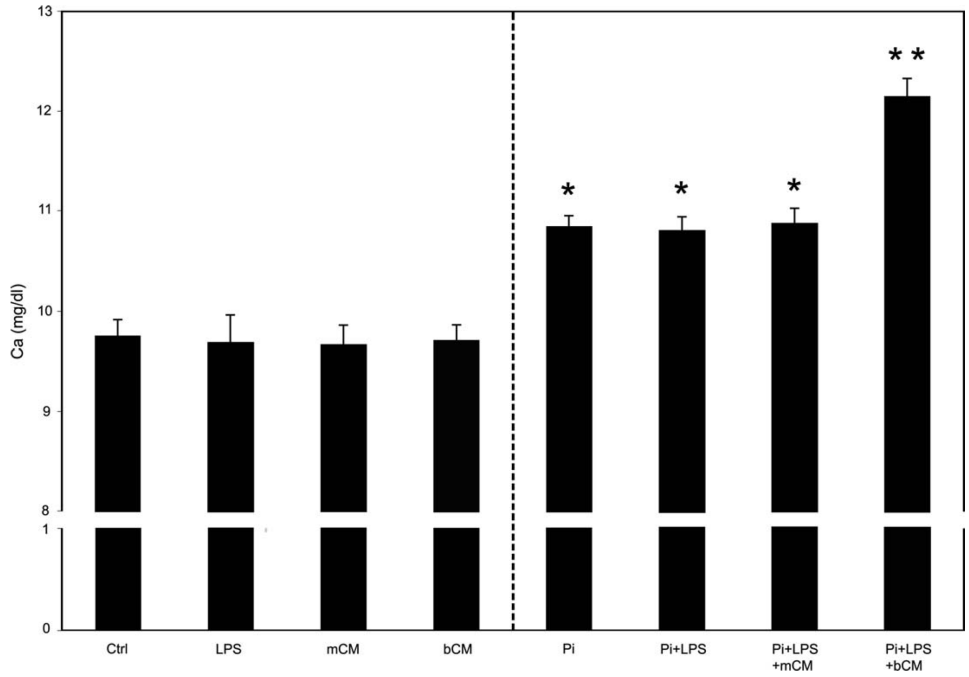

Fig. 1. Spectrophotometric estimation of calcium amounts for 9-day-long-cultured bovine AVICs with no treatment (Ctrl) or after different stimuli alone or combined, that is, lipopolysaccharide (LPS), murine conditioned medium (mCM), bovine conditioned medium (bCM), and elevated (2.6 mM) inorganic phosphate (Pi), with the vertical hatched line distinguishing Pi-lacking treatments from Pi-containing ones. The values are reported as mean ± SD. The values concerning the treated cultures are significantly different (*) from those of control-cultures, and those concerning Pi-LPS-bCM-cultures are significantly different (**) from all others; $P < 0.0001$.

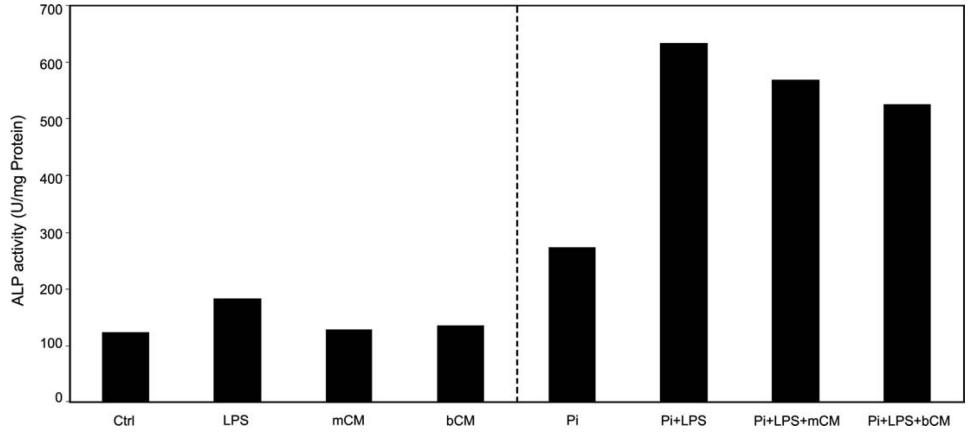

Fig. 2. Spectrophotometric estimation of ALP activity for 9-day-long-cultured bovine AVICs with no treatment or after the different stimulations as in Fig. 1.

long incubation for Pi-cultures, with a subsequent drop at 9 days. Conversely, enzymatic activity underwent a roughly linear increase up to day 9 for Pi-LPS-, Pi-LPS-mCM-, and Pi-LPS-bCM-cultures.

Morphologically, the mineralization rates induced by the applied treatments were readily recognizable under the inverted microscope on the basis of size and number of formed calcific nodules. The presence of calcific nodules only in Pi-containing cultures was apparent as well as the most marked calcification occurring in Pi-LPS-bCM cultures (Fig. 4).

Severity of cell alterations was assessed at the ultrastructural level on samples subjected to pre-embedding histochemical reactions based on the use of acidic

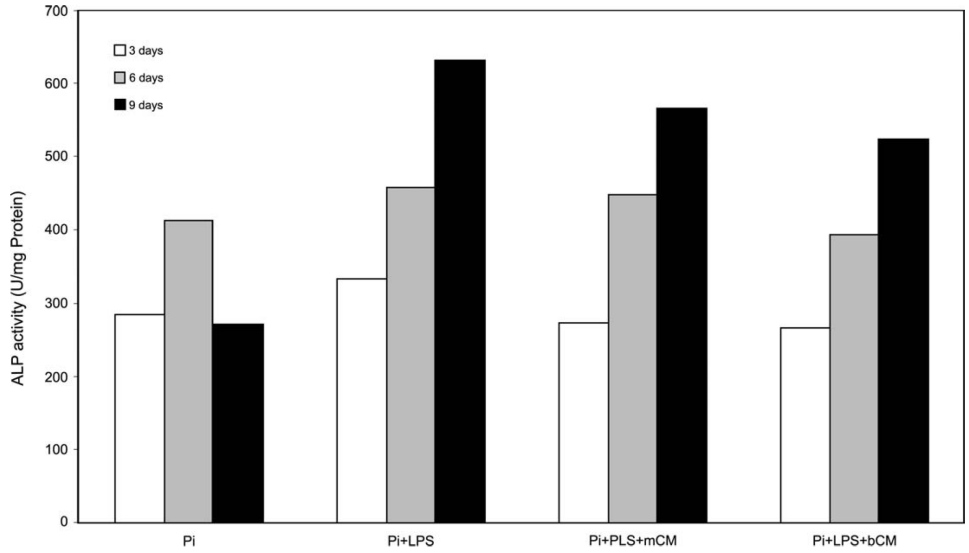

Fig. 3. Spectrophotometric estimation of ALP activity time course spanning 3–9 days for bovine AVIC cultures after all treatments involving the presence of elevated Pi.

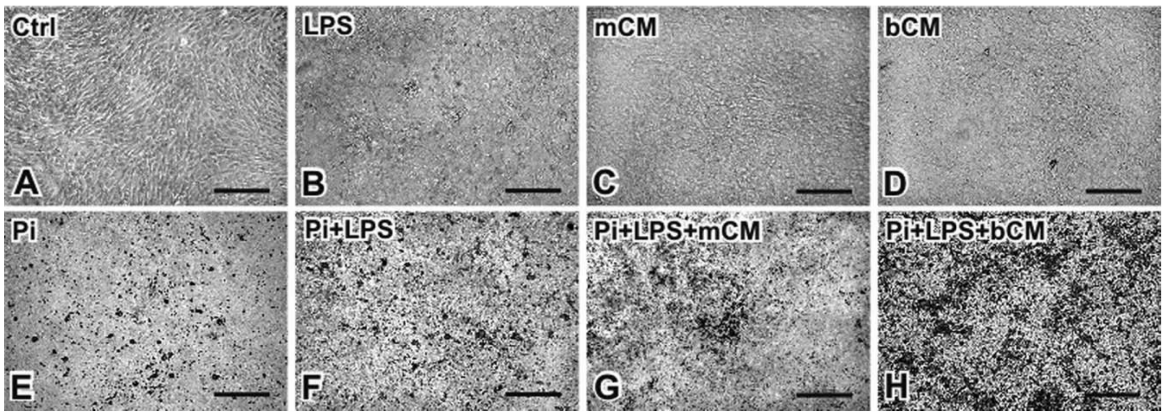

Fig. 4. Light microscopy micrographs of unstained AVIC monolayers. **A–D:** Absence of calcium precipitation in control cultures (Ctrl) and cultures treated with lipopolysaccharide alone (LPS), murine derived conditioned medium alone (mCM), and bovine derived conditioned medium alone (bCM). **E–H:** Presence of calcium precipitation in monolayer cultures treated with elevated (2.6 mM) inorganic phosphate alone (Pi), Pi+LPS, Pi+LPS+mCM, and Pi+LPS+bCM. Original magnification: 10×.

mixtures of glutaraldehyde and copper phthalocyanin Cuprolinic Blue (CB; see Materials and Methods session). Since this mixture allows sample decalcification with simultaneous retention of acidic-lipid-containing material resulting from the degradation of cytoplasmic organules and membranes, this method previously showed the peculiarity of the AVIC degeneration occurring in *in vivo* experimental models of accelerated calcification (Ortolani et al., 2002a,b, 2003, 2007) as well as in an *in vitro* model simulating dystrophic calcification (Ortolani et al., 2010). In addition, resin semithin sections of CB-reacted samples were subjected to post-embedding reactions based on metallic silver precipitation, namely the reaction of von Kossa, widely used on histological sections to detect calcific sites (see Materials and Methods session).

On thin sections, control AVICs showed well preserved intracytoplasmic organelles and lamellipodia with associated anchoring stress fibers (Fig. 5A,B), that is, the flat protoplasmic protrusions and cytoskeleton filaments which usually characterize adhering cultured cells.

As in controls, no apparent damage was appreciable for AVICs from mCM-cultures, bCM-cultures, and LPS-cultures (not shown). In all experiments in which elevated Pi was present, a distinct cell degenerative process was observed which included (i) degeneration of cytoplasmic organules, (ii) release of CB-reactive material, and (iii) margination of this material and its outward budding. In

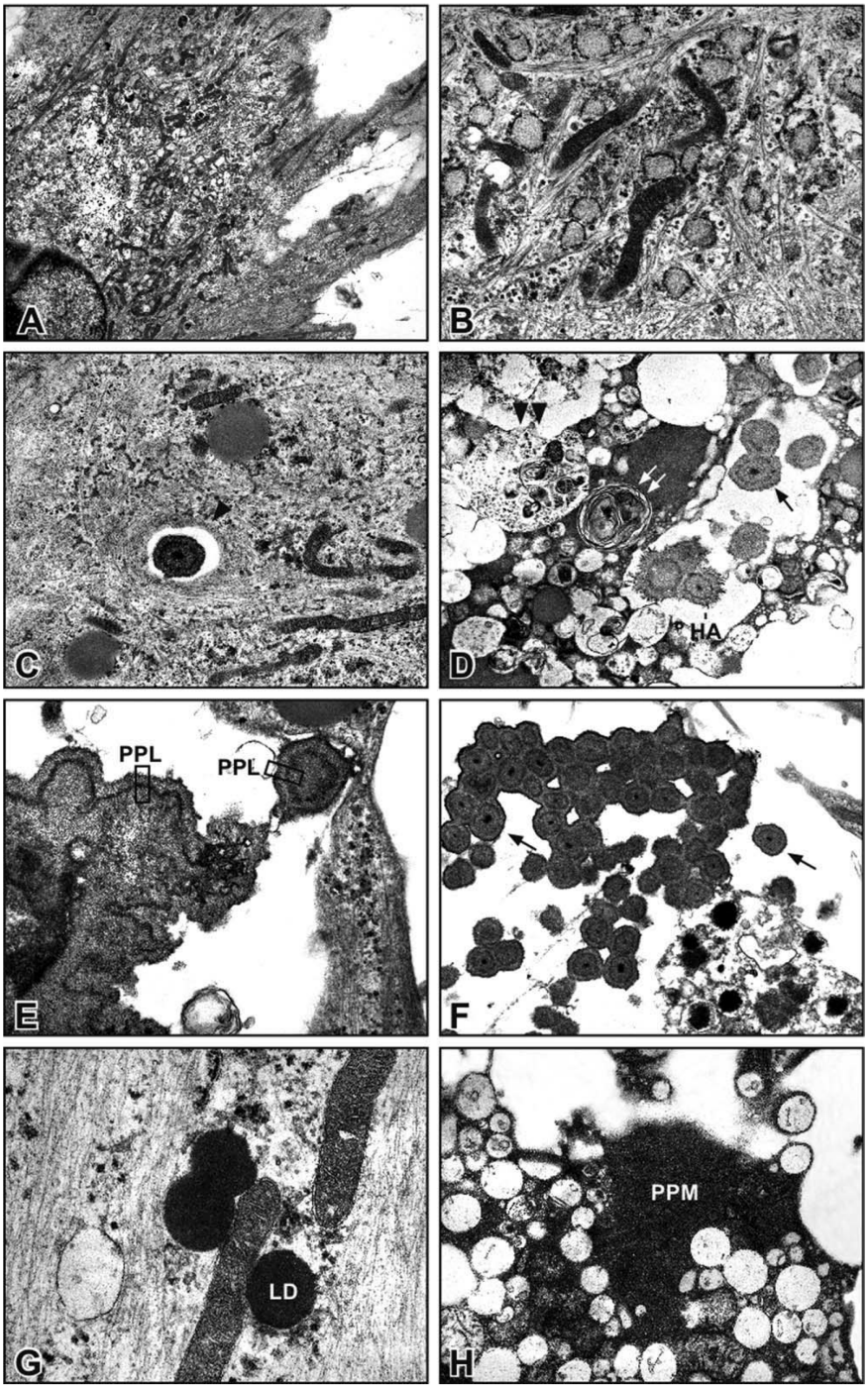

Fig. 5. **A** and **B:** Thin sections showing normal features in AVICs from control-cultures. **C–F:** Altered features in AVICs from cultures added with 2.6 mM Pi: autophagocytic vacuole (double arrowhead in D); myelin figure (double white arrow in D); CB-reactive layers (frame-PPL in E); calcospherulae (black arrows in D and F); phagocyted calcospherula (arrowhead in C); hydroxyapatite crystals (HA in D). **G:** CB-reactive lipid droplets (LD) in an AVIC cultured with Pi+LPS. **H:** Vesiculation and CB-reactive material (PPM) in an AVIC cultured with Pi+LPS+mCM. Magnifications: 3,000× (A); 12,000× (B); 9,000× (C and D); 20,000× (E); 7,000× (F); 25,000× (G); 11,000× (H).

more detail, initial AVIC alteration consisted in the abnormous dilation of rough endoplasmic reticulum, swelling of mitochondria with progressive dissolution of christae, cytoplasm vesiculation, mounting disruption/loss of all membrane-bound organelles and nuclear envelope, with the appearance of a lot of phthalocyanin-reactive lipid droplets, autophagocytic vacuoles/lysosomes, and myelin figures (Figs. 5D,G,H and 6A,C,D). Cytoplasm vacuolization also depended on depletion of swollen mitochondria and was complicated by their joining/fusion into greater vacuoles. During these processes, previously accumulated lipid-like amorphous material was poured into the major vacuoles, transforming them into lipid inclusions subsequent to fragmentation and dissolution of lining membranes (Figs. 5H and 6C). The resulting lipid inclusions underwent a progressive increase in reactivity to pre-embedding reaction with CB (Figs. 5G and 6A) and were selective sites for metallic silver particle deposition, after additional post-embedding von Kossa silver staining (Fig. 6B). An incipient increase in cytoplasm electrondensity seemed to result from the melting of these reactive lipid droplets with associated overgrowing of amorphous phthalocyanin-positive material (PPM), which entrapped organule-derived remnants and clusters of degrading ribosomes (Figs. 5H and 6D).

More advanced degenerative features were (i) shortening/disappearance of lamellipodia, with cells acquiring smoothed profiles and irregularly roundish shapes, (ii) complete colliquation of organules, and (iii) their replacement by increasing PPM. Centrifugal PPM spreading in waves followed, resulting in the appearance of multilaminated, CB-reactive PPLs outlining the body of cell remnants and being 100–200 nm thick (Figs. 5E and 6E). Initial pseudo-orthogonal precipitation of needle-like HA crystals appeared mostly to occur at level of PPLs, revealing their marked pro-calcific role (Fig. 6F). The same involvement was exhibited by initial PPL-derived bodies, detaching from cell surface and, to a lesser extent, intracellular transitional forms of PPM into PPLs. Co-localization between HA crystal nucleation and metallic silver precipitation was also evident after von Kossa reactions (Fig. 6G).

These degenerative phenomena appeared to end with the dead PPL-lined cells undergoing fragmentation into heterogeneously sized bubbling bodies (Fig. 7A,B), with overlapping sporulation-like PPL budding and pinching off, so generating rounded concentrically laminated calcospherulae mostly characterized by a punctate dense core, with diameters ranging between 130 nm and 1 μm (Fig. 7A–E). Also these PPL-derivatives were strongly reactive to silver von Kossa reactions (Fig. 7F).

It is worth noting that stimulation with elevated Pi alone was sufficient to give rise to all degenerative patterns including the genesis of calcospherulae (Fig. 5D). Of interest, calcospherulae phagocytated by still viable AVICs were encountered (Fig. 5C).

DISCUSSION

The elevated Pi concentration settled in the AVIC cultures was consistent with the hyperphosphatemic conditions in organisms, thus allowing to test the implications of this inorganic element, as well as bacterial endotoxin LPS and macrophage-derived inflammatory mediators, in a context reproducing metastatic calcification.

Aside from the additional stimulations, prominent calcific events occurred in all cultures containing elevated Pi. Since Pi concentration (3 mM) was consistent with conditions of severe hyperphosphatemia, such a condition seems to be capable of inducing ectopic calcification *per se*, consistently with the concept that elevated Ca x P product represents the most predictive parameter for cardiac valve calcification in hemodialysis patients (Ribeiro et al., 1998; Block, 2000; Tarrass et al., 2006).

Compared to Pi-cultures, additional increase in calcium amount resulted for Pi-LPS-bCM cultures exclusively. The absence of increase in calcium amounts after superstimulation of 9-day-cultured AVICs with endotoxin LPS is not consistent with a previous report of marked mineralization occurring in Pi-LPS treated AVIC cultures (Rattazzi et al., 2008). However, those results concerned longer incubation times. On the other hand, the highest ALP activity resulted for Pi-LPS treatment in the present investigation. Of note, direct pro-calcific effects by LPS, including ALP activity enhancement, were shown to occur for cultured AVICs with the involvement of specific LPS Toll-like receptors (TLRs; Babu et al., 2008; Meng et al., 2008; Yang et al., 2009). Thus, it seems likely that this bacterial endotoxin can exert some pro-calcific effect on AVICs, superimposing to that exerted by elevated Pi.

Additional stimulations with conditioned media derived from cultures of monocytes/macrophages, in their turn stimulated with LPS, were accomplished with the rationale of simulating inflammatory conditions due to a bacterial infection in the organism. A stimulation with conditioned medium from LPS-stimulated monocytes/macrophages was already used on a subset of bovine aorta-wall-derived smooth muscle cells (Tintut et al., 2002), named calcific vascular cells (CVCs; Watson et al., 1994), eliciting TNF-α secretion associated with increased ALP activity. Moreover, specific interaction of LPS with TLR-4 was reported to prime the activation of murine RAW264.7 macrophages, suggesting their contribution in mineralizing processes (Hume et al., 2001; Wu et al., 2009).

In this investigation, conditioned media from cultures of LPS-activated RAW264.7 macrophages did not cause increase in mineralization, whereas a clear calcific outgrowth occurred by using conditioned media from cultures of allogenic primary macrophages. Taking into account that macrophage activation by bacterial wall components correlates with secretion of species-specific chemo/cytokines (Nagao et al., 1992) and that equal pathogen doses can trigger different inflammatory cell responses (Munford, 2010; Warren et al., 2010), it is feasible that species-specific macrophage-derived cytokines are needed to enhance calcific responses by AVICs.

Together, the above results are in line with the concept that products derived from GRAM-negative bacteria may contribute in triggering cardiac valve calcification *via* inflammatory reactions, as suggested by the detection of Chlamydia pneumoniae in both stenotic and sclerotic semilunar valves (Juvonen et al., 1997; Nyström-Rosander et al., 1997), as well as the experimental demonstration that animal aortic valves undergo mineralizing effects after inoculation with oral bacteria (Cohen et al., 2004).

Concerning ALP activity in 9-day-long cultures, prominent increases were restricted to the three cultures

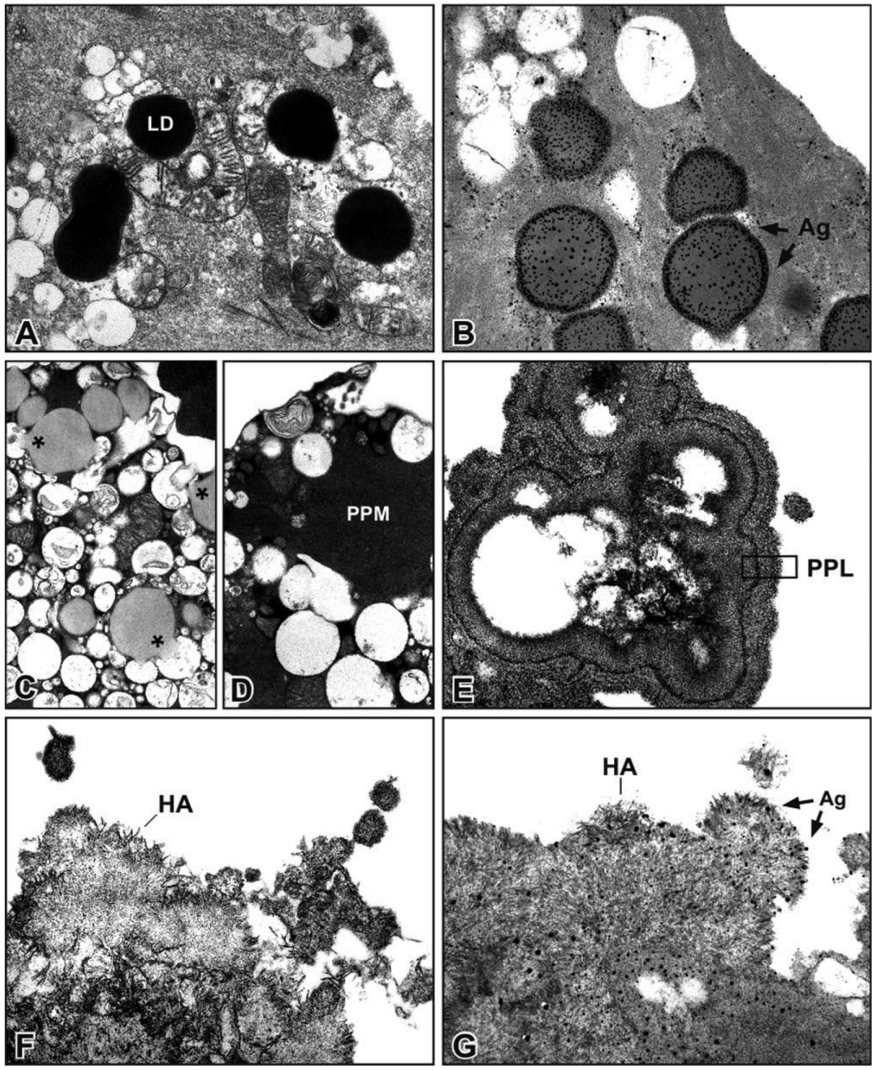

Fig. 6. **A–G:** Thin sections showing altered features in AVICs from cultures added with 2.6 mM-Pi+LPS+bCM: CB-reactive lipid droplets (LD in A); selective precipitation of metallic silver (Ag with arrows in B and G); vesiculation (in C and D) with inter-vesicule lipid material pouring (asterisks in C); CB-reactive material (PPM in D); CB-reactive multi-laminated layer (frame-PPL in E); hydroxyapatite crystals (HA in F and G). Magnifications: 14,000× (A); 20,000× (B); 11,000× (C); 13,000× (D); 17,000× (E and F); 25,000× (G).

subjected to superstimulation with LPS and LPS plus conditioned media. Since prominent increase in calcium amount was a response shared by Pi-cultures and all superstimulated cultures, analogous sharing was expected to exist for ALP activity. This was not the case because of lower enzyme activity for Pi-cultures. On extending the estimation of ALP activity to 3-day and 6-day long cultures, a similar increase was shared by all four culture types up to 6 incubation days, whereas there was a marked drop in Pi-cultures between the sixth and the ninth day, in contrast with a further increase occurring for the other three treatments. This was consistent with the reported finding of lower activity for AVIC Pi-cultures *versus* Pi-LPS cultures (Rattazzi et al., 2008). Thus, it is reasonable that ALP activity may be involved in mineralization but without acting as an exclusive driving factor.

Of interest, pro-inflammatory cytokines such as TNF-α were reported to induce over-expression of type III sodium-dependent Pi cotransporter PiT-1 (Li and Giachelli, 2007), with a possible increase in Pi uptake by cultured mineralizing vascular smooth muscle cells (Lau et al., 2010). Putatively, a differential cytokine-induced over-expression of PiT-1 by AVICs and consequent massive Pi uptake might enhance calcium phosphate formation, thereby eliciting greater HA precipitation at the edges of AVICs and AVIC-derived products in Pi-LPS-bCM cultures, independently from the rate of ALP activity.

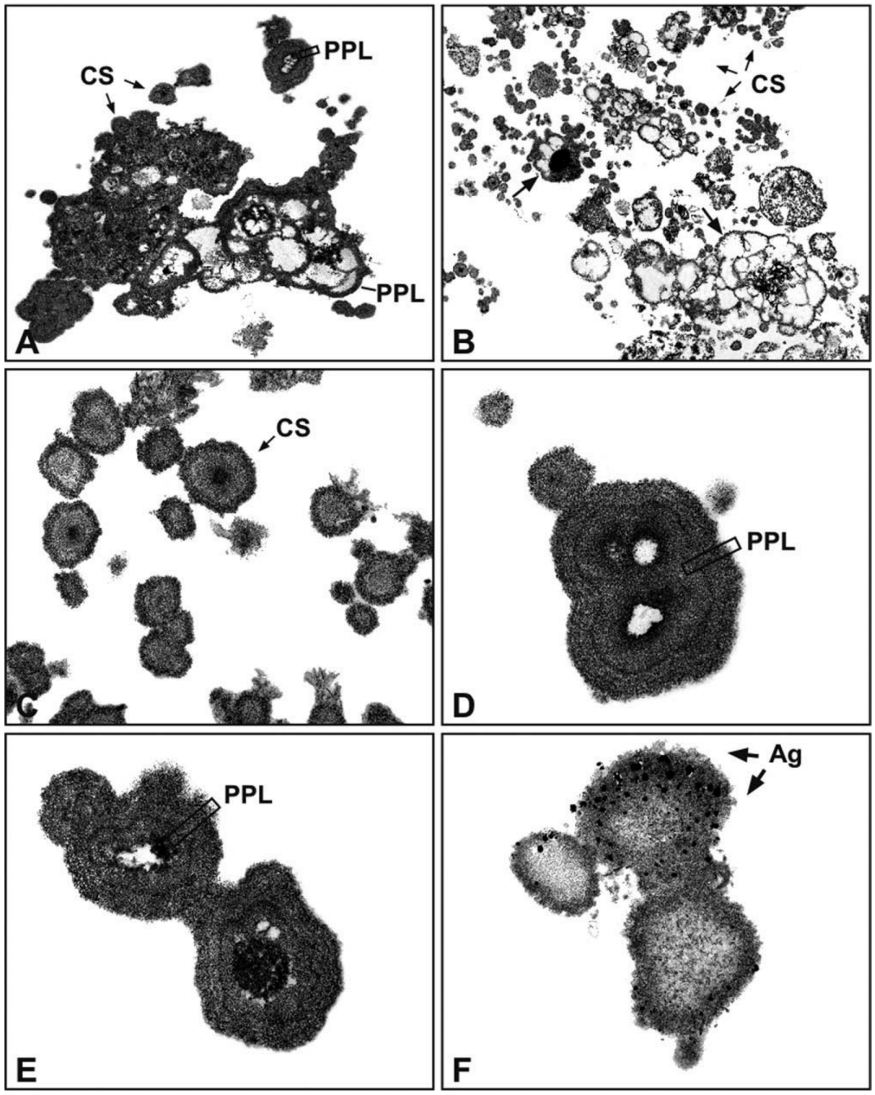

Fig. 7. **A–F:** Thin sections showing cell-derived products subsequent to fragmentation of AVICs from cultures added with 2.6 mM-Pi+LPS+bCM: concentrically laminated calcospherulae (CS with arrows in A–C); bubbling bodies (single arrows in B); and minor fragments showing CB-reactive layers (frame-PPL in A, D, and E); selective precipitation of metallic silver (Ag with arrows in F). Magnifications: 4,000× (A and B); 21,000× (C); 25,000× (D); 23,000× (E and F).

It is worth to note that increases in ALP activity were never associated with signs suggesting some AVIC trans-differentiation into osteoblast-like cells, being the progression of calcific processes exclusively accompanied by advancing of the described pro-calcific degenerative patterns showed by the dying/died cultured AVICs.

Although apoptosis was reported to occur for cultured ovine calcifying AVICs stimulated with transforming growth factor beta (TGF-β; Jian et al., 2003) as well as a specific clone of bovine AVICs after stimulation with LPS (Rattazzi et al., 2008), neither ultrastructural hallmarks nor positivity to TUNEL tests (not presented) were found in the present investigation. Rather, the observation of frequent macroautophagocytosis figures at the early treatment stages might suggest that autophagic cell death might be primed, as reported for calcified aortic valve stenosis (Somers et al., 2006), with the occurrence of unusually extensive lipolytic processes, possibly resulting in a prominent release of phospholipids and free fatty acids, consistently with the observed reactivity to cationic dye CB. Work is in progress to ascertain whether the observed degeneration patterns depend on a sudden unregulated cell breakdown or are the final steps of an aborted orthodox type of cell death, if not of a wholly undescribed type of regulated cell death.

Size and number of calcific nodules observed with light inverted microscope for Pi-containing cultures were morphological parameters fitting with the treatment-dependent increases in calcium amount spectrophotometrically estimated. Consistently, ultrastructural analysis clearly indicated that all treated AVICs underwent dramatic breakdown including intracellular release/accumulation of CB-reactive and silver-reactive material as well as its outcropping with formation of the pericellular dark layers named PPLs. A similar cell degradation process was already described for experimental *in vivo* calcification consisting in xenogenic subdermal implantation of glutaraldehyde-treated aortic valve cusps, with PPLs resulting to be largely formed by lipidic moieties including phospholipids and to contain calcium-binding sites (Ortolani et al., 2002a,b, 2003, 2007), as well as experimental *in vitro* models of ectopic calcification (Ortolani et al., 2010). Additionally, ultrastructural features reminiscent of PPLs were described for calcific aortic valves and other soft tissues affected by ectopic calcification as alcianophylic envelopes outlining so called "thick walled cell derived products" (CDPs; Kim and Huang, 1971; Kim, 1976; Boskey et al., 1988; Kim, 1995).

Since PPM production paralleled a progressive disappearance of all cytomembrane-bounded organelles, derived membranous residues and nuclear chromatin, it ensues that such a substance results from a complete colliquation of all these components. This was also confirmed by the observation of a lot of transitional patterns showing disrupting organelles or their ghosts to merge with PPM or to be embedded within such a material.

The role of these cell-derived products as major HA nucleators was supported by co-localization of calcium-binding sites, as revealed by the selective precipitation of metallic silver after von Kossa staining, as well as effective superimposition of HA crystals.

A further significant outcome in the present study was the identification of multilayered PPLs and concentrically laminated calcospherulae, these latter being closely reminiscent of the typical "porous particles in concentric layering" described for calcific aortic valves and other tissues affected by ectopic calcification (Kim, 1995) as well as failed calcific valve bioprostheses (Valente et al., 1985).

Because of affinity to von Kossa silver staining and superimposition by HA crystals, the calcospherulae seem to act as mineralization enhancers in the most advanced calcific stages, providing a widespread dissemination of supernumerary nucleation sites. This role is analogous to that played by matrix vesicles and/or apoptotic bodies in both physiological calcification and pathological one (Anderson, 1983; Kirsch, 2006), although being quite different cell-derived structures. In fact, calcospherulae appeared to result from a passive budding of PPLs and lack in cytoplasm, showing a roughly shared para-crystalline structure because of the presumable rearrangement of the pre-existent array of the lipid moiety at the level of the PPL-forming layers. Conversely, matrix vesicles and apoptotic bodies are described to result from distinct regulated mechanisms, contain organized cytoplasm, and are outlined by membranes with specific molecular architectures, including either inner location of phospholipids (Wu et al., 1997) or outer location (Bratton et al., 1997), respectively.

In conclusion, the used *in vitro* models represent reliable tools for simulating metastatic heart valve calcification, being calcospherulae actual structures characterizing ectopic mineralization, and the obtained results suggest that metastatic calcification in systemic conditions results from a peculiar AVIC degeneration and subsequent death which is triggered by hyperphosphatemia *per se*, with possible enhancing effects exerted by bacterial products and pro-inflammatory mediators.

LITERATURE CITED

Anderson HC. 1983. Calcific diseases: a concept. Arch Pathol Lab Med 107:341–348.

Babu AN, Meng X, Zou N, Yang X, Wang M, Song Y, Cleveland JC, Weyant M, Banerjee A, Fullerton DA. 2008. Lipopolysaccharide stimulation of human aortic valve interstitial cells activates inflammation and osteogenesis. Ann Thorac Surg 86:71–76.

Block GA. 2000. Prevalence and clinical consequences of elevated Ca x P product in hemodialysis patients. Clin Nephrol 54:318–324.

Boskey AL, Bullough PG, Vigorita V, Di Carlo E. 1988. Calcium-acidic phospholipid-phosphate complexes in human hydroxyapatite-containing pathologic deposits. Am J Pathol 133:22–29.

Bratton DL, Fadok VA, Richter DA, Kailey JM, Guthrie LA, Henson PM. 1997. Appearance of phosphatidylserine on apoptotic cells requires calcium-mediated nonspecific flip-flop and is enhanced by loss of the aminophospholipid translocase. J Biol Chem 272:26159–26165.

Cohen DJ, Malave D, Ghidoni JJ, Iakovidis P, Everett MM, You S, Liu Y, Boyan BD. 2004. Role of oral bacterial flora in calcific aortic stenosis: an animal model. Ann Thorac Surg 77:537–543.

Giachelli CM, Speer MY, Li X, Rajachar RM, Yang H. 2005. Regulation of vascular calcification: roles of phosphate and osteopontin. Circ Res 96:717–722.

Jian B, Narula N, Li QY, Mohler ER, III, Levy RJ. 2003. Progression of aortic valve stenosis: TGF-beta1 is present in calcified aortic valve cusps and promotes aortic valve interstitial cell calcification *via* apoptosis. Ann Thorac Surg 75:457–466.

Jono S, McKee MD, Murry CE, Shioi A, Nishizawa Y, Mori K, Morii H, Giachelli CM. 2000. Phosphate regulation of vascular smooth muscle cell calcification. Circ Res 87:e10–e17.

Juvonen J, Laurila A, Juvonen T, Aläkarppä H, Surcel HM, Lounatmaa K, Kuusisto J, Saikku P. 1997. Detection of Chlamydia pneumoniae in human nonrheumatic stenotic aortic valves. J Am Coll Cardiol 29:1054–1059.

Hume DA, Underhill DM, Sweet MJ, Ozinsky AO, Liew FY, Aderem A. 2001. Macrophages exposed continuously to lipopolysaccharide and other agonists that act *via* toll-like receptors exhibit a sustained and additive activation state. BMC Immunol 2:11.

Kaden JJ, Kiliç R, Sarikoç A, Hagl S, Lang S, Hoffmann U, Brueckmann M, Borggrete M. 2005. Tumor necrosis factor alpha promotes an osteoblast-like phenotype in human aortic valve myofibroblasts: a potential regulatory mechanism of valvular calcification. Int J Mol Med 16:869–872.

Kim KM. 1976. Calcification of matrix vesicles in human aortic valve and aortic media. Federation Proc 35:156–162.

Kim KM. 1995. Apoptosis and calcification. Scanning Microsc 9: 1137–1178.

Kim KM, Huang S. 1971. Ultrastructural study of calcification of human aortic valve. Lab Invest 25:357–366.

Kirsch T. 2006. Determinants of pathological mineralization. Curr Opin Rheumatol 18:174–180.

Lau WL, Festing MH, Giachelli CM. 2010. Phosphate and vascular calcification: emerging role of the sodium-dependent phosphate cotransporter PiT-1. Thromb Haemost 104:464–470.

Li X, Giachelli CM. 2007. Sodium-dependent phosphate cotransporters and vascular calcification. Curr Opin Nephrol Hypertens 16: 325–328.

Mathieu P, Voisine P, Pépin A, Shetty R, Savard N, Dagenais F. 2005. Calcification of human valve interstitial cells is dependent on alkaline phosphatase activity. J Heart Valve Dis 14:353–357.

Meng X, Ao L, Song Y, Babu A, Yang X, Wang M, Weyant MJ, Dinarello CA, Cleveland JC, Jr, Fullerton DA. 2008. Expression

of functional Toll-like receptors 2 and 4 in human aortic valve interstitial cells: potential roles in aortic valve inflammation and stenosis. Am J Physiol Cell Physiol 294:C29–C35.

Montasser D, Bahadi A, Zajjari J, Asserraji M, Aloyoude A, Moujoud O, Aattif T, Kadiri M, Zemraoui N, El Kabbaj D, Hassani M, Benyahia M, El Allam M, Oualim Z, Akhmouch I. 2011. Infective endocarditis in chronic hemodialysis patients: experience from Morocco. Saudi J Kidney Dis Transpl 22:160–166.

Munford RS. 2010. Murine responses to endotoxin: another dirty little secret? J Infect Dis 201:175–177.

Nagao S, Akagawa KS, Okada F, Harada Y, Yagawa K, Kato K, Tanigawa Y. 1992. Species dependency of *in vitro* macrophage activation by bacterial peptidoglycans. Microbiol Immunol 36: 1155–1171.

Nyström-Rosander C, Thelin S, Hjelm E, Lindquist O, Pahlson C, Friman G. 1997. High incidence of Chlamydia pneumoniae in sclerotic heart valves of patients undergoing aortic valve replacement. Scand J Infect Dis 29:361–365.

Ortolani F, Bonetti A, Tubaro F, Petrelli L, Contin M, Nori SL, Spina M, Marchini M. 2007. Ultrastructural characterization of calcification onset and progression in subdermally implanted aortic valves. Histochemical and spectrometric data. Histol Histopathol 22:261–272.

Ortolani F, Petrelli L, Tubaro F, Spina M, Marchini M. 2002a. Novel ultrastructural features as revealed by phthalocyanin reactions indicate cell priming for calcification in subdermally implanted aortic valves. Connect Tissue Res 43:44–55.

Ortolani F, Petrelli L, Nori SL, Spina M, Marchini M. 2003. Malachite green and phthalocyanin-silver reactions reveal acidic phospholipid involvement in calcification of porcine aortic valves in rat subdermal model. Histol Histopathol 18:1131–1140.

Ortolani F, Rigonat L, Bonetti A, Contin M, Tubaro F, Rattazzi M, Marchini M. 2010. Pro-calcific responses by aortic valve interstitial cells in a novel *in vitro* model simulating dystrophic calcification. Ital J Anat Embryol 115:135–139.

Ortolani F, Tubaro F, Petrelli L, Gandaglia A, Spina M, Marchini M. 2002b. Specific relation between mineralization and cuprolinic blue uptake as revealed by copper retention in calcified aortic valves and ultrastructural evidences. Histochem J 34:41–50.

Rattazzi M, Iop L, Faggin E, Bertacco E, Zoppellaro G, Baesso I, Puato M, Torregrossa G, Fadini GP, Agostini C, Gerosa G, Sartore S, Pauletto P. 2008. Clones of interstitial cells from bovine aortic valve exhibit different calcifying potential when exposed to endotoxin and phosphate. Arterioscler Thromb Vasc Biol 28:2165–2172.

Ribeiro S, Ramos A, Brandão A, Rebelo JR, Guerra A, Resina C, Vila-Lobos A, Carvalho F, Remédio F, Ribeiro F. 1998. Cardiac valve calcification in haemodyalisis patients. Role of calcium-phosphate metabolism. Nephrol Dial Transplant 13:2037–2040.

Somers P, Knaapen M, Kockx M, van Cauwelaert P, Bortier H, Mistiaen W. 2006. Histological evaluation of autophagic cell death in calcified aortic valve stenosis. J Heart Valve Dis 15:43–48.

Steitz SA, Speer MY, Curinga G, Yang HY, Haynes P, Aebersold R, Schinke T, Karsenty G, Giachelli CM. 2001. Smooth muscle cell phenotypic transition associated with calcification: upregulation of Cbfa1 and downregulation of smooth muscle lineage markers. Circ Res 89:1147–1154.

Tarrass F, Benjelloun M, Zamd M, Medkouri G, Hachim K, Benghanem MG, Ramdani B. 2006. Heart valve calcifications in patients with end-stage renal disease: analysis for risk factors. Nephrology 11:494–496.

Tintut Y, Patel J, Territo M, Saini T, Parhami F, Demer LL. 2002. Monocyte/macrophage regulation of vascular calcification *in vitro*. Circulation 105:650–655.

Torun D, Sezer S, Baltali M, Adam FU, Erdem A, Ozdemir FN, Haberal M. 2005. Association of cardiac valve calcification and inflammation in patients on hemodialysis. Ren Fail 27:221–226.

Valente M, Bortolotti U, Thiene G. 1985. Ultrastructural substrates of dystrophic calcification in porcine bioprosthetic valve failure. Am J Pathol 119:12–21.

Wang AYM. 2009. Vascular and other tissue calcification in peritoneal dialysis patients. Perit Dial Int 29:S9–S14.

Warren HS, Fitting C, Hoff E, Adib-Conquy M, Beasley-Topliffe L, Tesini B, Liang X, Valentine C, Hellman J, Hayden D, Cavaillon JM. 2010. Resilience of bacterial infection: difference between species could be due to proteins in serum. J Infect Dis 201:223–232.

Watson KE, Boström K, Ravindranath R, Lam T, Norton B, Demer LL. 1994. TGF-beta 1 and 25-hydroxycholesterol stimulate osteoblast-like vascular cells to calcify. J Clin Invest 93:2106–2113.

Wu LN, Genge BR, Dunkelberger DG, LeGeros RZ, Concannon B, Wuthier RE. 1997. Physicochemical characterization of the nucleational core of matrix vesicles. J Biol Chem 272:4404–4411.

Wu TT, Chen TL, Chen RM. 2009. Lipopolysaccharide triggers macrophage activation of inflammatory cytokine expression, chemotaxis, phagocytosis, and oxidative ability *via* a toll-like receptor 4-dependent pathway: validated by RNA interference. Toxicol Lett 191:195–202.

Xu Z, Huang CX, Li Y, Wang PZ, Ren GL, Chen CS, Shang FJ, Zhang Y, Liu QQ, Jia ZS, Nie QH, Sun YT, Bai XF. 2007. Toll-like receptor 4 siRNA attenuates LPS-induced secretion of inflammatory cytokines and chemokines by macrophages. J Infect 55: e1–e9.

Yang X, Fullerton DA, Su X, Ao L, Cleveland JC, Jr, Meng X. 2009. Pro-osteogenic phenotype of human aortic valve interstitial cells is associated with higher levels of Toll-like receptors 2 and 4 and enhanced expression of bone morphogenetic protein 2. J Am Coll Cardiol 53:491–500.